INTRATHECAL AAV9.TRASTUZUMAB TUMOR PROPHYLAXIS AND TREATMENT IN A MURINE XENOGRAFT MODEL OF HER2+ BREAST CANCER BRAIN METASTASES

William Thomas Rothwell

A DISSERTATION

in

Cell and Molecular Biology

Presented to the Faculties of the University of Pennsylvania

in

Partial Fulfillment of the Requirements for the

Degree of Doctor of Philosophy

2017

Supervisor of Dissertation	Graduate Group Chairperson
_____	_____
James M. Wilson, M.D., Ph.D.	Daniel S. Kessler, Ph.D.
Rose H. Weiss Professor and Director,	Chair, Cell and Molecular
Orphan Disease Center	Biology Graduate Group
Professor of Medicine and Pediatrics	Associate Professor of Cell and
Director, Gene Therapy Program	Developmental Biology

Dissertation Committee

Lewis A. Chodosh, M.D., Ph.D., Professor and Chair, Department of Cancer Biology

José R. Conejo-Garcia, M.D., Ph.D., Senior Member, Moffitt Cancer Center

Chi V. Dang, M.D., Ph.D., Professor, The Wistar Institute

Laura A. Johnson, Ph.D. Senior Director, GlaxoSmithKline

INTRATHECAL AAV9.TRASTUZUMAB TUMOR PROPHYLAXIS AND TREATMENT IN A MURINE XENOGRAFT MODEL OF HER2+ BREAST CANCER BRAIN METASTASES

COPYRIGHT

2017

William Thomas Rothwell

This work is licensed under the
Creative Commons Attribution-
NonCommercial-ShareAlike 3.0
License

To view a copy of this license, visit

https://creativecommons.org/licenses/by-nc-sa/3.0/us/

DEDICATION

For my mother and father

In memory of my grandmother and grandfather

For my friends

For my family

For my Wilson Lab family

For my teachers and mentors in science:

Lenora Crabtree, Rebecca Alexander, Paul Thomas, Stephen Turner, Nicole LaGruta,

Peter Doherty, James Wilson

For my teachers and mentors in writing and scholarship:

Nancy McDaniel, Tom Phillips

ACKNOWLEDGMENT

Thanks to Peter Bell who oversaw and provided guidance with histopathology, Laura Richman who provided guidance with histopathology and experimental design, Anna Tretiakova who provided guidance regarding antibody expression from AAV vectors, Maria Limberis who provided guidance in the design of mouse experiments, Mingyao Li who oversaw statistical analysis of data, and to James Wilson who originated the initial concept and provided direction for the program.

Thanks also to Lewis Chodosh and Jason Ruth for their generous gift of BT474-M1 cells; my thesis committee, Lewis Chodosh, José Conejo-Garcia, Chi Van Dang, and Laura A. Johnson, for their indispensable, generous guidance and advice; Tamara Goode for procedural instruction and advice with the xenograft model; Deirdre McMenamin, Christine Draper, and the Penn Gene Therapy Program (GTP) Program in Comparative Medicine for animal procedural assistance; Jamunabai Prakash and the Penn GTP Cell Morphology Core for exhaustive assistance with histopathology; the Penn Vector Core; Christian Hinderer for advice and direction; Jenny Greig for her generous gift of AAV9.2.10AmAb and for advice and direction; Jennifer Stewart for editorial assistance; and Tarek Sahmoud for his assistance with the clinical development plan.

Finally, thanks to my Wilson Lab family and their significant others for advice, direction, comfort, fun, and laughter over the past several years.

ABSTRACT

INTRATHECAL AAV9.TRASTUZUMAB FOR TUMOR PROPHYLAXIS AND TREATMENT IN A MURINE XENOGRAFT MODEL OF HER2+ BREAST CANCER BRAIN METASTASES

William Thomas Rothwell

James M. Wilson

Breast cancer brain metastases (BCBM) are a deadly sequela of breast tumors that overexpress human epidermal growth factor receptor 2 (HER2). HER2+ BCBM affects approximately 17,000 women in the US every year. Median survival is 10-13 months from the time of diagnosis of central nervous system (CNS) disease. Current therapeutic interventions are invasive, toxic, and largely ineffective, leaving a clear, unmet need for targeted HER2+ BCBM treatments. Trastuzumab(Herceptin®) is a monoclonal antibody used to treat HER2+ breast cancer successfully, but systemic trastuzumab cannot bypass the blood-brain barrier (BBB). To solve this problem, we have developed an adeno-associated virus serotype 9 (AAV9) vector to express trastuzumab *in vivo* after a single intrathecal (IT) injection. IT vector administration in an orthotopic Rag1-/- murine xenograft model of HER2+ BCBM led to a significant increase in median survival and attenuated brain tumor growth. We also report preservation of both the HER2 antigen specificity and the natural killer (NK) cell-associated mechanism of action of trastuzumab. Finally, we demonstrate increased median survival when IT AAV9.trastuzumab is administered as tumor treatment. Our results indicate that IT AAV9.trastuzumab may provide significant anti-tumor activity in patients with HER2+ BCBM.

TABLE OF CONTENTS

DEDICATION III

ACKNOWLEDGMENT IV

ABSTRACT V

LIST OF TABLES IX

LIST OF ILLUSTRATIONS X

CHAPTER 1 1

Adeno-associated virus (AAV) 1

AAV gene therapy vectors 2

Approved and forthcoming gene therapies 4

CHAPTER 2 9

The blood-brain barrier and cerebrospinal fluid 9

AAV serotype 9 (AAV9) 10

Intrathecal administration of AAV9 gene therapy vectors 11

When intra-cisterna magna vector administration is infeasible: The Ommaya reservoir versus lumbar puncture for access to cerebrospinal fluid 17

CHAPTER 3 26

Antibodies 26

AAV-mediated delivery of antibodies 32

CHAPTER 4 35

Human epidermal growth factor receptor 2 (HER2) 35

HER2 and trastuzumab (Herceptin®) **36**

The mechanisms of action of trastuzumab **41**

Trastuzumab-related cardiotoxicity **44**

CHAPTER 5 ..... **49**

HER2+ breast cancer brain metastases (BCBM) **49**

Intrathecal trastuzumab as HER2+ BCBM treatment **52**

CHAPTER 6
INTRATHECAL AAV9.TRASTUZUMAB TUMOR PROPHYLAXIS AND TREATMENT IN A MURINE XENOGRAFT MODEL OF HER2+ BREAST CANCER BRAIN METASTASES **56**

Hypotheses **58**

Introduction **56**

Results **58**
IT AAV9.trastuzumab provides tumor prophylaxis and treatment in a xenograft model of HER2+ BCBM 59
Prophylactic IT AAV9.trastuzumab slows tumor growth 61
Secreted trastuzumab binds to HER2+ brain tumors 61
NK cells, but not macrophages, mediate IT AAV9.trastuzumab tumor prophylaxis 62

Discussion and further directions **64**

Materials and Methods **68**
Experimental design 68
Statistics 69
Vector construction 70
Vector administration 70
Orthotopic xenograft model of HER2+ breast cancer brain tumors in Rag1-/- and NSG mice 71
Tumor diameter 73
NK cell depletion 73
Systemic macrophage depletion 73
Preparation of serum 74
Preparation of brain homogenate 74
Protein A ELISA 74
Biodistribution by qPCR 75
Histology 75
ICV Herceptin® and AAV9.trasstuzmab administration for quantification of trastuzumab in brain tissue 77
Study Approval and Animal Welfare 78

Tables & Table Legends **79**

Table 1. A summary of case reports of IT trastuzumab used to treat HER2+ BCBM. 79
Table 2. A summary of ongoing clinical trials using IT Herceptin® to treat HER2+ BCBM. 80

Figures & Figure Legends 81
Fig. 1. IT AAV9.trastuzumab tumor prophylaxis. 81
Fig. 2. IT AAV9.trastuzumab tumor treatment. 82
Fig. 3. Day 47 tumor diameter and IgG immunofluorescence microscopy. 83
Fig. 4. IT AAV9.trastuzumab tumor prophylaxis in NOD scid gamma mice. 84
Fig. 5. IT AAV9.trastuzumab tumor prophylaxis in the setting of continuous NK cell depletion. 86
Fig. 6. NK cell immunohistochemical staining of day 20 tumors. 87
Fig. 7. IT AAV9.trastuzumab tumor prophylaxis in the setting of continuous systemic macrophage depletion. 88

Supplementary Materials: 89
Fig S1. Biodistribution of vector genome copies in brain. 89
Fig S2. Trastuzumab quantified in brain tissue. 90
Fig S3. Anti-IgG immunofluorescence of day 20 and day 47 tumor cryosections. 91
Fig S4. IgG expression in brain tissue. 92
Fig S5. Human HER2 IHC staining of day 47 tumors. 92

BIBLIOGRAPHY 93

LIST OF TABLES

Table 1. A summary of case reports of IT Herceptin® used to treat HER2+ BCBM

Table 2. A summary of ongoing clinical trials using IT Herceptin® to treat HER2+ BCBM

LIST OF ILLUSTRATIONS

Figure 1. IT AAV9.trastuzumab tumor prophylaxis.

Figure 2. IT AAV9.trastuzumab tumor treatment.

Figure 3. Day 47 tumor diameter and IgG immunofluorescence microscopy.

Figure 4. IT AAV9.trastuzumab tumor prophylaxis in NOD *scid* gamma mice.

Figure 5. IT AAV9.trastuzumab tumor prophylaxis in the setting of continuous NK cell depletion.

Figure 6. NK cell immunohistochemical staining of day 20 tumors.

Figure 7. IT AAV9.trastuzumab tumor prophylaxis in the setting of continuous systemic macrophage depletion.

Figure S1. Biodistribution of vector genome copies in brain.

Figure S2. Trastuzumab quantified in brain homogenate.

Figure S3. Anti-IgG immunofluorescence of day 20 and day 47 tumor cryosections.

Figure S4. IgG expression in brain tissue.

Figure S5. Human HER2 IHC staining of day 47 tumors.

CHAPTER 1

Adeno-associated virus (AAV)

AAV is a small, non-enveloped parvovirus of the *dependoviridiae* family originally discovered as a contaminant in laboratory cultures of adenovirus in 1965 [1]. It has a single-stranded DNA genome which is about 4.7 kilobases in length and contains two genes, *rep* and *cap*. These genes code for full-length non-structural and viral capsid proteins, respectively, as well as multiple splice variants of each. These genes are flanked by inverted tandem repeat sequences (ITRs) of 145 base pairs in length, which serve to prime second strand synthesis of the viral genome in a host cell. They can also prime transcription of viral genes. AAV is not known to cause any disease in humans and can infect both dividing and non-dividing cells. [2-6]

Multiple AAV serotypes exist and are defined by differences in amino acid sequence of capsid proteins. Each serotype has a unique tropism for tissues in the body, thus allowing the engineering of AAV gene therapy vectors targeted to a particular organ or set of organs. The serotypes of the first nine AAVs discovered are indicated by a number (AAV1 or AAV2, for example). As more AAVs were discovered, this convention has changed to reflect the species of origin (AAVrh10 from rhesus macaques, AAVhu32 from humans, etc.) [7-12].

Wild-type AAV infection begins when a virion binds to a host cell. The full mechanism of attachment and entry is still incompletely understood. Recently, a pan-AAV receptor (AAVR) for AAV binding was reported [13]. Previously, Bell et al. showed that gene therapy vectors derived from AAV serotype 9 (AAV9) require a terminal galactose residue on host cell glycoproteins for entry [14]. In any case, binding to the

host cell leads to endocytosis of virions. Endocytosis of virions is necessary for successful infection, as direct injection of virions into the cytoplasm does not lead to virion localization to the nucleus. After trafficking through early endosomes, virions escape and are translocated to the nucleus where they uncoat. The AAV genome remains episomal in the nucleus, forming head-to-tail concatamers. [5, 15-23]

Whether or not AAV genomes have the ability to integrate into the host genome at a specific point on chromosome 19, termed AAVS1, is debated. Regardless, AAV infection alone is a lysogenic event. In order for wild-type AAV to replicate and complete a lytic cycle, coinfection with adenovirus and/or expression of required adenovirus proteins in the host cell is required. [5, 15-23]

AAV gene therapy vectors

To engineer a non-replicating AAV gene therapy vector from wild-type AAV, one simply replaces the *rep* and *cap* genes in the AAV genome with an expression cassette containing the therapeutic gene of interest (transgene) as well as necessary regulatory elements including an enhancer/promoter and polyadenylation signal. The ITRs are left intact, flanking the expression cassette. By convention, gene therapy vectors use ITR sequences from AAV2. Rather than relying on adenovirus coinfection to provide proteins required to complete the AAV life cycle, they are provided *in trans*. [24]

One common method of AAV vector production involves co-transfection of human embryonic kidney 293 cells (HEK293) with three plasmids. One plasmid is the vector genome itself containing the transgene expression cassette, another contains the necessary adenoviral protein genes, and a third contains the capsid protein gene for the

desired AAV serotype. Vector genomes are packaged into the AAV capsids that self-assemble intracellularly, and the host HEK293 cells are lysed to collect vector. Interestingly, HEK293 cells were first developed after transformation of embryonic kidney cells with sheared adenovirus DNA. Thus, HEK293 cells already possess some of the adenoviral proteins necessary for AAV vector production. [24]

Self-complementary (scAAV) AAV vectors were developed as a way to speed the onset of transgene expression. The genomes of these vectors are engineered to skip second strand synthesis, since a self-complementary genome will form a double-stranded molecule *in vivo* on its own. [24]

Most humans have been infected with at least one serotype of wild-type AAV, likely at a young age as antibodies to AAVs have been reported in children. Infection with either wild-type AAV or systemic administration of an AAV vector leads to a potent antibody response against the capsid protein. These antibodies may simply bind to the capsid protein, or the antibodies may neutralize the virus/vector (termed neutralizing antibodies or nAbs), rendering the particle unable to transduce a host cell. nAbs may be specific for one AAV serotype, or they may be cross-reactive, neutralizing multiple serotypes. Prevalence of antibodies against different serotypes of AAV is unique to the serotype in question. AAV9, for example, has a nAb prevalence in humans of about 15-30% and a binding antibody prevalence of about 45%. A person's geographic location correlates with the prevalence of anti-AAV antibodies, with higher titers of nAbs occurring in developing countries. [25-33]

The presence of neutralizing antibodies in a patient or laboratory animal are of particular concern in the field of gene therapy, as titers of neutralizing antibodies in blood

greater than 1:10 have been shown to prevent AAV transduction *in vivo* after systemic dosing. This would preclude either administration of gene therapy to an individual altogether or re-administration of an AAV vector of a given serotype to the same patient. Many laboratories which study AAV are employing various techniques to engineer AAVs to escape neutralization. It has been suggested that plasmapheresis may serve as a tool to temporarily lower the titer of anti-AAV antibodies in an individual before gene therapy vector administration, although multiple plasmapheresis sessions may be required, as a single session will lower a patient's AAV nAb titer by only 2 to 3-fold. [25-33]

Approved and forthcoming gene therapies

Several gene therapy products have been developed which have either been approved by either the Federal Drug Administration (FDA) or European Medicines Agency (EMA) or which are in clinical trials and are expected to be approved in the near future. Several of these are AAV gene therapies, but others use different vectors, such as lentiviral vectors derived from the human immunodeficiency virus (HIV).

The EMA approved the first gene therapy for commercial use in Europe. Glybera (apolipogene tiparvovec) is manufactured by uniQure based in the Netherlands. Glybera is an AAV1 gene therapy engineered to deliver the enzyme lipoprotein lipase (LPL) to patients harboring a very rare genetic deficiency of active enzyme. LPL helps to break down fat-laden chylomicrons which fill the blood after meals, and familial LDL deficiency may lead to chronic, life-threatening attacks of pancreatitis. Although Glybera administration was stated to have led to decreased number of pancreatitis episodes in patients with LPL deficiency, its true efficacy was hotly debated. To receive Glybera

treatment, patients are required to undergo 60 injections of the product into the quadriceps muscle. Its price tag proved daunting at the equivalent of 1 million USD per treatment. As such, uniQure announced in April 2017 that it would not seek renewal of Glybera marketing authorization by the EMA, allowing it to expire in October 2017. [34]

Another AAV gene therapy developed by Spark Therapeutics, voretigene niparvovec (Luxturna), has shown great promise in clinical trials. Luxturna is an AAV2 gene therapy to treat an inherited form of blindness call Leber congenital amaurosis (LCA). LCA can be caused by defects in several genes, one of which is *RPE65*, a protein that is expressed in retinal pigment epithelial cells and is required for normal visual function. Using a sub-retinal injection, AAV2 vector with an *RPE65* transgene has been administered to LCA patients and has shown promise in restoring vision, particularly in younger individuals. An FDA advisory committee recommended approval of Luxturna in October 2017, and it is likely that it will receive FDA approval in the fourth quarter of 2017 or first quarter of 2018, becoming the first gene therapy for a genetic disease licensed in the US. [35]

The very first gene therapy approved by the FDA is an *ex vivo* form of gene therapy called Kymriah (tisagenlecleucel). This treatment was approved in August 2017 and is comprised of genetically modified chimeric antigen receptor (CAR) T cells used to treat B cell acute lymphoblastic leukemia (ALL), an aggressive disease that kills 90% of patients in the first five years after diagnosis. 83% of patients treated with Kymriah experienced complete remissions of their disease in trials.

To understand how Kymriah works, it is necessary to elaborate briefly upon T cell biology. T cells are lymphocytes which form in the bone marrow and mature in the

thymus. They harbor a T cell receptor protein on their cell membranes. T cell receptors can recognize short peptides called epitopes. Epitopes can be derived from foreign proteins (for example, proteins from a virus or bacterium), self-proteins, mutant self-proteins, etc. Almost all self- reactive T cells are deleted by a complex process in the thymus during T cell development, although escapees can lead to autoimmunity.

Each T cell receptor recognizes a different epitope, which must be presented to the T cell receptor in the context of a major histocompatibility complex (MHC) protein. MHCs are present on all of our nucleated cells in the form of MHCI. MHCI presents intracellular self- and non-self-epitopes to the periphery. By the process of cross presentation, MHCI may present endocytosed antigens on specialized antigen presenting cells, primarily dendritic cells. MHCII is present on the surface of specialized antigen presenting cells such as dendritic cells, macrophages, or B cells. MHC II presents epitopes from endocytosed antigens.

Once a T cell encounters its cognate epitope-MHC complex on another cell, as well as the necessary costimulatory signals, the T cell is primed and activated to divide and exert effector functions. These effector functions could include killing target cells that express the cognate epitope of the T cell receptor. This function is mainly performed by cytotoxic T lymphocytes, which harbor a CD8 molecule. CD8 is costimulatory to MHCI-associated T cell priming. T cells may also exert effector function by releasing cytokines and signals crucial for priming other arms of the immune response. This function is mainly performed by T cells which harbor a CD4 molecule. CD4 is costimulatory to MHCII-associated T cell priming.

Rather than a conventional T cell receptor, CAR T cells express a receptor with an extracellular domain consisting of a small antibody construct. One antibody construct commonly used for this purpose is the short chain variable fragment (scFv), which is described further in “Antibodies” in chapter 3. In the case of Kymriah, the CAR scFv is murine and targets the human B cell protein CD19, which is expressed on all B cells including B cell leukemias and lymphomas. The advantage of using an antibody construct in this context is that the CD19 epitope does not have to be presented to the T cell in the context of an MHC. Rather, it can bind directly to its epitope. Additionally, the membrane-associated and intracellular domains of CAR T cells are engineered to provide potent co-stimulatory signaling machinery for the T cell to be induced to kill the target B cells. Thus, these CAR T cells are designed for fast, efficient, and specific recognition and killing of target cells.

Kymriah is derived from a patient’s own T cells, which are separated in the clinic from peripheral blood. Rather than AAV, lentiviral vectors are used to transfer the CAR gene to the T cells *ex vivo*, resulting in integration of the CAR expression cassette into the T cell genome. The cells are expanded and activated *in vitro*, then infused back into the patient. CAR T cells have led to ALL remissions in patients with high-stage disease who have failed other therapies. However, the toxicity associated with the release of large amounts of cytokines in these patients has resulted in patient mortality. As such, the FDA approved the use of Kymriah with an extensive risk evaluation and mitigation strategy over the next 5 years. Additionally, patients’ healthy B cells are also targeted by CD19 CAR T cells, necessitating regular infusions of intravenous immunoglobulin in recipients. [36, 37]

In summary, the field of gene therapy is growing at an exponential rate. New therapies for diseases once considered incurable are now contenders for cutting-edge treatments. The emergence of AAV gene vectors has contributed to this boom, and it is expected the FDA will soon approve more AAV gene therapies that are currently in clinical trials or pre-clinical development for use in patients.

CHAPTER 2

The blood-brain barrier and cerebrospinal fluid

The blood-brain barrier (BBB) is a physiological barrier separates the central nervous system (CNS) from the blood. It serves to protect the brain from organisms and toxins that may be present in the circulation. The BBB is formed both by astrocytyes and endothelial cells that line blood vessels in the CNS. These endothelial cells lack the usual fenestrations found in vascular endothelium elsewhere in the body; rather, they are held together by tight and adherens junctions. Astrocytic end feet also wrap around these blood vessels, forming another barrier. The BBB prevents the movement of large, polar, or charged molecules as well as cells from entering the CNS indiscriminately. Transport proteins expressed at the BBB do allow specific transfer of macromolecules from blood to CNS, and certain immune cells can access the CNS by moving intracellularly through the BBB. [38-40]

Cerebrospinal fluid (CSF) is the liquid that bathes the brain and spinal cord, serving both as a cushion to the brain as well as a source of nutrients and waste clearance for cells of the CNS. It is made from plasma that is transported by pinocytosis into the CNS by specialized anatomical structures such as the choroid plexus and ependymal cells, which are discussed below. CSF is much like plasma in composition except that most proteins and cells are excluded in its production. [38-40]

Traditionally, 80% of CSF is said to be secreted by a net-like structure called the choroid plexus, which floats in the lateral ventricles of the brain and is formed of a layer of cuboidal epithelial cells held together by tight junctions which line the outside of

capillaries. Other sources of CSF include ependymal cells, ciliated columnar epithelial cells which line both the lateral ventricles and central canal of the spinal cord, and the brain parenchyma itself. [38-40]

CSF flows around CNS structures and eventually joins back with venous blood at the one-way valve-like arachnoid granulations, also called arachnoid villi, located in the venous sinuses of the skull. A small portion of CSF is thought to return to venous circulation along the perineural spaces surrounding cranial nerves. CSF pulsates around CNS structures, moving with an individual's respiration. These pulsations are thought to originate at the choroid plexus and also by way of the ependymal cilia. In humans, the rate of CSF formation is 0.2-0.7 mL per minute, or 600-700 mL per day, and the total CSF volume is between 140 – 270 mL, depending on the age and sex of the individual. Thus, the CSF turns over rapidly. [38-40]

AAV serotype 9 (AAV9)

In the early 2000s, Gao et al. reported discovery of a number of new AAV serotypes in humans and non-human primates (NHPs) and characterization of their transduction patterns. A new AAV serotype, AAV9, emerged as a promising candidate for gene therapy in the central nervous system (CNS) due to its superior transduction of neurons and glial cells *in vivo*. AAV9 can also transduce liver, heart, and skeletal muscle. [10]

Cearley and Wolfe reported the widespread pattern of AAV9 CNS transduction in rodents after intravenous (IV) administration of vector, suggesting that AAV9 may cross the blood-brain barrier (BBB). Further studies in NHPs indicated that although IV-

administered AAV9 vectors may cross the blood-brain barrier to a small extent by way of an unknown mechanism, the amount of transduction in the brain itself after IV administration of vector is not enough to guarantee successful therapeutic efficacy of a gene therapy unless exceptionally large doses are used. As such, a more targeted route of administration (ROA) for AAV9 delivery to the CNS was in order. [41-48]

Intrathecal administration of AAV9 gene therapy vectors

Several groups have demonstrated that bypassing the BBB with an intrathecal (IT) injection of AAV9 directly into central nervous system (CNS) leads to superior transduction of cortical and cerebellar brain structures compared to IV AAV9 vector administration. Additionally, IT administration of AAV9 will not expose vector to neutralizing antibodies (nAbs) circulating in the blood. Thus, individuals with high titers of nAbs may still be eligible to receive IT AAV gene therapy.

There are multiple ways to access the CNS for IT vector administration. One may inject vector directly into the brain tissue itself (intraparenchymal injection). This technique involves making multiple needle tracks in the brain parenchyma and releasing several boluses of vector as the needle is drawn back up the needle track. This may be the route of administration (ROA) of choice if one desires high levels of local transduction of small structures in the brain such as the basal ganglia. However, this technique would not be suitable if one desires widespread AAV transduction in the CNS as these intraparenchymal injections lead to poor penetration of vector into the brain parenchyma. In fact, the majority of transduced cells are located in the area immediately surrounding the needle tracks. To guarantee widespread transduction throughout the

cortex by intraparenchymal injection, as is accomplished by roughly 4 intraparenchymal injections in mice, over 100 individual needle tracks would likely need to be made in the human brain. Additionally, disruption of brain tissue during intraparenchymal vector administration can lead to the initiation of an inflammatory response in the brain. This, in turn, can prime potent immune responses against the vector capsid and transgene which can damage CNS tissue. [49-51]

One may also inject vector directly into the cerebrospinal fluid (CSF), the fluid that bathes the brain and spinal cord and is contiguous with brain interstitial fluid. Vector thus percolates with the CSF around CNS cells leading to widespread transduction of structures throughout the brain. There are multiple ways by which one may access the CSF. A lumbar puncture (LP) would involve administering vector directly into the CSF surrounding the lumbar spinal cord. Intracranioventricular (ICV) administration would likely involve neurosurgical placement of an Ommaya reservoir, a plastic, dome-shaped reservoir attached to a catheter. The catheter penetrates the skull and brain parenchyma, and the tip of the catheter rests in one of the lateral ventricles. CSF flows out of the ventricles through the catheter and into the bulb portion of the reservoir, which sits subcutaneously outside of the skull. After placement, one simply pierces the skin and reservoir with a needle to access CSF. Finally, one may deliver vector by way of direct injection into the cisterna magna (intra-cisterna magna, ICM), an anatomical reservoir of CSF located directly below the occipital portion of the skull. [49, 52-55]

AAV9 transduction in the murine CNS has been described in many publications. Cearley and Wolfe administered AAV9 by direct stereotaxic intraparenchymal injection of vector into the brains of mice that lacked a lysosomal enzyme required to break down long carbohydrate molecules called glycosaminoglycans. Patients with family of genetic

diseases called mucopolysaccharidoses can lack one of a family of these lysosomal enzymes, leading to toxic accumulation of glycosaminoglycans in the CNS and other organs of the body.

After intraparenchymal administration of AAV9 vector, transduction of cortical neurons was evident in cerebral hemisphere ipsilateral to the injections, as expected. Interestingly, cortical structures in the hemisphere contralateral to the side of vector administration were also transduced. It was postulated that AAV9 was taken up by neurons around the injection site and trafficked by way of axons which cross the cerebral hemispheres, leading to enzyme expression in the contralateral hemisphere. The hippocampal commissure, septal nuclei, and entorhinal commissure were identified as candidate structures for this phenomenon, as they contain neurons that send axons to the contralateral hemisphere. Trafficking of AAV9 along axons was subsequently confirmed in later papers from the same group. [15, 56]

Schuster et al. described transduction of AAV9 after ICV administration of AAV9.GFP in mice. GFP expression was widespread throughout the CNS including in cortical neurons and astrocytes. Specific structures observed to be transduced included “cranial nerve nuclei, ventral pons, cerebellar cortex, hippocampus, pituitary, choroid plexus, and selected nuclei of midbrain, thalamus and hypothalamus.” Interestingly, transduction of the enteric nervous system was also observed. [57]

Many labs have compared administration of AAV9 vector by way of LP or by ICM injection in large animals, particularly in NHPs. Two reports by Samaranch et al. describe ICM administration of 1.8e13 genome copies (GC) of scAAV9 vector to a total of 4 cynomolgus macaques. The transgene expression cassette of the vector was

comprised of a cytomegalovirus immediate/early enhancer-promoter (CMV) and a green fluorescent protein (GFP) transgene (scAAV9.CMV.GFP). 3 weeks after vector administration, animals were euthanized and GFP was detected in CNS tissues both by immunohistochemistry (IHC) and immunofluorescence (IF) microscopy.

In all animals, GFP was expressed in cells from the prefrontal to occipital cortex and at all levels of spinal cord. Types of cells transduced included neurons, astrocytes, and ependymal cells. In the earlier of the two reports, Purkinje cells in the cerebellum were found to have the strongest GFP expression. GFP expression was also shown to cluster in cells surrounding blood vessels. In the earlier report, colocalization of GFP expression with cell type-specific markers showed that GABAergic interneurons were transduced. In the later report, the authors describe sparse transduction of cells in spleen and liver, suggesting that vector does indeed escape from the CNS after IT administration, likely with CSF as it empties into the venous circulation at the arachnoid granulations. [44, 58]

Grey et al. described administration of scAAV9 vector with a different promoter-enhancer, derived from chicken beta-actin (CBh), to express GFP in ten cynomolgus macaques. Two of these animals received scAAV9.CBh.GFP vector by ICM administration, and eight received vector by LP. Most animals received 1.83e12 GC vector, although two animals that received LP vector were dosed at 5.5e12 GC vector. After four weeks, animals were euthanized, and GFP expression was detected in cells throughout the cortex by IHC only.

LP vector administration led to greatest GFP expression in lumbar segments of spinal cord. Using quantitative PCR (qPCR) to determine number of GC in specific

anatomical structures, the authors indicated that ICM vector administration led to spinal cord transduction at a level of 0.08 GC per diploid genome (DG) while LP vector administration yielded only 0.02 GC/DG. This suggests that ICM administration of vector is a superior ROA to LP, even for spinal cord gene transfer. Interestingly, qPCR of CSF collected two hours after vector administration detected no vector, suggesting that the rapid turnover of CSF also leads to rapid vector clearance. [41]

A pivotal report by Hinderer et al. compares ICM and LP dosing of 6 cynomolgus macaques with AAV9.GFP. Four animals received vector ICM, two at a dose of 2.5e12 GC/kg and two at a dose of 5e12 GC/kg. The two animals that received vector by LP were dosed at 2.5e12 GC/kg. One animal also received vector IV at 2e13 GC/kg. This IV dose was 8-fold higher per kg body weight than the dose given to monkeys by LP and the lower dose administered to monkeys ICM.

After 14 days, expression of GFP throughout the cortex and spinal cord was visualized by IF, and GFP-positive neurons were quantified in an automated fashion by software. Importantly, animals that received vector by ICM dosing showed 10- to 100-fold higher levels of gene transfer in the cortical CNS than animals that received vector by LP. In fact, ICM vector administration in these animals led to better gene transfer in all divisions of the spinal cord than LP vector administration. Additionally, IV vector delivery led to similar levels of gene transfer throughout the CNS when compared to LP vector administration, although the IV dose was much higher. IF colocalization of cell-type specific markers demonstrated that AAV9 vector transduced neurons and glia, including astrocytes. Although the number of lymphocytes in CSF increased after vector administration, no clinically appreciable or histological toxicity was noted in the animals during the course of the experiments. [49]

NHPs are not the only large animals used to study IT administration of AAV9 vector, as porcine models are becoming increasingly prevalent. One report by Federici et al. describes LP delivery of scAAV9.CBh.GFP to twelve pigs at one of two doses, 4.28e10 GC/kg or 1.7e11 GC/kg. Vector was administered after single level lumbar laminectomy and catheter placement either “locally,” as a 1.5 mL bolus at the lumbar level, or “diffusely,” as three 0.5 mL boluses at the cervical, thoracic, and lumbar levels 10 cm apart.

After four weeks, “local” administration led to greater GFP expression at lumbar levels of the spinal cord, greater GFP expression in spinal cord at the higher dose, and GFP expression in dura up to the level of the cervical spinal cord. “Diffuse” administration led to transduction of all segments of spinal cord, but with very little transduction at the low dose. qPCR analysis of DNA from various tissues showed only small amounts of transduction of peripheral tissues. Only IHC was used to visualize GFP expression, with microscopic quantification of transduced neurons performed manually. [59]

Overall, these studies suggest that unless one desires to target spinal cord locally, ICM AAV9 vector administration leads to the most extensive transduction of cortical and cerebellar structures compared LP vector administration. As such, ICM is the most promising IT ROA for gene therapies that require widespread transduction of the CNS and expression of either intracellular or secreted transgenes by neurons and glia throughout the cortex and cerebellum.

When intra-cisterna magna vector administration is infeasible: The Ommaya reservoir versus lumbar puncture for access to cerebrospinal fluid

Although ICM vector administration will likely be the preferred method of AAV9 vector delivery for CNS gene therapies going forward, there may be instances where this ROA is not feasible. In these cases, an LP or Ommaya reservoir may be preferred methods of access to CSF. The following is an in-depth comparison of both techniques in terms of safety and feasibility as ROAs for gene therapy vectors targeting the CNS.

The Ommaya reservoir was developed in 1963 by Dr. Ayub Ommaya as a way to provide easy, subcutaneous access to patients' CSF to administer drugs for fungal meningitis [53]. Since then, it has become the method of choice to administer chemotherapeutic agents directly into the CSF of patients with CNS malignancies.

As described above, the reservoir consists of a plastic, dome-shaped structure connected to a catheter. To insert it, neurosurgeons shave and incise skin overlying the non-dominant hemisphere of the brain to expose the skull. Next, a burr hole is drilled in the skull that is large enough to accommodate the catheter. After penetrating the dura, the catheter is inserted into the brain parenchyma and advanced to the ventricle. Correct trajectory of the catheter may be assisted by ultrasound guidance, a stereotactic frame, or a device such as a Ghajar Guide (Neurodynamics, Inc.) to ensure that the catheter travels perpendicularly relative to the plane of the patient's skull. To confirm entry into the ventricle, the surgeon will test for CSF flow through the catheter. Further intraoperative fluoroscopic or endoscopic imaging can be used to determine the precise location of the catheter tip.

After confirming proper placement of the catheter, the reservoir is connected, secured to the skull with suture, and the overlying skin is closed. A computed tomography (CT) scan may be performed postoperatively to confirm correct placement of the catheter [54]. To access the reservoir, the overlaying skin is disinfected, and a needle and syringe is used to puncture the reservoir and withdraw CSF. According to one study, reservoirs have remained in place anywhere from 2 days to 4.6 years, with a median of 4.1 months [60]. Both pediatric and adult patients may have an Ommaya reservoir implanted.

Major complications resulting from placement and access of the Ommaya reservoir include infection, hemorrhage, and catheter misplacement. One study reported that 10% of patients with an Ommaya reservoir experienced some sort of complication [54].

Infections comprise a large portion of these Ommaya reservoir complications. Two recent retrospective case analyses surveyed reservoir infections at two separate institutions over a 10 and 16-year period, respectively. 5.5 [61] and 8% [62] of patients with Ommaya reservoirs developed a device-related infection, which falls within the previously reported 2-15% infection rate [63-66]. Meningitis or meningoencephalitis represented the majority of infections.

Most infections occurred soon after the device was accessed (within 7 days [62] or 30 days [61]). The studies also reported that 32 [61] and 40% [62] of reservoir infections occurred within the first month after placement. The median number of reservoir punctures before infection reported in the respective studies was 3 [62] and 5[61], although the range was broad for both studies (0-105 [61]; 2-17 [62]).

The most commonly isolated bacteria from CSF cultures of patients with infected reservoirs are normal skin flora, particularly coagulase negative staphylococci (e.g. *Staphylococcus epidermidis*) and *Proprionibacterium acnes*. However, *Staphylococcus aureus*, *Pseudomonas spp.*, enteric bacteria, mouth flora, and even *Candida spp.* have been cultured as infectious agents [61, 62]. Reported treatments for reservoir infection range from device removal to intravenous and/or intrathecal antibiotics [62, 67]. Patients have died as a result of reservoir infections [61, 62].

It is important to note that the majority of patients that receive Ommaya reservoirs do not contract an infection. One Canadian study reports that 85% of patients with Ommaya reservoirs had no infection within the first year post-implantation [60]. In addition, it is important to consider that many patients that receive Ommaya reservoirs are cancer patients who are likely immunosuppressed and therefore more susceptible to infection in general.

Hemorrhage is a second complication resulting from reservoir placement, occurring in anywhere from 1-2.8% of patients [54, 60, 63]. Subarachnoid, subdural, and intraventricular hematomas may occur. One retrospective study indicates that two of three reported reservoir-related hemorrhages were fatal. However, these deaths were associated with anticoagulation or development of thrombocytopenia unrelated to device placement [54].

Misplacement of the reservoir catheter tip is another significant complication of Ommaya reservoir implantation, occurring in 2.7-12.5% of patients [54, 68, 69]. Although various imaging modalities can be used both intraoperatively and postoperatively to confirm catheter tip placement, there are multiple reports of the catheter tip piercing the

brain parenchyma postoperatively [70]. One study reports the death of a patient due to catheter advancement through the wall of the lateral ventricle, thalamus, and into the midbrain [60].

Despite these morbidities, the Ommaya reservoir offers several advantages to patients who would receive intrathecal gene therapy. Only one procedure is needed to provide CSF access for both vector administration and subsequent sampling. CSF access requires a simple subcutaneous needle stick. Finally, the Ommaya reservoir is reported to be more comfortable for patients than serial LPs [71].

Alternatively, clinicians may use LP as a method to access the CSF for gene therapy. LP was first reported by Heinrich Quincke in 1891 as a method to drain CSF from pediatric patients who had increased intracranial pressure due to tuberculous meningitis [72]. Today, it is a commonly used technique in both adults and children to diagnose CNS infections and to identify suspected subarachnoid hemorrhages when CT scans are negative [55].

To perform a LP, the patient may sit or lie on his or her side in a fetal position with the back and head bent forward. The clinician palpates the vertebrae of the spine to locate the 3rd, 4th, and/or 5th lumbar vertebrae (L3, L4, and L5), which are located below the termination of the spinal cord. The skin above this area is disinfected and draped, and local anesthesia to the skin is administered. A spinal needle is advanced between L3 and L4 or L4 and 5 until the CSF from the subarachnoid space begins to flow through the needle. Often a “pop” is felt as the needle penetrates the dura. The clinician can then instill medication or anesthesia or withdraw CSF for analysis. Up to 40 mL of CSF may

be taken from a patient, although a 8-15 mL volume is more commonly collected for analytic purposes [73].

LPs are usually conducted freehand, although fluoroscopic or ultrasound guidance can increase the success of the procedure [74-76]. In children, LPs are performed using the same procedure as in adults with one exception. At birth, the termination of the spinal cord is located at L3, thus a patient younger than 1 year should receive a LP below the L2 and L3 vertebrae to avoid piercing the spinal cord [77].

Minor complications associated with LP include post-LP spinal headache, back pain, radicular pain and limb numbness, and abducens nerve palsy. These sequelae occur with much greater frequency than the major complications that include hemorrhage, cerebral herniation, and epidermoid tumors [78].

The most common sequela of LP is the post-LP spinal headache. The onset of the headache is usually within 5 days of the procedure [79] and occurs commonly in the front-temporal or occipital regions [80]. It is exacerbated by sitting upright or standing, and it is ameliorated by reclining [80]. The reported incidence of spinal headache post-LP is variable depending on the case series. One study examined several case reports and reported spinal headache incidence anywhere from 12-40%. This large range is due to several factors including the gauge of needle used to perform the LP as well as technique of the clinician [79]. In adults, it has been shown that using a needle with a smaller diameter lessens the incidence of spinal headaches, as does using a pencil-point spinal needle rather than one with a beveled end [81-85]. These alterations do not lessen the incidence of spinal headache in children [86].

There are several proposed pathophysiological mechanisms to explain the etiology of the spinal headache including persistent CSF leakage from the LP access point, decreased CSF pressure causing tension on the pain-sensitive lining of the brain and CNS blood vessels, and increased vasodilatation in the brain [87, 88]. Regardless, the headache is usually self-limiting, with 70% of patients recovering within a week [89, 90]. Caffeine can be taken to relieve pain and possibly decrease the duration of the headache [91, 92]. In cases where the headache is especially severe or abates slowly, an epidural blood patch or surgical closure of the hole in the dura can be employed to stop the headache [83, 93, 94].

Blood in the CSF is a relatively common occurrence in CSF collection and is referred to as a “traumatic” or “bloody tap.” This occurs if the spinal needle pierces an epidural vein [78]. Rarely, however, severe hemorrhage due to severing of subdural and subarachnoid vessels can lead to subarachnoid, epidural, or subdural hematomas that may compresses the spinal cord causing neurologic deficits and possibly death [95]. As is the case for patients that receive Ommaya reservoirs, patients that are anticoagulated after the LP procedure or who have a bleeding diathesis are at higher risk for hematoma post-LP [95]. If a hematoma does form in the spinal canal, it may require surgical decompression. Additionally, the patient may experience permanent sensory or motor damage [96].

Other complications of LP include back pain and paresthesia in the lower extremities and groin [73]; these are relatively common during and immediately after the procedure. Cerebral herniation through the foramen magnum due to increased intracranial pressure (ICP) is a fatal complication of LP. A CT scan should thus be conducted for all patients exhibiting signs of increased ICP before LP is performed [73].

Meningitis is rarely experienced following an LP obtained for diagnostic purposes [97] and is usually associated with poor disinfection of skin or instruments used for the procedure, poor aseptic technique, or (somewhat controversially) contamination by mouth flora of the clinician or hospital staff performing or assisting with the LP [98]. Epidermoid tumors are another uncommon sequela of LP and are thought to result from seeding of the subarachnoid space with epidermoid tissue dislodged during the procedure. Most of these epidermoid tumors are discovered in early to late childhood in patients who received LPs as infants [78, 99, 100].

LPs are advantageous for gene therapy applications because they do not require a specialist to perform. Most internal medicine or pediatric clinicians are trained to perform an LP. LPs are much less invasive, quicker, and cheaper than implanting an Ommaya reservor. In addition, the incidence of severe complications or infections for LPs is universally recognized to be very low.

In order to choose the best route of administration and subsequent access to CSF for gene therapies in the CNS, one may consider how treatment may progress for a patient who undergoes Ommaya reservoir implantation versus one who receives serial LPs.

In one case, the patient would undergo surgery to implant the Ommaya reservoir prior to vector administration. In the absence of subsequent infection, it is feasible to assume that vector may be instilled through the reservoir soon after recovery from the implantation procedure. CSF would be collected from the reservoir, perhaps at 7, 14, 30, 60, and 90 days after vector administration to evaluate transgene expression and immune responses.

A high index of suspicion for infection would be maintained through the course of treatment and evaluation given the increased likelihood of infection within 7 to 30 days of last reservoir access. The number of reservoir taps may be increased, although this would exceed the 3 and 5 taps reported above as the median number of reservoir accesses before infection occurs. The risk of infection may be mitigated if the patient is not immunocompromised due to cancer or chemotherapy treatment. Patients with a bleeding diathesis due to thrombocytopenia or clotting factor deficiencies would require close monitoring and a low threshold for CT imaging to catch hemorrhages early. Adult patients or families of pediatric patients who experience great distress at the prospect of serial LPs or who find LPs unbearably painful or uncomfortable may decide that the convenience of an Ommaya reservoir outweighs its risk of morbidity and mortality.

In the second case, the patient would receive a gene therapy vector intrathecally by any number of methods including but not limited to instillation through an Ommaya reservoir that is removed within days of treatment. The patient would then experience serial LPs punctures to collect CSF for transgene and immunological analysis, again perhaps at 7, 14, 30, 60, and 90 days post-treatment. The risk of infection due to LP for this patient would be low, thus clinical suspicion in response to CNS abnormalities would be focused on complications caused by gene therapy. The same precautions for patients prone to hemorrhage would be taken in this instance as described above. It is likely that at least one of these LPs would result in a spinal headache and back pain, both of which would likely dissipate within several days to a week. It is possible that the patient will experience radiculopathy and paresthesia during or after the procedure, and it would be very unlikely for the patient will develop an epidermoid tumor, abducens palsy, or cerebral herniation (unless, in the latter case, the gene therapy treatment leads to

increased ICP that is not detected before LP is performed). Overall, serial LPs would be relatively safe following gene therapy treatment.

Ultimately, the factors that will determine whether the Ommaya reservoir or serial LPs are chosen for an individual patient or specific treatment may be further dictated by the expertise of the clinician and center at which therapy is initiated, the patient's immune competency, the patient's propensity to bleed, whether spinal cord cells are the targets of gene transfer for a given therapy, and the level of comfort the patient or his or her family has for either modality.

CHAPTER 3

Antibodies

Antibodies are proteins produced by the immune system in response to the introduction of proteins that the body senses as foreign. These foreign proteins could come from a virus, bacterium, or a transplanted organ. Each individual antibody attaches to a very specific region of this foreign protein. This region of binding is called an epitope. The epitope may be linear, composed of an adjacent sequence of 5 to 20 amino acids, or the epitope may be conformational, meaning that it is comprised of non-adjacent amino acids that exist near each other in the three-dimensional confirmation of the protein. The protein containing these epitopes is called an antigenic protein or antigen. This antigen may also be another macromolecule, for example a carbohydrate or glycoprotein.

Antibodies are produced by a specialized immune cell called a B cell, a lymphocyte of the immune system which develops and matures in the bone marrow. Each B cell produces an antibody that has unique specificity for a particular epitope. Upon exposure to its specific antigen along with costimulatory signals from other immune cells, B cells begin to secrete antibodies. At first, the antibodies tend to have a relatively low affinity for a particular antigen, meaning the strength of the attachment is relatively low. As time goes by, the B cells undergo a process called affinity maturation whereby the strength of attachment of these secreted antibodies increases due to random mutations specifically in the antibody gene.

Activated B cells will divide to produce a clone of cells. Some members of this clone will become plasma cells, which are long-lived cells and specialized to produce a

large amount of antibody. As the immune response progresses and diminishes, some B cells become memory cells, specialized to re-activate upon secondary exposure to antigen and secrete antibodies again.

Antibodies are also called immunoglobulins (Ig). There are several types of Igs including IgG, IgM, IgA, IgE, and IgD, each of which have structural similarity and serve a specific purpose in an immune response. IgM, for example, is a large, bulky molecule of approximately 970 kDa that is the first type of antibody secreted by a B cell when it encounters its antigen. IgA is shaped like two Ys connected at their stalks and is produced at mucosal surfaces. IgE is a Y-shaped molecule secreted in response to allergens. IgG is described in the next paragraph.

After a B cell encounters its antigen and secretes IgM, the B cell undergoes a process called class switching and begins to secrete IgG, a 150 kDa Y-shaped Ig made of four polypeptide chains, two heavy and two light chains. The stalk of the Y is called the crystallizable fragment (Fc), and the two shorter “prongs” are each called antigen-binding fragments (Fab). An IgG has two sites for antigen attachment, one at each end of the two Fabs. The sites of antigen attachment are comprised of complementarity determining regions (CDRs) and confer the antigen/epitope specificity of a given antibody. This specificity is unique to the antibodies produced by a single B cell or clone of B cells.

The structure of an antibody can also be described with respect to protein domains or regions. An IgG is made of four types of domains, three constant domains comprised of the Fc plus the lower portion of the Fab and one variable domain at the end of the Fab prongs. The variable domain encompasses the CDRs. Constant domains

on the heavy chain of an IgG are numbered (CH1, CH2, CH3), with CH3 existing at the bottom of the stalk of the IgG. The light chain constant regions are termed CL. Variable regions on the heavy and light chains are called VH and VL, respectively, and the combined heavy and light chain variable regions are termed Fv.

When an antigen is delivered to an individual, many B cells may be stimulated to produce antibodies against different parts of the antigenic protein. If one were to harvest these B cells, each antibody produced by different clones of B cells would have a unique set of CDRs, and each antibody may play one of many different functions in the clearance of the antigen from the body. Some antibodies may opsonize the foreign protein, binding to it and signaling to phagocytic cells to engulf the protein or organism on which the protein is found. This is called opsonization. At other times antibodies serve as flags to other immune cells such as natural killer (NK) cells to kill the cell harboring the antigen. Antibodies may also activate the complement cascade.

The antibodies produced by a single B cell or a genetically identical clone of B cells are called monoclonal antibodies. These antibodies have the same amino acid sequence and CDRs, and they attach to the same epitope on a given protein. In contrast, polyclonal antibodies are antibodies all targeted against the same antigen, but they are produced by multiple B cells or B cell clones. The epitopes of polyclonal antibodies are located on many different places on the same antigenic protein.

IgGs can be further divided into sub-classes which differ from each other slightly in the sequence of the Fc and their functions in the body. In humans, the four IgG subclasses are IgG1, IgG2, IgG3, and IgG4. Each sub-class differs in its affinity for Fc receptors on effector cells, complement cascade factor C1, the neonatal Fc receptor

(described below), etc. Fc-binding receptors are generally called Fc receptors (FcRs), with FcγRs being FcRs that bind to IgG as opposed to IgA (FcαRs) or IgE (FcεRs).

Different IgG subclasses mediate different IgG effector functions. IgG1, for example, has a high affinity for activating FcγRs, while IgG4 has a much lower affinity for these receptors. As such, immune cells such as NK cells that express activating FcγRs will bind to the Fc region of IgG1 and be stimulated to exert their effector functions. IgG4, however, has low affinity for activating FcγRs, so NK cell effector function is not induced by IgG4.

To make a monoclonal antibody in the laboratory, B cells are harvested from an individual or animal and are fused with a myeloma tumor cell to immortalize it. The resulting “hybridoma” cells are individually sorted into cell culture plates. They divide continuously forming a clone which secretes a unique monoclonal antibody into cell culture supernatant. The antibody can be purified from this supernatant and characterized in terms of its epitope and function.

Scientists and physicians have used monoclonal antibodies for decades in applications from the laboratory to the clinic. The first report of production of monoclonal antibodies by the hybridoma method described above was in 1975 [101]. From 1980 to 1982, monoclonal antibodies against human lymphoma-associated antigen were first administered to human patients to treat T cell lymphoma as well as gastrointestinal tumors. The Nobel Prize in Medicine was awarded in 1984 to Niels K. Jerne, Georges J.F. Köhler and César Milstein for “the specificity in development and control of the immune system" and the discovery of "the [hybridoma] principle for production of monoclonal antibodies.” In 1997, the FDA approved the first therapeutic monoclonal

antibody to treat B cell non-Hodgkin lymphomas, rituximab (Rituxan). Although the US patent for rituximab expired in 2015, it is still used today in the clinic. [102-105]

Proteins that are introduced from one species of animal into another are often immunogenic in the recipient animal and lead to production of antibodies against the foreign protein. Introduction of a mouse protein into a goat, for example, will likely cause the goat to develop an IgM and then IgG response to the mouse protein. This anti-species antibody production can be utilized by scientists to raise antibodies against human proteins for therapeutic use.

Of note, amino acid sequences of antibodies also differ among species. This means that introduction of a mouse IgG into a goat could cause the goat to develop anti-mouse IgG antibodies. Therefore, if scientists isolate an IgG with therapeutic potential from a mouse, it is possible that patients that receive that same IgG will develop an immune response against it, rendering it ineffective.

To prevent this from happening, recombinant DNA techniques can be used to produce chimeric antibodies. Chimeric antibodies are made by grafting the Fv portion of the desired, non-human IgG onto the constant regions of a human IgG. Rituximab, described above, is a chimeric IgG specific for human CD20 protein on B cells that was originally raised in a mouse injected with human CD20 protein [106-108]. During the development of rituximab, the murine constant regions of the most therapeutically promising mouse anti-human CD20 monoclonal antibody was replaced with human constant regions, making rituximab less immunogenic to patients.

So called humanized antibodies replace the non-human IgG constant regions and almost all of the Fv with human IgG sequence. The non-human CDRs, which

include several “framework” amino acids that play a necessary role in CDR-epitope binding, are left intact. The result is an even less immunogenic IgG. Fully human antibody sequences can either be directly isolated from humans or from mice genetically engineered to express human antibodies.

Genetic engineering can also be used to make antibody constructs, non-naturally occurring antibody-like proteins that maintain the antigen specificity of an antibody with or without the associated Fc-mediated effector function. One example of an antibody construct is an immunoadhesin. Immunoadhesins are proteins that are translated in a single reading frame as opposed to multiple reading frames as is the case for a full-length antibody. The immunoadhesin heavy and light chain sequences are connected by a linker peptide that allows the expressed protein to form the Y-shaped structure of an IgG. Immunoadhesins lack CH1, located on the lower portion of the prongs of the IgG, making the DNA sequence of an immunoadhesin shorter than that of a full-length IgG. Because the immunoadhesin maintains a normal stalk portion of the IgG Y-shape, it can still mediate FcR functions and has a half-life similar to full-length antibodies.

Another antibody construct is the scFv. Here, the VH and VL of an antibody are also translated in a single reading frame, connected by a linker peptide of 10-25 amino acids. *In vivo*, these proteins form into an Fv-like structure which can bind to an epitope. scFvs do not have an Fc, therefore they cannot mediate Fc effector functions. Their half-life in blood is also much shorter than that of full-length IgG.

In fact, IgG has an unusually long half-life in blood, 10 to 18 days, compared to other Igs. IgA or IgM have a half-life of only 5 to 6 days. This longer IgG half-life is due to the recycling function of the neonatal Fc receptor (FcRn). FcRn was originally

discovered in placenta where it transports antibodies from the blood of a mother to her fetus. It is expressed on many other tissues in the body where it plays various roles.

In the circulatory system, FcRn is expressed on the apical surface of endothelial cells lining blood vessels. These endothelial cells constitutively pinocytose plasma, which contains IgG as well as other Igs and proteins. The endosomes resulting from this pinocytosis are acidified and traffic to lysosomes where protein contents are normally degraded. However, IgG escapes this fate. As endosomes are acidified, IgG binds to FcRn in the lumen of the endosome. The FcRn-IgG complexes are then sorted into recycling endosomes which transport the IgG back to the apical plasma membrane. After the recycling endosome fuses with the plasma membrane, IgG dissociates from FcRn at physiological pH. This recycling function of FcRn is what gives IgG a long half-life in the blood. [109]

Section References

Male, D.K., *Immunology*. 8th ed. 2013, Elsevier/Saunders: United States, 472 pp.[110]

Murphy, K.P., et al., *Janeway's Immunobiology*. 8th ed. 2012, New York: Garland Science. 868 pp. [111]

AAV-mediated delivery of antibodies

IgG antibodies are proteins coded by genes. The human IgG heavy and light chain DNA sequences are approximately 1345 base pairs (bp) and 645b bp long, respectively. An antibody gene sequence can easily fit into an AAV genome along with the requisite regulatory elements. Thus, AAV vectors can be used to deliver the gene for

a monoclonal antibody to patients so that the patients' own cells will produce the therapeutic antibody *in vivo*. [112]

Expression cassettes designed for whole antibody gene transfer by AAV vectors must be engineered to express both the heavy and the light chains of an antibody. This can be accomplished from the same expression cassette in several ways. One method is to place an internal ribosome entry site (IRES) between the heavy and light chain sequences in the expression construct. However, for successful expression of a whole antibody, it is necessary for the light and heavy chain proteins to be produced at a 1:1 ratio. Greater expression of light chain over heavy chain, for example, can lead to intracellular toxicity as well as pathologic deposition of complexes formed by aggregation of light chain in various organs. As the sequence upstream of the IRES in the expression construct may be translated more efficiently, using an IRES may cause unequal production of heavy and light chains. [113]

Instead, using a so-called 2A peptide motif between the light and heavy chain sequences allows for translation of the heavy and light chains together followed by a "self-cleavage" event during translation. 2A motifs are derived from viruses. For example, F2A was derived from foot-in-mouth virus. Self-cleavage of the 2A polypeptide occurs between a glycine and proline residue at the C terminus. The addition of a furin recognition sequence upstream of the 2A but downstream of the first gene allows removal of the 2A residues from the upstream gene by furin enzymatic cleavage. Using this technique, equal ratios of heavy and light chains are produced, increasing the efficiency and safety of antibody gene translation over the use of an IRES. [113]

An alternative to expressing a whole antibody is expressing an antibody construct, many of which are transcribed in a single reading frame and form the correct conformation *in vivo*. These antibody constructs may include the immunoadhesin or scFv, described above.

Using AAV vectors to deliver monoclonal antibodies to patients is not a novel concept. Balazs et al. and Johnson et al. pursued this technique to introduce antibodies to animal models for "vectored immunoprophylaxis" against HIV. This may be conceptualized as an *in vivo* passive vaccination. Using the gene sequence of a broadly neutralizing antibody to the human immunodeficiency virus (HIV) as a transgene, AAV vectors were manufactured for intramuscular (IM) delivery. Muscle cells transduced by the vector would produce the anti-HIV antibody constitutively. The antibody would distribute into the circulatory system and throughout the body, thus conferring protection from HIV infection. [114, 115]

In one report, HIV-susceptible humanized mice were injected intramuscularly (IM) with an AAV vector containing a broadly-neutralizing HIV antibody transgene. The full-length antibody was detected in mouse serum, and subsequent challenge with very high doses of replication-competent HIV yielded no successful infection. A later report described intramuscular administration in NHPs of 2e13 GC of an AAV vector with an anti-simian immunodeficiency virus (SIV) antibody transgene. Subsequent IV challenge with virulent SIV yielded no productive infection; all animals were completely protected. [114, 115] Going forward, AAV delivery of antibodies thus shows promise for a variety of gene therapy applications.

CHAPTER 4

Human epidermal growth factor receptor 2 (HER2)

Human epidermal growth factor receptor 2 (HER2) is a 185 kDa membrane-associated tyrosine kinase that is expressed on cells throughout the body. It is one of four members of the HER family of proteins which serve to transduce extracellular growth signals and thus regulate cell survival and differentiation. HER2 has no known ligand, unlike other members of the HER family of proteins which bind such ligands as neuregulin (NRG) and extracellular growth factor (EGF, hence the more common name of the HER1 protein, extracellular growth factor receptor or EGFR). Rather, the native conformation of HER2 resembles that of other ligand-bound HER proteins. [116-124]

HER2 signal transduction begins with heterodimerization of ligand-bound members of the HER family with HER2, the most potent combination of which is the HER2/HER3 heterodimer. In normal cells, HER2 may homodimerize relatively infrequently. These dimerization events lead to auto-phosphorylation and recruitment of intracellular adapter proteins at the plasma membrane. This, in turn, leads to activation of master regulators of cell growth and survival, including the phosphatidylinositol 3-kinase/Akt (protein kinase B)/NFkB pathway and the mitogen-activated protein kinase (MAPK) pathway. HER2 signal transduction is also associated with organogenesis during fetal development and with tissue maintenance in adults. [116-124]

Overexpression of HER2 due to gene amplification is oncogenic. Cancer cells that overexpress HER2 are termed HER2+ and may have up to 2- to over 20-fold more HER2 expression than normal cells [125, 126]. As such, HER2 homodimerization occurs more frequently in these cells, leading to greater ligand-independent growth signal

transduction. Several types of cancers may overexpress HER2 including breast, stomach, uterine, and ovarian.

Breast cancers are of particular interest with respect to HER2 overexpression, as approximately 20% of these cancers are HER2+, portending more aggressive disease with a poorer prognosis than HER2- cancer. Whether or not a tumor is deemed HER2+ is determined either by a tumor HER2 IHC status of 3+ or greater, a HER2 gene copy number of 6 or more by fluorescence *in situ* hybridization (FISH), or a HER2/CEP17 ratio of greater than 210 by FISH on chromosome 17. [117, 118, 120, 125-133]

HER2 and trastuzumab (Herceptin®)

Trastuzumab was the first therapeutic monoclonal antibody to target HER2. It was developed by Genentech, and in 1998 it was approved for first-line treatment of metastatic HER2+ disease in combination with paclitaxel chemotherapy or as a second- or third-line agent by itself. In the 1980s, scientists at Genentech and the National Cancer Institute discovered that HER2 overexpression was linked to breast cancer and that cancers in which HER2 was overexpressed led to more aggressive disease, as described above. [134] Genentech then developed a series of monoclonal antibodies raised in mice against human HER2. One of these mouse anti-human HER2 IgGs, termed 4D5, bound to the extracellular domain IV of HER2 and was able to suppress the growth of HER2+human cancer cells both *in vitro* and in murine xenograft tumor models. [118, 119, 135, 136]

To lessen the chance that 4D5 would induce an anti-mouse IgG immune response in patients, it was humanized as described above in “Antibodies” in Chapter 3.

Briefly, the antigen-binding portions of 4D5, including the CDRs, were inserted into the framework of a human IgG1. The resulting “humab4D5-8” antibody is what is known today as trastuzumab. Trastuzumab was found to bind to HER2+ cancer cells with a dissociation constant of 0.1 nM. [118, 137, 138]

Trastuzumab has become part of the standard of care for patients with HER2+ primary and metastatic breast cancer. It is also approved for the treatment of HER2+ gastric cancer. Trastuzumab may be administered as adjuvant to chemotherapy, meaning it is administered along with chemotherapy after surgery or radiation to reduce the risk of recurrence or metastasis, or as neoadjuvant therapy, meaning as an agent that is used to shrink a tumor before surgical resection. It is usually given at a loading dose of 4 mg/kg body weight and at 2 mg/kg body weight for the duration of therapy. This regimen maintains the trastuzumab serum trough concentration at around 10-20 µg/mL in serum. [127]

Many clinical trials were initiated beginning in the 1990s to evaluate trastuzumab as an agent to treat HER2+ metastatic breast cancer, both as a single agent and along with chemotherapy. To evaluate the safety of trastuzumab and its pharmacokinetics, phase I clinical studies were conducted in patients with metastatic HER2+ breast cancer refractory to treatment. In one study, patients were dosed IV either a single time or weekly with 10-500 mg of trastuzumab along with cisplatin chemotherapy. No serious adverse events (SAEs) related to trastuzumab administration were reported. A maximum tolerated dose was not reached in this trial, and the half-life of trastuzumab in blood at the 500 mg dose was determined to be 2 weeks. [118, 139]

Phase II studies to evaluate the efficacy of trastuzumab were initiated with trastuzumab as a single agent in patients with metastatic HER2+ breast cancer. The first phase II trial involved 43 evaluable patients. The trastuzumab dose was 250 mg in the first week and 100 mg every week subsequently for 10 weeks. One patient in this study achieved a complete response to therapy for 6 years, and 4 patients achieved a partial response. The combination of complete responders and partial responders represents the overall response rate to treatment, in this study equal to 11.6%. 37% of the patients experienced a minimal response to treatment, and disease progressed in the remaining 22 individuals. The median time to disease progression after initiation of therapy was 5.1 months [118, 138, 140, 141]

Another phase II study administered trastuzumab with cisplatin chemotherapy to 39 patients with HER2+ metastatic breast cancers that were treated with previous chemotherapy but had relapsed. The dose of trastuzumab was the same as the single-agent phase II trial above. There were 37 evaluable patients in this trial. Though none had a complete response, 9 patients experienced a partial response. 3 patients had a minor response. Disease stabilized in 6 patients and progressed in 19 patients. The overall response rate was thus calculated to be 24.3%. The median survival was 11 months, and the median response duration was 5.3 months. [118, 138]

The largest phase II trastuzumab clinical trial was an open-label, single-arm study conducted across 54 centers. 222 patients were included who had been treated with one or two previous cytotoxic chemotherapy regimens but in whom disease had relapsed. In this trial, trastuzumab dose was calculated based on body weight of the patients at a 4 mg/kg loading dose (first dose) and a 2 mg/kg maintenance dose (subsequent doses). Patients also received chemotherapy in the form of doxorubicin or

epirubicin plus cyclophosphamide or, if patients had already received anthracycline chemotherapy, paclitaxel. Of 204 evaluable patients, eight achieved a complete response and 26 achieved a partial response. The overall response rate was calculated to be 15%. 12 patients had a minimal response to trastuzumab treatment and 62 had stable disease. The rest of the patients experienced disease progression. The median duration of response to therapy was determined to be 9.1 months, and median survival was 13 months.

Interestingly, patients whose disease showed greater HER2 overexpression by immunohistochemistry responded better to trastuzumab therapy in this trial. Average serum trastuzumab peak and trough concentrations among all patients were calculated to be 100.3 µg/mL and 25 µg/mL, respectively. Mean trough trastuzumab concentrations in patients with complete responses were higher at weeks 7 and 8 of therapy (70.3 µg/mL) as opposed to serum trastuzumab concentration in patients with partial responses (54.8 µg/mL). The half-life of trastuzumab in this study was calculated to be 6.2 days. [118, 138, 142]

Following these phase I and II studies, phase III randomized, placebo-controlled, multi-center trials were conducted in over 900 women with HER2+ metastatic disease. In the pivotal phase III trial, 469 patients were included with a median follow-up time of 29 months. These women had received prior chemotherapy. The trastuzumab dose was 4 mg/kg in the first week followed by 2 mg/kg in subsequent weeks. More patients who received trastuzumab plus chemotherapy in this trial were still living one year after initiation of treatment (79%) compared to women who received chemotherapy only (68%). Patients who received trastuzumab also had a significantly longer median survival, 25.4 months compared to 20.3 months in patients who received chemotherapy

alone. The approximate increase in median survival was calculated to be 25%. Time to disease progression was longer in patients in the trastuzumab arm of the trial, 7.6 months compared with 4.6 months in the chemotherapy arm. The overall response rate was higher in patients who received trastuzumab and chemotherapy, 49% compared to 32% in patients who received chemotherapy alone. [143-145]

Further phase III trials were conducted in over 3500 patients with operable, node positive HER2+ breast cancer. These studies compared treatment with 1 year of adjuvant trastuzumab plus chemotherapy (doxorubicin plus cyclophosphamide followed by paclitaxel) to chemotherapy alone. When analyzed together, the studies indicated that patients who received adjuvant trastuzumab in addition to chemotherapy experienced recurrence of their tumors at a 52% lower rate than patients who received chemotherapy alone. The risk of death after 24 months of follow-up was calculated to be 33% lower in patients in the trastuzumab arm. [146]

Even after metastatic HER2+ breast cancer progresses, trastuzumab treatment has been shown to extend median overall survival as demonstrated in five randomized clinical trials (114, 118-123). Additionally, a study of 247 patients who continued to receive trastuzumab after disease progression found it to be well-tolerated without increased incidence of adverse events such as cardiotoxicity (170).

Following the approval of trastuzumab by the FDA in 1998, the repertoire of targeted treatments for HER2+ cancer has continued to expand. One of these drugs is a modified trastuzumab treatment called trastuzumab emtansine (Kadcyla). Kadcycla is trastuzumab conjugated to the cytotoxic agent emtansine (DM1), an inhibitor of microtubule assembly. Trastuzumab emtansine takes advantage of the ability of

trastuzumab to home to cells that overexpress HER2, allowing for localized, effectively concentrated delivery of emtansine to tumors.

In clinical trials of Kadcyla, patients with locally advanced or metastatic breast cancer previously given trastuzumab and chemotherapy were included. A median survival was not reached in patients who received trastuzumab emtansine, but a median survival of 23.3 months was reported in patients that received a chemotherapeutic regimen of capecitabine and lapatinib (described below). The overall response rate in patients that received trastuzumab emtansine was 43.6% as opposed to 30.8% of patients who received chemotherapy. [147]

Another HER2-targeted agent is the monoclonal antibody pertuzumab. Pertuzumab works synergistically with trastuzumab, binding to the extracellular domain of HER2 to disrupt HER2/HER3 dimerization. In patients with operable HER2+ breast cancer, adding pertuzumab to trastuzumab therapy increases the duration of disease-free survival.[148]

Finally, lapatinib is a small molecule inhibitor of HER1 and HER2, targeting the intracellular domain of these proteins. It is used to treat patients with metastatic HER2+ breast cancer and is discussed further in Chapter 6 “HER2+ breast cancer brain metastases.”

The mechanisms of action of trastuzumab

Therapeutic monoclonal antibodies targeted against cancer may exert their effects in many different ways. The first FDA-approved monoclonal antibody developed against cancer, rituximab, was shown to work mainly by activation of the complement cascade, leading to tumor cell lysis. However, its other mechanisms of action have been

elucidated in the literature, including interruption of cell signaling and immune cell-mediated cytotoxicity. [149]. The various methods by which trastuzumab exerts its anti-tumor activity have also been extensively studied.

The main mechanism of action of trastuzumab is mediating a process called antibody-dependent cell-mediated cytotoxicity (ADCC). Trastuzumab bound to HER2 on a tumor cell is engaged by an NK cell possessing an activating FcR, such as FcγRIIIa. The activating FcR binds to the Fc portion of trastuzumab, inducing the NK cell to release cytotoxic proteins such as perforins, which form holes in the tumor cell membrane, and granzymes, proteases which activate apoptosis of the targeted cell, leading to tumor cell death. Other immune cells such as macrophages also possess activating Fc receptors and can undergo antibody-dependent cell-mediated phagocytosis (ADCP), a process by which the macrophage devours the trastuzumab-decorated tumor cell. *In vivo*, NK cells are the main effector cells governing trastuzumab-mediated cytoxicity.[150]

Several studies have demonstrated that trastuzumab mediates ADCC both *in vitro* and *in vivo*. In 2001, Clynes et al. reported failure of trastuzumab treatment to arrest growth of HER2+ xenografted tumors both in nude mice lacking activating FcRs and in mice treated with an antibody to disrupt Fc binding to FcRs. It was determined that an activating FcR is necessary for trastuzumab to exert an anti-tumor response. [151]

Gennari et al. studied peripheral blood mononuclear cells (PBMCs) from breast cancer patients treated with trastuzumab as a single agent in the neoadjuvant setting, with surgical resection of tumor 7 days after trastuzumab administration. *In vitro* ADCC assays were performed using patient serum from before or after trastuzumab treatment

applied to HER2+ target cells. This was followed by application of autologous PBMCs. In most patients who had received trastuzumab therapy, there was significant killing of HER2+ target cells by autologous PBMCs. Interestingly, using PBMCs from patients with a better clinical response to trastuzumab therapy led to a higher degree of tumor cell death *in vitro*. Additionally, tumor samples from patients treated with trastuzumab were unable to be stained histologically by trastuzumab conjugated to horseradish peroxidase (HRP), suggesting that available antigen binding sites on the tumor cells were saturated by already-bound trastuzumab [152].

Arnould et al. used histology techniques to study immune cell infiltrates in tumor samples of patients also treated with trastuzumab in the neoadjuvant setting. 23 patients who received trastuzumab and docetaxel for 17 weeks underwent surgical resection of the primary tumor after the last cycle of combined trastuzumab and docetaxel treatment. Case-matched controls received docetaxel without trastuzumab. Pathologists analyzed tumor slides for the presence of B cells, T cells, macrophages, dendritic cells, and NK cells. Trastuzumab treatment resulted in an increase in the number of NK cells associated with the tumor and increased expression of granzymes and TiA1, a pro-apoptotic protein, in tumor-infiltrating lymphocytes. [153]

Trastuzumab has been shown to exert its anti-tumor effect by other mechanisms as well. Trastuzumab blocks homodimerization of the HER2 protein, preventing signal transduction and leading to inhibition of pathways associated with cell survival. For example, when tumor cells are exposed to trastuzumab *in vitro*, MAPK and PI3K/AKT cell growth-associated pathways are downregulated. [150, 154, 155]

Trastuzumab has also been shown to prevent cleavage of the extracellular domain of HER2 on tumor cells, which occurs normally and is mediated by 5-aminophenymercuric acetate matrix metalloproteinase activator. The remaining p95 membrane-associated protein is able to transduce growth signals by itself. [155-157]

Trastuzumab has also been shown to inhibit tumor-associated angiogenesis. Tumors normally secrete vascular endothelial growth factor (VEGF), and increased VEGF expression is associated with HER2 overexpression. In a xenograft model, trastuzumab administration led to decreased tumor vascularization as well as normalization of tumor vascular permeability, diameter, and volume. VEGF mRNA expression was also decreased in trastuzumab-treated tumor cells in this experiment. [158]

Finally, HER2 signaling is important for activating DNA repair pathways. Treating cancer cells with trastuzumab downregulates these DNA repair pathways. Studies by Pietras et al. in 1998 and 1999 in murine xenografts showed a 35-40% reduction of cisplatin-induced DNA damage *in vivo* after trastuzumab treatment as well as prevention of a slow S phase necessary for tumor cells to repair radiation-induced DNA damage [159, 160].

Trastuzumab-related cardiotoxicity

A small number of patients who received trastuzumab in the pivotal phase III clinical trial described above developed cardiac dysfunction. Those who received concurrent anthracycline chemotherapy, such as doxorubicin (Adriamycin) were particularly affected. 27% of patients who received trastuzumab plus an anthracycline

developed systolic dysfunction compared with 8% of patients who received an anthracycline alone.

At first, it was believed that the combination of trastuzumab and anthracyclines led to this cardiac dysfunction. However, endomyocardial biopsies of patients with trastuzumab-associated cardiotoxicity did not show the same ultrastructural changes known prior to be associated with anthracycline-associated cardiotoxicity. The dose of trastuzumab that a given patient received also did not correlate with the development of cardiotoxicity. Later studies conducted in patients without previously diagnosed cardiovascular disease who did not receive anthracyclines simultaneously with trastuzumab still reported cases of cardiotoxicity. In these reports, the risk of trastuzumab-associated heart failure was 3.9%. [116, 161-163]

Although the exact mechanism of trastuzumab-induced cardiotoxicity is not fully understood, scientists have discovered that cardiomyocytes require some baseline level of HER2 signaling for normal function [161]. Mouse models were developed with conditional knock-outs of HER2 and HER4 in ventricular tissue. By 8-12 weeks of age, these mice had already developed dilated cardiomyopathy, and the cardiomyocytes of these mice were more susceptible to anthracycline-induced death. NRG, which binds to HER4, was found to play a large role in the recovery of cardiomyocytes after stress. HER2 signaling was also suggested to be involved in formation and maintenance of the conduction system of the heart, contractility, regulating myofilament architecture, glucose metabolism, and angiogenesis. [162, 164-168]

Extensive research has been performed to determine a patient's risk for developing trastuzumab-associated cardiotoxicity. A 2012 meta-analysis of multiple

large clinical trials (11,911 women total) indicated that trastuzumab treatment was associated with an increased risk for severe heart failure (2.5 vs. 0.4%) and a reduction in left ventricular ejection fraction (LVEF), a measure of heart function. This trastuzumab-associated reduction in LVEF manifests asymptomatically in the majority of patients who experience it. [169]

The National Adjuvant Breast and Bowel Project (NSABP) B31 7-year follow-up found that patients who received trastuzumab had a 4% 7-year cumulative risk of a cardiac event compared to a 1.3% cumulative risk for patients who did not receive trastuzumab. A cardiac event was defined as definite or probable cardiac death, heart failure (dyspnea with normal activity or at rest) with an LVEF decline of greater than 10% from baseline, or an LVEF of <55%. [170]

The Herceptin Adjuvant Trial (HERA, BIG1-01) 8-year follow-up compared patients who received 2 years of trastuzumab (n=1673), 1 year of trastuzumab (n=1682), or observation (n=1744). Congestive heart failure was reported in 0.8%, 0.8%, and 0% of patients, respectively. A significant LVEF decrease was reported in 7.2%, 4.1%, and 0.9% of these patients, respectively. Severe congestive heart failure and cardiac death were found to be rare in all study arms. Of patients who experienced a significant decrease in LVEF, acute recovery was reached in 87.5% of patients who received 2 years of trastuzumab treatment and 81.2% of patients who received 1 year of trastuzumab treatment. [171]

Another phase III trial reported that 33 patients who developed a cardiac event (most often an asymptomatic decline in LVEF) continued trastuzumab treatment. 85% of these patients' cardiac function eventually improved or remained the same. This study

also found that 75% of patients with symptomatic cardiotoxicity experienced reversal of symptoms when treated with standard heart failure therapy (including, but not limited to, angiotensin converting enzyme inhibitors, aldosterone antagonists, angiotensin receptor blockers, or beta blockers) [161].

A retrospective review of 49 patients with trastuzumab cardiotoxicity drew similar conclusions. In this study, 79% of patients who experienced cardiotoxicity subsequently recovered with appropriate heart failure therapy and withdrawal of trastuzumab. Of these patients, 26 resumed trastuzumab treatment. Only 10 patients developed cardiac dysfunction again, and 5 of these patients continued to receive trastuzumab therapy, with a slight decrease in LVEF as the only indication of cardiotoxicity. [172]

In another study, risk factors associated with trastuzumab cardiotoxicity were found to be patient age greater than 50 years, previous or concurrent use of anthracycline chemotherapy, preexisting cardiac dysfunction, and overweight (>30) body mass index. Antihypertensive therapy, diabetes, valvular heart disease, and coronary artery disease were not found to increase the risk of cardiotoxicity [173].

Other HER2-targeted chemotherapies have also been reported to cause cardiotoxicity. Pertuzumab is another monoclonal antibody that targets a different epitope of HER2 than trastuzumab, and it is often co-administered with trastuzumab. In the CLEOPATRA trial, 8.3% of patients who received placebo, trastuzumab, and docetaxel experienced decreased LVEF compared with 4.4% who received pertuzumab, trastuzumab, and docetaxel. The cardiotoxicity of lapatinib has also been studied. A meta-analysis of 49 trials in (n=3689 patients total) concluded that 1.4% of patients who

received lapatinib experienced asymptomatic cardiac events and 0.2% of patients experienced congestive heart failure. [173]

In summary, trastuzumab cardiotoxicity occurs in a small but significant percentage of patients treated with trastuzumab. The exact percentage varies depending on the study but ranges from less than 1% to about 10%. In the majority of these patients, cardiotoxicity manifests as an asymptomatic decline in LVEF, with many fewer developing fulminant heart failure. The occurrence of cardiotoxicity is not related to the dose of trastuzumab that patients receive. Instead, cardiotoxicity is more likely to occur if a patient received or is receiving anthracycline chemotherapy or if they have preexisting cardiac dysfunction such as a low baseline LVEF. Older and overweight individuals are also at higher risk for developing cardiotoxicity. Most patients who experience cardiotoxicity recover baseline cardiac function after trastuzumab is withdrawn and/or standard heart failure drugs are administered. A large subset of the patients who experience trastuzumab cardiotoxicity will resume trastuzumab treatment and experience no further cardiac episodes. The mechanism of cardiotoxicity is not fully understood, but it known that HER2 signaling is linked to cardiomyocyte survival. Importantly, studies have shown that long-term administration of trastuzumab is generally well-tolerated.

CHAPTER 5

HER2+ breast cancer brain metastases (BCBM)

Compared to other subtypes of breast cancer, HER2+ disease has the second poorest overall prognosis, tends to be more aggressive, and has a higher propensity to metastasize to other organs, including the brain [119, 125]. Brain metastases are a devastating sequela of HER2+ breast cancer, with reports indicating an incidence of 15-35.2% among patients with HER2+ disease compared to 10-16% of patients with any type of breast cancer. [129, 174-193] Interestingly, autopsies of patients with any type of breast cancer and no clinical evidence of brain metastases have found that up to 30% of patients have pathologically evident metastases or micrometastases at death [161, 194-196]. 80% of brain metastases are detected after the diagnosis of systemically metastatic disease. There is a 75% chance that if primary breast tumor is HER2+, brain metastases will also be HER2+. [127, 128, 197]. In most retrospective studies of patients presenting with breast cancer brain metastases (BCBM), CNS disease was discovered after clinical reports of headache or neurological deficits due to the mass effect of brain tumors. [194]

Approximately 17,000 women every year will be diagnosed with HER2+ BCBM in the US, and the median survival of these patients will be 10-13 months from the time of diagnosis [174], although the RegistHER prospective observational study results published by Brufsky et al report a median survival of 17.5 months [198]. Other studies indicate that only 20% of HER2+ BCBM patients will be alive a year after diagnosis of CNS disease and that these patients these patients tend to be younger (less than 50 years old) and have 2 or more metastatic foci outside of the CNS [198-200]. A reported

41-52% of patients die as a result of BCBM progression as opposed to other causes including progression of systemically metastatic disease. [174, 194, 198, 201-204]

A small percentage of patients with HER2+ BCBM will present with leptomeningeal carcinomatosis (LC), a rare type of brain metastasis with that accounts for 5% of patients with HER2+ BCBM [181, 204, 205]. In LC, tumor cells cloak the brain, spreading along the leptomeninges, a term that refers to the pia and arachnoid mater, which are membranous coverings of the brain between which flows CSF. Patients with LC have an even poorer prognosis than those with focal metastases, with median overall survival ranging from 2 to 5.2 months from the time of LC diagnosis. Most patients survive less than a year from the time of LC diagnosis. [204-209]

Current treatments for HER2+ BCBM do not confer substantial survival benefit. The presence of the BBB excludes many chemotherapeutics and biological therapies that are used successfully to treat systemically metastatic disease, including anti-HER2 monoclonal antibodies such as trastuzumab. The standard of care for patients with HER2+ BCBM depends on the number of tumor foci or whether the patient has LC. Patients with one or a limited number of focal metastases will typically undergo neurosurgical resection of their tumor(s) along with systemically-administered chemotherapy and/or trastuzumab plus pertuzuamb, despite the poor penetration of these treatments into the CNS [198]. A response to single-agent IV trastuzumab therapy is only seen in 11-15% of patients with HER2+ BCBM [140, 210].

If feasible, stereotaxic radiosurgery, a high-energy type of focused radiation therapy, may be used against HER2+ BCBM, particularly in patients with a limited number of metastases or for whom surgical resection is contraindicated. If stereotaxic

radiosurgery is not available or if surgical resection is impossible, patients with multiple metastases will undergo whole brain radiation therapy, which can improve survival and reduce the frequency of intracranial relapse from 80% to 50% [185]. However, whole brain radiation therapy can carry a set of side effects including decreased IQ, cognitive deficits, urinary incontinence, and dementia [211]. Neither radiation treatment nor chemotherapy improves prognosis for patients with leptomeningeal disease [186, 193, 206]. All too often, patients with systemically metastatic HER2+ disease receiving therapies including intravenous trastuzumab therapy will experience regression in visceral disease in response to treatment while CNS disease simultaneously progresses. [211]

Patients with HER2+ primary or systemically metastatic disease treated with trastuzumab are at higher risk for developing brain metastases. This was discovered as a result of post-hoc anslysis of clinical trials including the NSABP B-31 and HERA studies mentioned above. In these trials, CNS metastases were recorded more frequently in patients who received trastuzumab therapy as opposed to control treatments.

A few factors have been postulated to account for the increased incidence in HER2+ BCBM over the past several decades among patients who have received trastuzumab to treat visceral disease. The increasing efficacy of chemotherapeutic regimens and anti-HER2 agents to treat systemically metastatic HER2+ breast cancer and the corresponding increase in overall survival for these patients may allow time for the outgrowth of brain metastases that in the past may have remained undetectable before death. Additionally, poor penetration of trastuzumab into the CNS due to its size and thus a lack of HER2 blockade in HER2+ tumor deposits that are unappreciable

clinically or by imaging modalities may contribute to the increasing incidence of HER2+ BCBM. [129, 174, 177, 186, 193, 194, 198, 212]

For patients with HER2+ BCBM, the small molecule lapatinib offers some clinical benefit. Lapatinib is an inhibitor of HER1 and HER2, targeting the intracellular domain of these proteins. In the LANDSCAPE phase II trial, which included patients with HER2+ BCBM that were previously untreated, 65.9% of patients experienced a partial response to lapatinib plus capecitabine. However, one phase III trial, called CEREBEL, studied the effect of lapatanib on the incidence of CNS metastases in patients with HER2+ systemically metastatic disease who did not yet have CNS metastases. Patients were treated either with lapatinib plus capecitabine or trastuzumab plus capecitabine. The study did not find a significant difference between the two treatment regimens in terms of incidence of CNS disease, progression-free survival, or overall survival. Other phase III studies with lapatinib are ongoing as of October 2017. [213, 214] Additional small molecule inhibitors of HER2 which may cross the blood-brain barrier to target HER2+ brain metastases are in development [215].

Intrathecal trastuzumab as HER2+ BCBM treatment

When administered IV, trastuzumab penetrates poorly into the CNS. Pestalozzi et al. illustrated this point in 2000, describing weekly IV trastuzumab administration in a patient with LC. On week one, a loading dose of 240 mg was administered. The following week, 120 mg trastuzumab was administered, and the patient's serum and CSF were collected for ELISA. The trastuzumab concentration was determined to be 61.392 µg/mL in serum and 0.210 µg/mL in CSF. Another week later, another 120 mg

trastuzumab was administered again, and serum and CSF were collected for ELISA. Serum trastuzumab was measured to be 70.336 µg/mL and CSF trastuzumab to be 0.212 µg/mL [216]. This phenomenon is not limited to humans. In a preclinical study in mice by Abukayyas et al., a radio-labeled human IgG1 antibody was administered intravenously. The resulting brain-to-blood ratio of IgG in was determined to be 0.7%. [217, 218]

Because IV trastuzumab does not cross the BBB effectively, many clinicians have administered trastuzumab intrathecally to patients with HER2+ BCBM "off-label." Table 1, found in Chapter 6, lists case reports of patients with HER2+ BCBM, either LC or intraparenchymal disease. The table includes trastuzumab dose, dose frequency, indicated concurrent treatments, degree of clinical response, duration of response, adverse events (AEs) or serious adverse events (SAEs), and overall survival. For most of these patients, IT trastuzumab provides some clinical benefit. No AEs or SAEs have been reported related to IT trastuzumab administration.

To examine the significance of the clinical benefit of IT trastuzumab, Zagouri et al. conducted a meta-analysis in 2013 of patients with LC who received IT trastuzumab treatment. The analysis concluded that overall survival increases from 5.9 months in historical controls to 13.5 months in patients who received IT trastuzumab. Additionally, 68.8% of patients experienced significant clinical improvement. [219]

Two case reports have reported that IT trastuzumab can provide clinical benefit to patients with intraparenchymal disease. Bousquet and colleagues gave IT trastuzumab to a patient with HER2+ cerebellar and epidural breast cancer metastases, resulting in a six-month halt in disease progression [220]. Colozza and colleagues

describe a patient with HER2+ intraparenchymal cortical metastases who was treated for 19 months with IT trastuzumab [221]. Both patients were still alive at the time of publication.

As a result of these successful reports, several clinical trials have been initiated to examine the effect of IT trastuzumab in patients with LC. Table 2 in Chapter 6 lists these ongoing trials, compiled from clinicaltrials.gov. Of note, IT trastuzumab is dosed in these trials within the range of 30-150 mg per administration. Interestingly, trastuzumab is not the only monoclonal antibody to show promise after IT administration for CNS malignancy. Rituximab administered IT has been tested in two phase I clinical trials and has shown benefit for patients with CNS B cell lymphoma [222, 223]. The anti-epidermal growth factor receptor (EGFR) antibody panitumumab has also administered to single a patient with EGFR mutant lung adenocarcinoma that metastasized to the brain [224].

Although IT trastuzumab has shown promise, it is likely that the normal, rapid clearance of CSF compromises the efficacy of IT trastuzumab. In a study by Braen et al., cynomolgus macaques were given 3mg or 15mg trastuzumab by intrathecal infusion, with 3 macaques in each dose group. The mean concentration of trastuzumab in CSF in the 3 mg dose cohort one day after trastuzumab infusion was around 10,000 ng/mL. One week after infusion, the trastuzumab concentration in CSF was around 50 ng/mL. In the 15 mg dose cohort, the mean concentration of trastuzumab in CSF one day after infusion was around 20,000 ng/mL, and one week after infusion, the trastuzumab concentration was around 200 ng/mL [225].

In the report by Bousquet et al where IT trastuzumab was administered to a patient with HER2+ cerebellar and epidural BCBM, the half-life of trastuzumab in CSF

was calculated to be around 12 hours. The half-life of trastuzumab in blood has been calculated by multiple studies. These include a trastuzumab half-life of 8.3 days after a 100 mg IV dose in 45 patients [140], 28.5 days after a 2 mg/kg IV dose in 476 patients [226], and 6 mg/kg after the 12^{th} IV dose in 15 patients [227]. Of note, the clinical trial conducted by Gutierrez et al. listed in Table 2 aims to achieve a CSF trastuzumab concentration of 30 µg/mL to maximize potential therapeutic effect.

In summary, HER2+ BCBM are a devastating diagnosis that leave patients with few options for treatment. IT administration of trastuzumab has shown promise in several case reports, and clinical trials are being conducted to evaluate its efficacy in an official setting. Still, it is possible that combining an intrathecal trastuzumab treatment approach with AAV gene therapy techniques may improve survival for patients with HER2+ BCBM. It is also conceivable that an IT AAV gene therapy to express trastuzumab behind the BBB may serve as prophylaxis for patients with systemically metastatic HER2+ disease at risk for developing CNS disease.

CHAPTER 6

Intrathecal AAV9.trastuzumab tumor prophylaxis and treatment in a murine xenograft model of HER2+ breast cancer brain metastases

Introduction

Breast cancer is the most commonly diagnosed malignancy in women in the US with an estimated 252,710 new cases in 2017 [228]. Approximately 20% of breast cancers overexpress HER2 and are considered to be more aggressive and more likely to metastasize to the brain than other breast cancer subtypes [175, 191, 229]. About 30% of patients with metastatic HER2+ breast cancer will develop BCBM [174, 178, 193, 230]. The registHER prospective study of patients with newly-diagnosed HER2+ metastatic breast cancer found that 37.3% of the 1012 patients studied developed brain metastases within 10.8 months from the initial diagnosis of metastatic disease [198]. Brain metastases can significantly lower patient quality of life by inducing nausea, sensory loss, aphasia, motor deficits, ataxia, seizures, stroke, and paralysis [175, 231-233]. The median age at diagnosis of HER2+ BCBM is 48 years [234], and the incidence of HER2+ BCBM is rising [191]. It has been suggested that this increase is due to many factors. Targeted, effective therapies for HER2+ tumors in the periphery have increased the duration of patient survival, thereby allowing adequate time for outgrowth of brain metastases that would have otherwise remained subclinical before death [231, 235]. Many of these therapies, including biological therapeutics, do not reach adequate concentrations in cerebrospinal fluid (CSF) after systemic administration [216, 236].

Current standard of care treatments for HER2+ BCBM are invasive, can cause cognitive impairment, and provide suboptimal survival benefit. Patients often undergo a combination of neurosurgical tumor resection, stereotaxic radiosurgery, whole brain

radiation therapy, systemic and/or intrathecal chemotherapy, steroids, or anti-HER2 agents [175, 231, 235]. Even with these treatments, survival from the time of diagnosis of HER2+ BCBM ranges from 3 to 25 months with a median of 10-13 months [174, 188, 198, 237]. Clearly, there is an unmet need for more effective, targeted treatments for patients with HER2+ BCBM.

Trastuzumab (Herceptin®, Roche) is a humanized monoclonal antibody (mAb) directed against HER2 that extends survival of patients when used with chemotherapy to treat primary and systemically metastatic HER2+ disease [174, 210, 238]. However, trastuzumab does not cross the intact blood-brain barrier to treat central nervous system (CNS) tumors [175, 229]. Additionally, the CSF concentration of trastuzumab after intravenous (IV) administration is 300 to 400-fold lower than in serum [216, 236]. As such, patients with concurrent HER2+ BCBM and systemic HER2+ disease who receive IV trastuzumab often experience regression or stabilization of systemic tumor burden while brain metastases progress [174].

Trastuzumab administered IT has been reported to increase survival and delay progression of HER2+ brain metastases. Bousquet and colleagues gave IT trastuzumab to a patient with HER2+ cerebellar and epidural breast cancer metastases, resulting in a six-month halt in disease progression [220]. Colozza and colleagues describe a patient with HER2+ intraparenchymal cortical metastases who was treated for 19 months with IT trastuzumab [221]. In both case reports, patients were still alive at the time of publication. A 2013 meta-analysis by Zagouri and colleagues demonstrated that the median survival of patients with HER2+ leptomeningeal carcinomatosis (LC), a particularly deadly form of BCBM, increases from 5.9 months in historical controls to 13.5 months with IT trastuzumab treatment [219].

Despite these promising reports, IT administration of trastuzumab has disadvantages. Multiple intrathecal administrations are required. Perhaps more importantly, the normal, rapid turnover of cerebrospinal fluid (CSF) results in a widely-fluctuating pharmacokinetic profile of trastuzumab in CSF, resulting in a CSF half-life of just 12 hours in one case report [220, 239]. It is therefore unlikely that tumor cells in the CNS receive optimal exposure to trastuzumab after IT administration.

Gene therapy offers the potential for a one-shot solution to the problem of mAb delivery across the blood-brain barrier. Adeno-associated viral (AAV) vectors, particularly serotype 9, can safely and efficiently deliver exogenous genes, such as the gene for trastuzumab, to neurons and astrocytes throughout the brain and spinal cord after a single IT administration. This results in long-term, stable expression of the transgene product in the brain parenchyma and CSF [49, 56].

We aim to use AAV9.trastuzumab delivered IT to bypass the blood-brain barrier for localized expression of trastuzumab *in situ*. Using a Rag1-/- murine orthotopic xenograft model of HER2+ BCBM, we delivered AAV9.trastuzumab IT by intracranioventricular (ICV) injection either as tumor prophylaxis or as tumor treatment. In both cases, a single dose of IT AAV9.trastuzumab significantly extended median survival of mice compared to no treatment or control AAV vector treatment. Looking ahead, we predict that IT AAV9.trastuzumab could prolong survival of patients with existing HER2+ CNS metastases in addition to patients with primary or metastatic HER2+ breast cancer at risk for developing BCBM.

Hypotheses

Using an orthotopic murine xenograft model of human HER2+ BCBM, we aimed to express trastuzumab in the CNS by administering AAV9.trastuzumab IT by way of

ICV injection. Vector was administered as tumor prophylaxis 21 days before tumor implantation or as tumor treatment 3 days after tumor implantation. In both the prophylactic and treatment setting, we expected mice that received AAV9.trastuzumab to survive longer than mice that received an AAV9 vector to express an irrelevant antibody or mice that received no treatment.

The main mechanism of action by which trastuzumab exerts its anti-tumor effect *in* vivo is by mediating ADCC of tumor cells, chiefly by NK cells. We sought to demonstrate that this primary mechanism of action was preserved in our model and in the CNS compartment. When an NK cell depleting agent was administered systemically, we expected the median survival of mice that received AAV9.trastuzumab tumor prophylaxis to decrease compared to mice that received AAV9.trastuzumab tumor prophylaxis without the NK cell depleting agent. Given that macrophages may perform ADCP on tumor cells, we also hypothesized that depleting macrophages in the systemic compartment of mice that received AAV9.trastuzumab tumor prophylaxis would lead to a shorter median survival than mice given AAV9.trastuzumab tumor prophylaxis without macrophage depletion.

Results

IT AAV9.trastuzumab provides tumor prophylaxis and treatment in a xenograft model of HER2+ BCBM

We first tested AAV9.trastuzumab as HER2+ CNS tumor prophylaxis in our Rag1-/- xenograft model. No treatment, AAV9.trastuzumab, or AAV9.2.10AmAb (a negative control vector expressing a rhesus anti-simian/human immunodeficiency virus IgG) were administered IT by ICV injection at least 21 days before tumor implantation.

HER2+ BT474-M1.ffluc cells (100,000) were implanted in the brain parenchyma stereotaxically, and mice were monitored daily until moribund. Kaplan-Meyer survival curves (Fig. 1A-B) indicate that the median survival of mice that received IT AAV9.trastuzumab tumor prophylaxis was significantly greater than mice that received AAV9.2.10AmAb (124 days vs 46.5 days; $p<0.0001$, hazard ratio = 0.0306). The median survival of mice that received AAV9.2.10AmAb was not significantly different from mice without treatment (46.5 days vs 50 days; $p=0.4306$, hazard ratio = 1.1868). Protein A ELISA quantification of IgG transgene expression in serum (Fig. 1C-D) and brain tissue homogenate, normalized to total protein in brain homogenate (Fig. 1E), indicates that transgene expression was similar between groups that received AAV9.trastuzumab and AAV9.2.10AmAb. Tumors remained HER2+ at the time of necropsy (Fig. 1F). Biodistribution analysis of AAV9 vector genome copies in brain tissue demonstrates equivalent genome deposition between groups that received vector (Fig. S1).

To determine if IT AAV9.trastuzumab can serve as treatment for existing HER2+ BCBM, we implanted HER2+ BT474-M1.ffluc tumors in Rag1-/- mice and administered IT AAV9.trastuzumab or no treatment three days after tumor implantation. Kaplan-Meyer survival curves (Fig. 2) indicate that the median survival of mice that received AAV9.trastuzumab (82 days, $p=0.002$) is significantly greater than mice that received no treatment (61 days).

To compare the amount of trastuzumab in brain tissue after ICV administration of AAV9.trastuzumab versus Herceptin®, 1e11 GC AAV9.trastuzumab or 15 µg Herceptin® were administered ICV to Rag1-/- mice. Assuming a mouse brain mass of 0.4g, the 15 µg trastuzumab dose is equivalent to 37.5 µg trastuzumab/g brain mass. This dose would be the equivalent of a 50.625 mg dose of trastuzumab in a 1350 g

human brain. Brains from mice that received AAV9.trastuzumab were harvested 2 weeks after vector administration, while brains that received Herceptin® were harvested 24, 48, and 168 hours after antibody administration. Fig. S2 indicates that the median amount of trastuzumab expressed in brains tissue in mice that received AAV9.trastuzumab is slightly higher than the amount of Herceptin® in brain tissue 24 hours after administration of 15 µg antibody. Over time, the amount of Herceptin® in brain tissue decreases, as expected.

Prophylactic IT AAV9.trastuzumab slows tumor growth

To determine if IT AAV9.trastuzumab tumor prophylaxis slows tumor growth, we measured tumor diameter 47 days after implantation. The median diameter of tumors from mice that received AAV9.trastuzumab tumor prophylaxis (1.2 mm, n=5) was significantly smaller than mice that received AAV9.2.10AmAb (5.7 mm, n=5) or no treatment (7.2 mm, n=4) (Fig. 3A). Transgene expression in brain tissue and in serum collected before tumor implantation shows higher but comparable median 2.10A mAb expression (Fig. 3B-C).

Secreted trastuzumab binds to HER2+ brain tumors

Anti-IgG immunofluorescence of day 47 tumor cryosections was employed to determine if secreted trastuzumab could bind to HER2+ tumor cells *in vivo*. Micrographs show trastuzumab decorating tumors from mice that received IT AAV9.trastuzumab but not tumors from mice that received IT AAV9.2.10AmAb or no treatment (Fig. 3D, overexposures Fig. S3A). Additionally, neurons transduced by AAV9.trastuzumab or

AAV9.2.10AmAb stain positive for IgG. Secreted trastuzumab also decorated day 20 tumors from mice that received AAV9.trastuzumab (Fig. S3B). Tumors remain HER2+ on the day of necropsy (Fig. S5).

NK cells, but not macrophages, mediate IT AAV9.trastuzumab tumor prophylaxis

Trastuzumab exerts its effect against peripheral tumors mainly by facilitating antibody-dependent cell-mediated cytotoxicity (ADCC) of HER2+ tumor cells [120, 151, 240]. We hypothesized that the same mechanism would govern AAV9.trastuzumab tumor prophylaxis in the CNS. We first evaluated AAV9.trastuzumab tumor prophylaxis in NOD *scid* gamma (NSG) mice, which lack NK cells and functional macrophages. As expected, AAV9.trastuzumab tumor prophylaxis fails in NSG mice (Fig. 4). Survival was comparable between groups that received no treatment (37 days) or AAV9.trastuzumab (40 days, $p=0.862$). Transgene expression in brain tissue was similar among mice that received vector (Fig. S4).

We next sought to determine if NK cells or macrophages played a larger role in IT AAV9.trastuzumab tumor prophylaxis in the CNS. To do so, we first employed continuous NK cell depletion by intraperitoneal (IP) administration of the anti-NK1.1 antibody PK136 in our Rag1-/- xenograft tumor model (Fig. 5A-B). Mice that received AAV9.2.10AmAb with or without NK cell depletion survived a median of 53 and 50 days, respectively. Mice that received AAV9.trastuzumab tumor prophylaxis and no NK cell depletion lived a median of 156 days. Median survival of mice that received AAV9.trastuzumab tumor prophylaxis with continuous NK cell depletion was significantly shorter, 73 days ($p<0.0001$, compared to AAV9.trastuzumab without NK cell depletion).

Formalin-fixed tumors from mice in the NK cell depletion experiment were subjected to *in situ* hybridization (ISH) for NK cell-specific *Ncr1* (*NKp46*) RNA. NK cells infiltrated only tumors from mice given AAV9.trastuzumab without NK cell depletion (Fig. 5C). IgG transgene expression in brain tissue homogenate was comparable between groups that received vector (Fig. 5D). *Ncr1* ISH of spleens was used to confirm successful depletion of NK cells (Fig. 5E). We also cryosectioned day 20 tumors from mice given AAV9.trastuzumab, AAV9.2.10AmAb, or no treatment without NK cell depletion. Immunohistochemical (IHC) staining for Ly-49G2 (Fig. 6) confirms that NK cells infiltrated day 20 tumors only from mice that received AAV9.trastuzumab tumor prophylaxis.

To determine if systemically-circulating macrophages play any role in AAV9.trastuzumab tumor prophylaxis in our model, we employed continuous macrophage depletion by IP administration of clodronate liposomes. Mice that received no treatment with or without macrophage depletion survived a median of 53 and 50 days, respectively (Fig. 7A-B). Mice that received AAV9.trastuzumab without macrophage depletion survived a median of 92 days ($p=<0.0001$ compared to mice that received no treatment without macrophage depletion). Mice that received AAV9.trastuzumab with macrophage depletion survived a median of 70.5 days ($p=0.3268$, compared to AAV9.trastuzumab without macrophage depletion). IgG transgene expression in brain tissue was comparable among groups that received vector (Fig. 7C), and macrophage depletion was confirmed by IHC staining of spleens for CD68 (Fig. 7D).

Discussion and further directions

Metastasis of HER2+ breast cancer to the brain is a devastating diagnosis with a poor prognosis due to a lack of targeted and effective treatments. Although IT administration of trastuzumab has been reported to slow disease progression and prolong survival, the benefit is modest, likely due to the rapid turnover of CSF resulting in poor tumor exposure to antibody. An unmet need for effective treatments exists for patients with this disease.

The advent of AAV vectors for gene transfer has revolutionized the field of gene therapy. The discovery of CNS-tropic vectors, such as AAV9, represents a boon for clinicians seeking to localize biological treatments behind the blood-brain barrier. A single IT administration of AAV9 vector into the CSF by way of the lateral ventricles or cisterna magna leads to widespread transduction of neurons and astrocytes throughout the cortex, cerebellum, and spinal cord, resulting in long-lived production of transgene product in the CNS compartment [14, 49, 56].

We have successfully demonstrated that AAV9.trastuzumab administered IT at a moderate vector dose, both as tumor prophylaxis and as tumor treatment, significantly extends median survival in a xenograft mouse model where the human HER2+ cancer cell line BT747-M1.ffluc is implanted into the brains of Rag1-/- mice. In the prophylactic setting, median survival is 2.48 times greater for mice that received AAV9.trastuzumab tumor prophylaxis than mice that received control AAV vector treatment or no treatment. Additionally, tumors in mice given AAV9.trastuzumab are smaller at day 47 than tumors from untreated or AAV9.2.10AmAb-treated mice. In the treatment setting, the median survival benefit is significant but less, perhaps in part due to the shorter total duration of exposure of tumor cells to expressed trastuzumab. Additionally, we report that a dose of

1e11 GC AAV9.trastuzumab administered ICV yields a similar amount of trastuzumab in brain tissue as does an ICV dose of Herceptin® equivalent to 50 mg in humans when measured 24 hours after antibody administration.

Our studies also indicate that trastuzumab secreted by neurons and astrocytes maintains its antigen specificity and effector function despite the fact that these cells do not normally produce IgG. Using immunofluorescence microscopy, we showed that HER2+ tumors from mice treated with AAV9.trastuzumab, but not AAV9.2.10AmAb, are decorated with expressed IgG.

The effector functions of trastuzumab have been widely studied [120, 240]. Trastuzumab bound to HER2 on tumor cells (i) mediates ADCC when its Fc binds to activating Fcγ receptors (e.g. FcγRIIIa) on immune cells such as NK cells and macrophages; (ii) prevents initiation of signal transduction when HER2 homodimerizes or heterodimerizes with other members of the HER family, thus slowing tumor growth; (iii) blocks proteolytic cleavage of the HER2 ectodomain preventing the remaining membrane-bound p96 protein from activating pro-growth signaling pathways; (iv) disrupts pro-angiogenic pathways; and (v) disrupts DNA repair pathways.

The predominant mechanism by which trastuzumab acts against peripheral HER2+ tumors in patients is ADCC by immune cells carrying activating Fcγ receptors, such as NK cells and macrophages. We hypothesized that the same would be the case in our xenograft model. It is important to note that the mouse FcγRs do indeed bind to human IgG1. Overdijk et al. demonstrate that mouse FcγRs bind to human IgG1 and activate ADCC, and Bruhns reports that all human IgG subclasses are bound efficiently by mouse FcgRs and FcRn [241, 242].

AAV9.trastuzumab tumor prophylaxis fails when administered to NSG mice, which lack NK cells and functional macrophages compared to Rag1-/- mice, suggesting an NK cell- or macrophage-mediated mechanism of tumor prophylaxis. When we depleted NK cells in the Rag1-/- model, the median survival of mice decreased substantially, indicating that NK cell-driven ADCC of tumor cells is responsible for a majority of the survival benefit. Additionally, immunofluorescence and immunohistochemical staining of NK cells in tumors indicates that NK cells infiltrated only into tumors of mice that received AAV9.trastuzumab tumor prophylaxis, not untreated or control-treated mice. These NK cells are present in tumors as early as 20 days after tumor implantation and as late as the time of necropsy. To our knowledge, this is the first time that the predominant mechanism by which trastuzumab works against HER2+ tumors in the CNS has been reported.

Our macrophage depletion studies indicate that these cells do not contribute significantly to the anti-tumor effect of AAV9.trastuzumab tumor prophylaxis in this model. However, as clodronate liposomes do not cross the blood-brain barrier, these experiments can only address whether systemically-circulating macrophages play a role in AAV9.trastuzumab tumor prophylaxis. Tissue resident macrophages/microglia may still contribute in small part to the anti-tumor effect of AAV9.trastuzumab in this model.

Limitations of our studies include our use of a single vector dose, although studies to determine a minimally effective dose (MED) are in progress. Our mice bore one brain tumor, but patients often develop multiple metastases. Testing AAV9.trastuzumab tumor prophylaxis in a model where tumor cells are administered via carotid artery injection or where brain metastases arise after implantation of a peripheral tumor would indicate whether our treatment is effective against multiple brain tumors.

We also employed AAV9.trastuzumab in these studies as a monotherapy. Unsurprisingly, all mice eventually succumb to outgrowth of tumors, which remain HER2+ at necropsy. Combining AAV.trastuzumab with chemotherapy and/or radiotherapy will likely be synergistic against HER2+ BCBM, both in this xenograft model and in patients.

Trastuzumab infusion is standard of care for patients with HER2-overexpressing breast cancer, and IT delivery of trastuzumab has been shown to be beneficial. However, trastuzumab expression cannot be turned off after AAV9-mediated gene transfer. Related to this, cardiotoxicity is a known side-effect that occurs in a small subset of patients who receive systemic trastuzumab treatment. Risk factors for cardiotoxicity have been identified, including previous anthracycline-containing chemotherapeutic regimens, age, and existing cardiac dysfunction [243-245].

With IT administration of IT AAV9.trastuzumab, we anticipate a lower concentration of trastuzumab in blood than after IV administration of Herceptin®, which would be less likely to lead to cardiotoxicity. Regardless, women with CNS metastasis from HER2+ breast cancer almost always have systemic disease necessitating treatment with systemic administration of trastuzumab where safety monitoring of cardiac function is standard. This aspect will be incorporated into the design of our first in human phase I safety trial.

We plan to first assess the safety, efficacy, and pharmacokinetics of AAV9.trastuzumab in women with documented CNS lesions from HER2+ breast cancer. Subject to safety and efficacy in this setting, AAV9.trastuzumab will be subsequently assessed in a similar patient population with systemically metastatic HER2+ disease prior to clinical or radiological diagnosis of CNS lesions. Given that AAV transgene

expression has been documented to persist for years in non-human primates and humans [246, 247], this approach has the potential to be an integral part of the adjuvant therapy for patients with early diagnosis of HER2+ breast cancer after curative resection of the breast lesion.

Given this fact and the results of our experiments, we intend to move AAV9.trastuzumab toward the clinic. Going forward, our AAV platform has the potential to be expanded to express other therapeutic antibodies behind the blood brain barrier to treat CNS diseases and address other unmet needs.

Materials and Methods

Experimental design

IT-administered trastuzumab can increase survival and delay tumor progression in patients with HER2+ BCBM. However, trastuzumab has been reported to have a half-life in CSF of 12 hours [220]. We aim to administer AAV9.trastuzumab IT such that trastuzumab can be constitutively secreted by neurons and astrocytes *in situ* leading to better tumor exposure to trastuzumab and thus longer median survival. To test our hypothesis, we chose Rag1-/- mice due to their lack of endogenous IgG and T cell "leakiness" that can occur in nude mice often used for HER2+ brain tumor xenografts in the literature. Both Rag1-/- and NSG mice used in these experiments were obtained from The Jackson Laboratory (Bar Harbor, ME, USA), housed at the barrier facility of the Translational Research Laboratories (TRL) Vivarium at the University of Pennsylvania, and maintained according to NIH guidelines for the care and use of animals in research. All procedures and protocols were approved by the Institutional Animal Care and Use

Committee (IACUC) of the University of Pennsylvania. The 2.10A mAb control antibody is a rhesus anti-simian/human immunodeficiency virus (SHIV) IgG, and the AAV9.2.10AmAb expression construct has the same regulatory elements as AAV9.trastuzumab. We administered vector to mice at least 21 days before tumor implantation in the prophylaxis studies and 3 days after tumor implantation in the treatment studies, because at least 10-14 days are required for vector expression to reach steady state. Sample size was determined to be a minimum of 8 mice per experimental group to allow for robust statistical analysis if mice were euthanized due to complications during or post-tumor implantation. The large prophylaxis study began with 20 mice per group, the treatment study with 8 mice per group, and the NSG and NK cell depletion studies with 12 mice per group. Macrophage depletion studies began with 9 mice per group, with an additional 2 mice added to AAV9.trastuzumab-treated arms due to clodronate-related toxicity. Mice found dead rather than euthanized were included only in the survival analyses and not in downstream transgene expression, histological, or biodistribution analysis. Studies were conducted without blinding.

Statistics

Survival study p values were calculated using the Log-Rank (Mantel-Cox) test in GraphPad Prism for Windows version 7 (GraphPad Software). Hazard ratios were calculated with a Cox regression model using the *sts* package in Stata (StataCorp). Tumor diameter comparisons were carried out using Wilcoxon rank-sum test within the R program (version 3.3.1; https//cran.r-project.org) using the function “wilcox.test.”

Vector construction

Sequences matching the WHO published amino acid sequences of the heavy and light chains of trastuzumab were back-translated, codon-optimized, and synthesized by GeneArt (Life Technologies). Heavy and light chain sequences were preceded by a human IL-2 secretion signal. The heavy and light chain sequences were cloned into an AAV expression construct containing an upstream hybrid CMV immediate early enhancer/chicken beta-actin promoter and a Promega chimeric intron and a downstream SV40 polyadenylation signal. The heavy and light chain sequences were separated from each other by an F2A self-cleaving peptide to ensure 1:1 production of heavy and light chain protein. The construct was flanked by AAV2 inverted terminal repeats. The resulting pAAV.CMV.PI.trastuzumab.SV40 expression construct was packaged in an AAV9 capsid by triple transfection of 293 cells and purified as previously described [24]. Vector was titrated using standard qPCR. AAV9.CMV.PI.2.10AmAb.SV40 was obtained from the Penn Vector Core.

Vector administration

Six to nine-week-old female Rag1-/- (B6.129S7-Rag1tm1Mom/J) mice were obtained from The Jackson Laboratory (Bar Harbor, ME, USA) and housed at the TRL Vivarium at the University of Pennsylvania. All animal procedures and protocols were approved by the IACUC of the University of Pennsylvania. Vector was diluted in sterile PBS. For IT administration by ICV injection, vector was diluted to 1×10^{11} GC per 5 µL.

For tumor prophylaxis, mice were injected ICV with 1×10^{11} GC of AAV9.CMV.PI.trastuzumab.SV40 or AAV9.CMV.PI.2.10AmAb.SV40 at least 21 days

prior to BT474-M1.ffluc tumor implantation. For tumor treatment, mice received BT474-M1.ffluc tumors first, and vector was administered by ICV injection 3 days after tumor implantation.

Orthotopic xenograft model of HER2+ breast cancer brain tumors in Rag1-/- and NSG mice

The xenograft model was based on previous HER2+ BCBM models reported in the literature [248-252]. The HER2+ BT474.M1 human ductal carcinoma cell line, transduced with the lentiviral vector VSVG.HIV.SIN.cPPT.CMV.ffluciferase.WPRE (Penn Vector Core), was cryopreserved in liquid nitrogen. One week before tumor implantation, BT474-M1.ffluc cells at passage 56 were thawed, expanded in DMEM/F12 (Corning) with 10% FBS and 1% penicillin/streptomycin at 37°C and 5% CO_2, and passaged three days before tumor cell implantation. On the day of tumor injection, cells were counted with a Countess II cytometer (Life Technologies), and suspended at $1x10^5$ cells per 5 µL in 50%/50% (v/v) PBS/MatriGel® (Corning).

For the injection procedure, mice were anesthetized with ketamine/xylazine. Fur on the scalp and neck was sheared. A time-release 17-β estradiol pellet (1.7 mg, 90-day release, Innovative Research of America) was implanted subcutaneously in the dorsum of the neck and re-administered every 90 days during the study. Mice were fixed in a stereotaxic apparatus. Exposed skin was cleansed with povidone iodine and 70% ethanol. A 1 cm anterior-posterior incision was made over the top of the skull. Bregma was identified. A pneumatic drill was positioned at bregma then moved 0.8 mm posterior and 2.2 mm left of bregma where a burr hole was drilled in the skull.

A 25 µL Hamilton syringe was loaded with 5 µL of cell suspension and positioned in a mechanical injector on the stereotaxic frame. After bringing the needle to 0.8 mm posterior and 2.2 mm left of bregma, the needle was moved 4.0 mm deep into brain parenchyma then lifted 1.0 mm to create a pocket into which to inject cells. The needle was left in place for 5 minutes. The cell suspension was mechanically injected over 10 minutes, and the needle was left in place another 5 minutes before being removed slowly. After suturing incisions, mice recovered on a 37°C heating pad and were given 100 µL of 2 mg/kg enrofloxacin in PBS and 0.3 mg/kg buprenorphine in PBS subcutaneously.

Firefly luciferase imaging of tumor growth was not conducted in these studies. Our previous attempts to do so resulted in many mice developing acute urinary and kidney complications including hydronephrosis, kidney and bladder stones, and gross hematuria in the days immediately following the imaging procedure, necessitating euthanasia of affected mice. 17β estradiol, released from the subcutaneous pellet, has been reported in the literature to cause renal and urinary pathology[253-255]. It is possible that some aspect of our model exacerbated underlying kidney or urinary pathology associated chronic exposure to 17β estradiol.

Mice were monitored daily. When moribund, mice were euthanized by overexposure to CO_2 followed by cervical dislocation. At necropsy, brains and tumor were either snap-frozen on dry ice and stored at -80°C for transgene expression and genome copy analysis, cryopreserved in OTC medium using liquid nitrogen, or preserved in formalin.

Tumor diameter

Measurement of day 47 tumor diameter was performed with digital Vernier calipers (Thermo-Fisher). Brains were harvested at necropsy and cut coronally through the visible tumor injection needle track. The diameter of the tumor in the anterior section was calculated as the geometric mean of two perpendicular diameter measurements.

NK cell depletion

PK136 (anti-mouse NK1.1) antibody was purified from PK136 hybridoma supernatant (ATCC® HB-191™) using the protein A purification kit (Sigma) and supplemented as needed with PK136 available commercially (Leinco Technologies). Mice were given 100 µg PK136 or PBS intraperitoneally on days 5 and 1 before tumor implantation, then weekly for the duration of the experiment.

Systemic macrophage depletion

Chlodronate liposomes or PBS liposomes (Nico van Rooijen, Vrije University Medical Center, Amsterdam, the Netherlands) were injected intraperitoneally at 10 µL per g body weight on days 5 and 1 before tumor implantation, then weekly for the duration of the experiment.

Preparation of serum

Blood was collected by retro-orbital or sub-mandibular bleed into Z-Gel microtube serum separators (Sarstedt) and incubated at room temperature for 20 minutes. After centrifuging for 5 minutes at 5000 RPM in a tabletop microcentrifuge (accuSpin micro 17, Thermo-Fisher), serum was stored at -80°C.

Preparation of brain homogenate

Brain homogenates were prepared by chipping frozen brain into tissue lysis buffer (25 mM Tris-HCl, 5 mM EDTA, 1% Triton-X, 150 mM NaCl, pH 7.6) containing 3 times the normal concentration of cOmplete™ Protease Inhibitor Cocktail Tablets (Roche). Samples were homogenized with stainless-steal beads on a TissueLyzer II (Qiagen) at 30 Hz for 2 minutes, frozen at -80°C, thawed, then centrifuged at 17K x g for 60 minutes at 4°C to remove myelin debris. BCA assay (Thermo-Fisher) was used to determine protein concentration of brain homogenates.

Protein A ELISA

Protein A ELISA was used to quantify trastuzumab and 2.10A mAb expression in serum and brain homogenates. All steps were performed at room temperature unless otherwise stated. Plates were washed with a BioTek 405TS microplate washer with PBS + 0.05% Tween-20. Protein A (Sigma) was suspended in PBS and stored at -20°C. Costar® 96-well EasyWash™ ELISA assay plates (Corning) were coated with 5 µg/mL protein A in PBS overnight at 4°C then blocked with PBS + 0.5% bovine serum albumin

(Sigma). Samples were diluted in PBS and plated. Herceptin® (Roche) was used as a quantitative standard. For brain homogenate ELISAs, brain homogenate from untransduced mice was spiked into the standard curve wells at a dilution equal to that of samples on the plate. After washing, plates were incubated with AffiniPure polyclonal goat anti-human IgG-biotin (Jackson ImmunoResearch Labs) followed by streptavidin-horseradish peroxidase (Abcam). Plates were developed with TMB substrate, stopped with 2N H_2SO_4, then read using a SpectraMax M3 (Molecular Devices) plate reader at 450 nm.

Biodistribution by qPCR

AAV9 vector genome copies in brain were quantified using TaqMan qPCR (Thermo-Fisher). Briefly, frozen brain tissue was chipped into ALT Buffer (Qiagen) and homogenized with steel beads using a TissueLyzerII. Phenol:chloroform:isoamyl alcohol (25:24:1, Sigma) extraction and isopropanol precipitation was used to isolate tissue DNA. For TaqMan qPCR, primers and probe were designed against the SV40 polyadenylation signal of the vector.

Histology

HER2 staining was performed on formalin-fixed paraffin-embedded tissue samples. Sections were deparaffinized through a xylene and ethanol series, boiled in a microwave for 6 min in 10 mM citrate buffer (pH 6.0) for antigen retrieval, treated sequentially with 2% H_2O_2 (15 min; Sigma), avidin/biotin blocking reagents (15 min each; Vector Laboratories), and blocking buffer (1% donkey serum in PBS + 0.2% Triton for 10

min) followed by incubation with primary antibody (1 h, rabbit anti-HER2, Abcam ab2428) and biotinylated secondary antibody (45 min; biotinylated donkey anti-rabbit, Jackson Immunoresearch, West Grove, PA) diluted in blocking buffer. Bound antibodies were visualized with a Vectastain Elite ABC kit (Vector Laboratories) using DAB as substrate. Sections were counterstained with hematoxylin to show nuclei.

Immunofluorescence staining for human IgG was performed on cryosections. Sections were fixed in 4% paraformaldehyde in PBS for 10 minutes, permeabilized and blocked in 0.2% Triton in PBS containing 1% donkey serum for 30 minutes, and incubated for 1 hour with a goat antibody against the crystalizable fragment (Fc) of human IgG (Jackson Immunoresearch Laboratories, West Grove, PA; 109-005-098) diluted in 1% donkey serum/PBS. After washing sections in PBS, bound primary antibodies were detected with FITC-labeled secondary donkey anti-goat antibodies (Jackson Immunoresearch Laboratories) diluted in 1% donkey serum/PBS. After washing in PBS, sections were mounted with Vectashield containing DAPI as nuclear counterstain.

Immunohistochemistry to detect NK cells and HER2 was also performed on cryosections. Sections for NK cell staining were fixed in acetone at -20ºC for 7 minutes, air dried, sequentially treated with 0.3% H_2O_2 in PBS for 10 minutes, avidin/biotin blocking reagents (15 minutes each; Vector Laboratories), and blocking buffer (1% donkey serum in PBS, 20 minutes). Sections for HER2 staining were fixed in 4% paraformaldehyde in PBS for 10 minutes, then permeabilized in 0.2% Triton in PBS (30 minutes) and sequentially treated with 0.3% H_2O_2 in PBS (10 minutes) and avidin/biotin blocking reagents (15 minutes each; Vector Laboratories). Sections were then blocked with 1% donkey serum in PBS for 20 minutes, then treated with primary (1 hour) and

corresponding biotinylated secondary antibodies (45 minutes; Jackson Immunoresearch) diluted in 1% donkey serum in PBS. Primary antibodies were as follows: rat anti-mouse Ly-49G2 (clone 4D11, BD Pharmingen) for NK cells or rabbit anti-mouse Erb2 (Abcam ab2428) for HER2. A Vectastain Elite ABC kit was used according to the manufacturer's instructions with DAB as substrate.

To detect NK cells on formalin-fixed paraffin-embedded sections, *in situ* hybridization was performed using the ViewRNA ISH Tissue Assay Kit (Thermo Fisher) according to the manufacturer's protocol. Z-shaped probe pairs specific for mouse *Ncr1* (natural cytotoxicity triggering receptor 1, *NKp46*) RNA were synthesized by the kit manufacturer. The deposition of Fast Red precipitates indicating positive signals was imaged by fluorescence microscopy using a rhodamine filter set. Sections were counterstained with DAPI to show nuclei.

ICV Herceptin® and AAV9.trastuzumab administration for quantification of trastuzumab in brain tissue

AAV9.trastuzumab was diluted in PBS. 1e11 GC per Rag1-/- mouse was delivered ICV in a final volume of 10 µL. Two weeks later, brains were harvested.

Herceptin® was diluted in PBS and administered ICV in a 10 µL volume at a dose of 15 µg/mouse brain, which is roughly equivalent to a 50 mg IT dose in humans by brain mass. Brains were harvested 24, 48, and 168 hours after ICV administration of Herceptin®. Brains were homogenized as described above in 1 mL tissue lysis buffer. Protein A ELISA, performed as described above, was used to determine ng/mL of

trastuzumab in brain homogenate. Multiplying this trastuzumab concentration by the homogenate volume of 1 mL yielded approximate ng trastuzumab per brain.

Study Approval and Animal Welfare

All procedures and protocols were approved by the Institutional Animal Care and Use Committee (IACUC) of the University of Pennsylvania.

Tables & Table Legends

Reference	LM or Intraparenchymal	Dose (total cumulative dose)	Frequency	Concurrent treatments (if indicated)	MRI or Clinical Response	Duration of response (months)	AEs/SAEs	OS (months)
Preusser et al.	LC	5-100mg (250 mg)	Twice weekly	IV PLD, IV trastuzumab	MRI progression	NR	None	1.5 months
Hofer et al.	LC	100-150mg (1110 mg)	Every 2-3 weeks	IV trastuzumab	CR	>5.4	None	5.4 months
Mego et al.	LC	20-40mg (180 mg)	Weekly	IT MTX, IT cytarabine, IT hydrocortisone	PR	13.5 months	Postradiation leukoencephalopathy, ischemic lesion in fronto-temporal region of left brain	13.5
Mego et al.	LC	20-100mg (440 mg)	Weekly	IT MTX, IT cytarabine, IT hydrocortisone	PR	7.5 months	None	7.5 months
Oliviera et al.	LC	25 mg (825 mg)	Weekly	IT prednisone, IT capecitabine, IV trastuzumab	SD	9	None	18.4 months
Ferrario et al.	LC	20-40 mg (610 mg)	Weekly	IT MTX, IT cytarabine, IT hydrocortisone, IV trastuzumab, IV PLV	PR	10	G3: anemia, neutropenia	>23
Colozza et al.	Intraparenchymal	12.5 mg (287.5 mg)	Every 3 weeks	IV trastuzumab	SD	19	None	>37
Allison et al.	LC	20-60 mg	Every 1-2 weeks		Clinical improvement	>1	None	>1
Allison et al.	LC	20-60 mg	Every 1-2 weeks		Clinical improvement	>3.5	None	>3.5
Allison et al.	LC	20-60 mg	Every 1-2 weeks		SD --> progression	Not reported	None	Not reported
Allison et al.	LC	20-60 mg	Every 1-2 weeks		SD --> progression	Not reported	None	Not reported
Stemmler et al. 2008	LC	20 mg (80mg)	Twice weekly	IT MTX	Clinical improvement	1.3	None	1.3
Mir et al.	LC	20-100 mg (460mg)	Every week		SD	2	None	7
Shojima et al.	LC	25 mg/kg (>150 mg/kg)	Every week		PR	>1.5	None	>1.5
Platini et al.	LC	20-25 mg (405-495 mg)	Every week	IV paclitaxel, IV trastuzumab	MRI progression	5	None	>21
Stemmler et al. 2006	LC	4-20 mg (70 mg)	Twice weekly	IV trastuzumab, PO capecitabine	Clinical improvement	5.2	None	>5.2
Laufman and Forstoefel	LC	5-20 mg (35 mg)	Over 2 weeks	IT MTX, IT Thiotepa, IV paclitaxel, IV trastuzumab	SD	1.5	None	2.2
Brandt et al.	LC	25 mg	Every other day for 3 weeks, then weekly	IV trastuzumab, IV capecitabine, IV lapatinib	Clinical improvement	>46 months	None	>46 months
Kordbacheh et al.	LC	40-105 mg (1090 mg)	Every 1-2 weeks	IT MTX	CR	>7.4	None	7.4
Lu et al.	LC	5-80 mg	Twice weekly for one month then every two weeks	Lapatinib, IV trastuzumab emtansine	SD	46	Meningitis (Ommaya replaced)	46
Bousquet et al.	Intraparenchymal	25-100 mg	Every 3 weeks, then weekly, then every three days		SD	>6	None	>6
Dumitrescu et al.	LC	20-100 mg	Weekly	IV trastuzumab	PR	2	None	2
Park et al.	LC	25-50 mg	Weekly	IT methotrexate	PR	18	None	20
Park et al.	LC	25-50 mg	Weekly	IV trastuzumab, IV paclitaxel	PR	13	None	>13
Pluchart et al.	LC	21mg	Weekly	IV trastuzumab, lapatinib	PR	14	None	>14
Gulia et al.	LC	50-150mg	Twice weekly, weekly, every 3 weeks	lapatinib, letrozole, IT hydrocortisone	PR	4	None	Not reported
Giulia et al.	LC	150mg	Every 3 weeks, weekly, every 3 days	IV trastuzumab, lapatinib, IT hydrocortisone	SD	7	None	>7

Table 1. A summary of case reports of IT trastuzumab used to treat HER2+ BCBM. [219-221, 256-276]. Table adapted from [219, 257-259]. (MTX, methotrexate; OS, overall survival; CR, complete response; PR, partial response; SD, stable disease; AE, adverse event; SAE, serious adverse event; LC, leptomeningeal carcinomatosis; PO, by mouth)

IT Trastuzumab Clinical Trials	PI	Size	Dose	Safety	Phase II study?	Expected completion dates	Clinical benefit so far?
Intrathecal Trastuzumab for Leptomeningeal Metastases in HER2+ Breast Cancer (Phase I)	Raizer et al. (Northwestern)	13 women with HER2 positive BC, 1 man with glioblastoma, and one woman with anaplastic ependymoma	3 patients at 10mg, 3 at 20mg, 1 at 40mg, 1 at 60mg, and 7 at 80	AEs/SAEs = 1 patient had grade 4 dose-limiting toxicity (arachnoiditis); one patient had ommaya removed due to infection	Phase I/II study at 40 mg max dose in progress	Expected primary endpoint results 3/2018, estimated study completion date 3/2019	N/A
Safety and Efficacy of Intrathecal Trastuzumab Administration in Metastatic HER2 Positive Breast Cancer Patients Developing Carcinomatous Meningitis (Phase I/II Study)	Gutierrez et al. (Institut Curie)	19 patients	30-150mg (aimed for 30 ug/mL in CSF)	No >3 tox or neuro toxicity; maximum tolerated dose not reached; treatment well-tolerated in general	Phase II at 150 mg dose in progress	Expected primary endpoint results 9/2017, estimated study completion date 5/2018	*5 patients out of 19 had evident clinical benefit *All had 8 or more administrations of IT Herceptin® (mean 23) *Effective dose(s) not mentioned
Intrathecal Pertuzumab and Trastuzumab in Patients with New Untreated Asymptomatic or Low Symptomatic Brain Metastasis in HER2 Positive Breast Cancer (Phase I/II)	Blackwell et al. (Duke)	36 patients	80 mg trastuzumab, 10-80 mg pertuzumab	N/A	N/A	Expected primary endpoint results 2/2019, study complete 8/2019	N/A

Table 2. A summary of ongoing clinical trials using IT Herceptin® to treat HER2+ BCBM. (clinicaltrials.gov)

Figures & Figure Legends

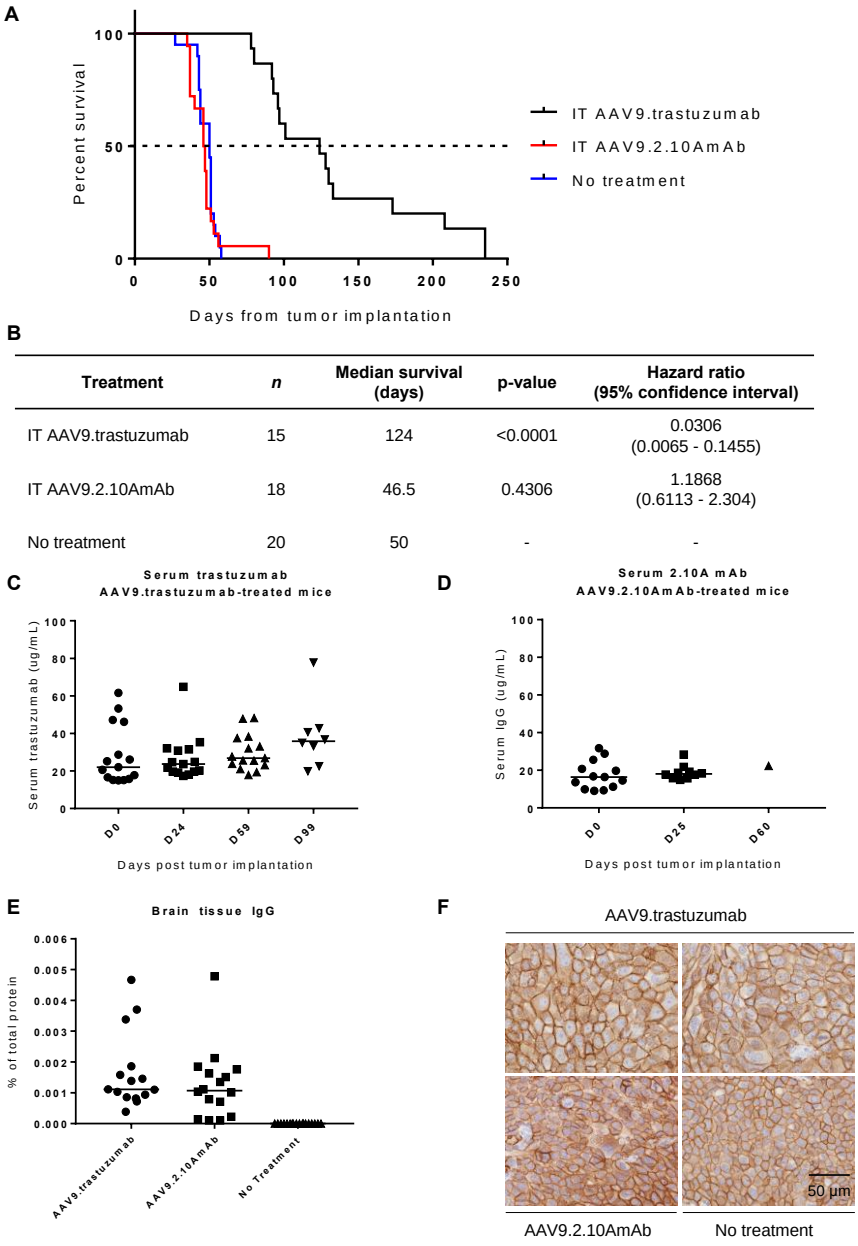

Treatment	*n*	Median survival (days)	p-value	Hazard ratio (95% confidence interval)
IT AAV9.trastuzumab	15	124	<0.0001	0.0306 (0.0065 - 0.1455)
IT AAV9.2.10AmAb	18	46.5	0.4306	1.1868 (0.6113 - 2.304)
No treatment	20	50	-	-

Fig. 1. IT AAV9.trastuzumab tumor prophylaxis. (A) Kaplan-Meyer survival curves for mice that received IT AAV9.trastuzumab tumor prophylaxis, IT AAV9.2.10AmAb control treatment, or no treatment at least 21 days before tumor challenge. (B) Tabulated survival and statistical data for Fig. 1A. (C-D) Serum expression of trastuzumab and 2.10A mAb measured by protein A ELISA. (E) IgG transgene expression in brain tissue measured by protein A ELISA of brain homogenate and graphed as a percent of total protein in brain homogenate. (F) Positive HER2 immunohistochemistry (IHC) staining of BT474.M1.ffluc tumors from the necropsies of mice from Fig. 1A.

A

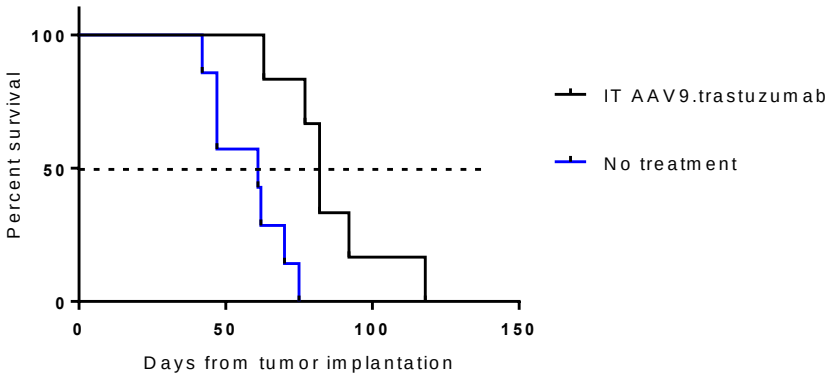

B

Treatment	*n*	Median survival (days)	p-value
IT AAV9.trastuzumab	6	82	0.002
No treatment	7	61	-

Fig. 2. IT AAV9.trastuzumab tumor treatment. (A) Kaplan-Meyer survival curves for mice that received IT AAV9.trastuzumab tumor treatment, IT AAV9.2.10AmAb control treatment, or no treatment 3 days after tumor challenge. (B) Tabulated survival and statistical data for Fig. 2A.

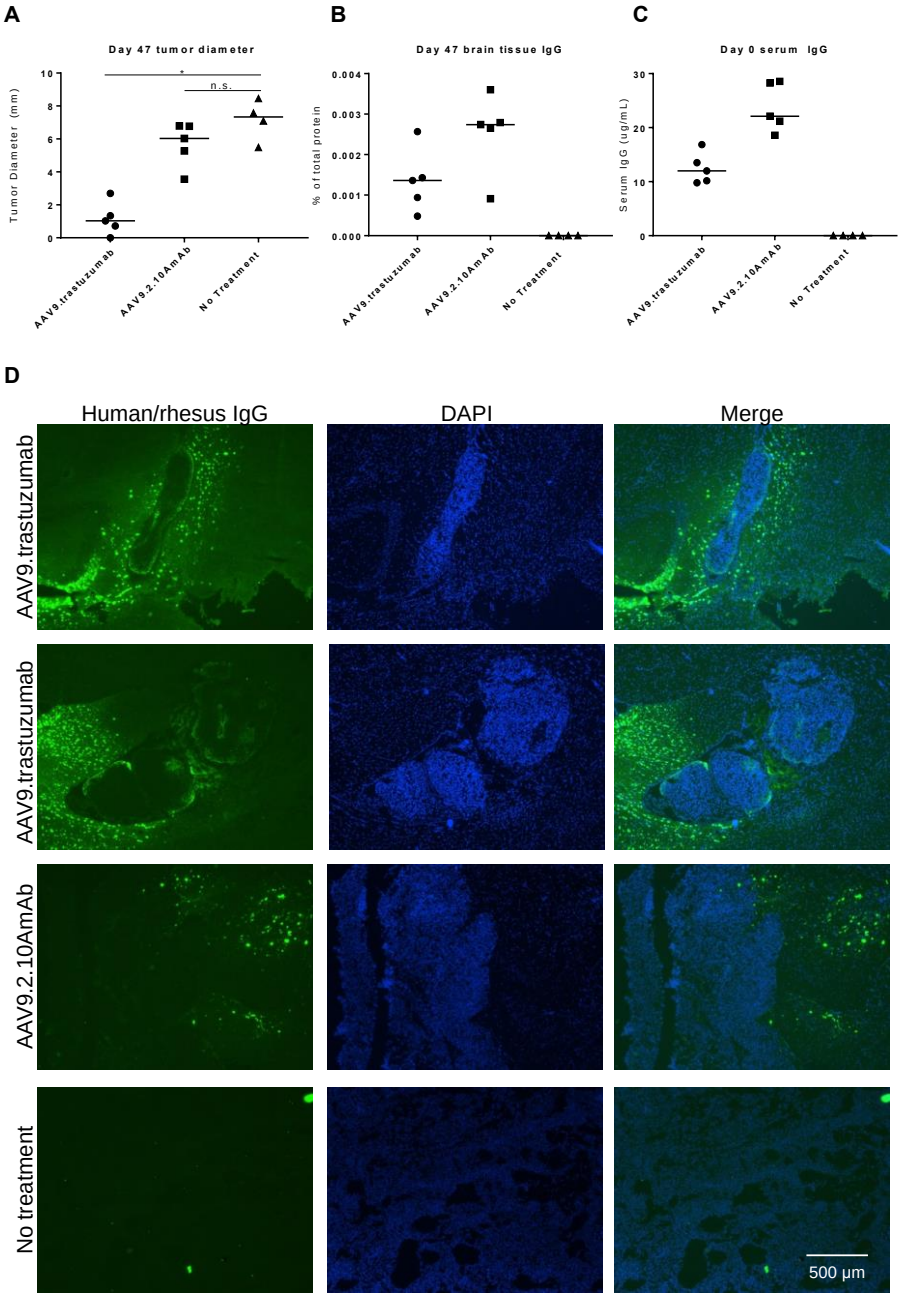

Fig. 3. Day 47 tumor diameter and IgG immunofluorescence microscopy. (A) IT AAV9.trastuzumab tumor prophylaxis yielded tumors of significantly smaller diameter than IT AAV9.2.10AmAb control treatment or no treatment when measured 47 days after tumor cell implantation (p=0.0159). (B) IgG transgene expression in brain tissue measured by protein A ELISA of brain homogenate and reported as a percent of total protein in brain homogenate. (C) Serum IgG transgene expression on the day of tumor challenge (day 0) measured by protein A ELISA. (D) Immunofluorescence staining for human/rhesus IgG in day 47 tumor cryosections. Representative HER2 IHC staining is shown in Fig. S5

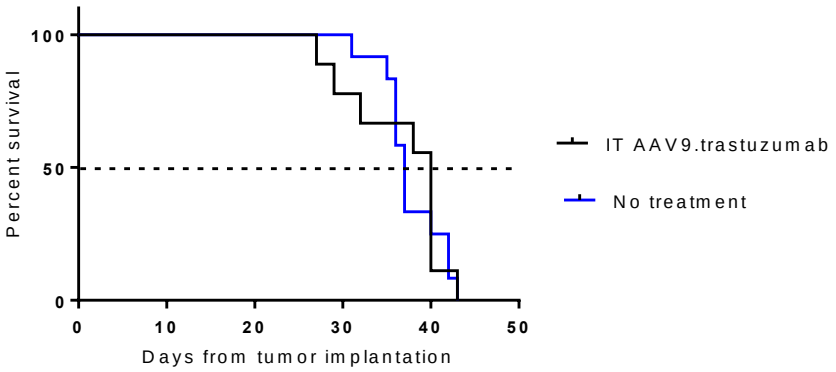

Treatment	*n*	Median survival (days)	p-value
IT AAV9.trastuzumab	9	40	0.862
No treatment	12	37	-

Fig. 4. IT AAV9.trastuzumab tumor prophylaxis in NOD scid gamma mice. (A) Kaplan-Meyer survival curves for mice that received IT AAV9.trastuzumab tumor treatment or no treatment at least 21 days before tumor challenge. (B) Tabulated survival and statistical data for Fig. 4A.

A

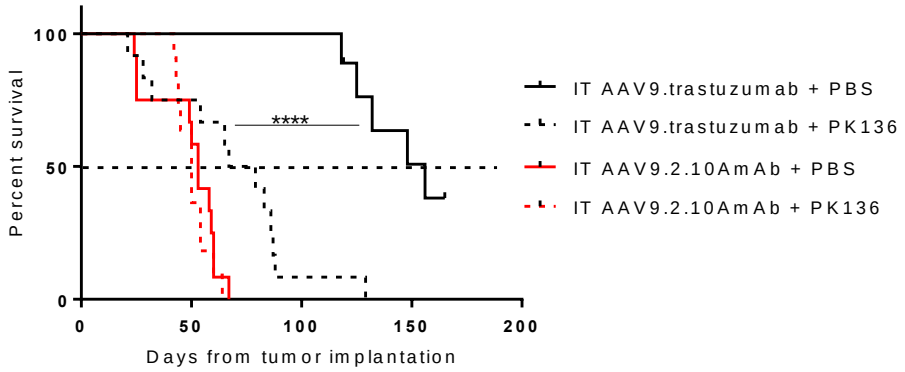

B

Treatment	*n*	Median survival (days)	p-value
IT AAV9.trastuzumab + PBS	9	156	<0.0001
IT AAV9.trastuzumab + PK136	12	73	0.0070
IT AAV9.2.10AmAb + PBS	12	50	-
IT AAV9.2.10AmAb + PK136	11	53	0.5661

C

AAV9.trastuzumab + PBS

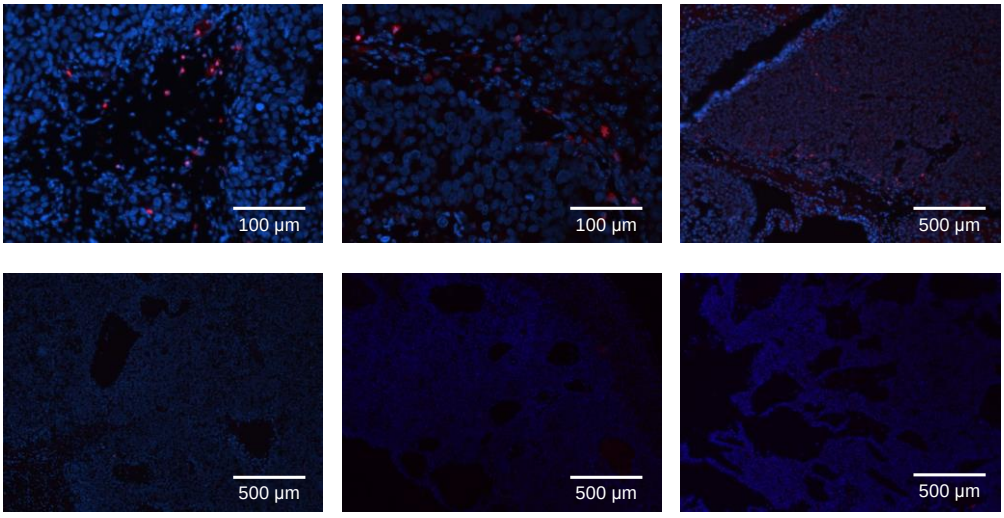

AAV9.trastuzumab + PK136

AAV9.2.10AmAb + PBS

AAV9.2.10AmAb + PK136

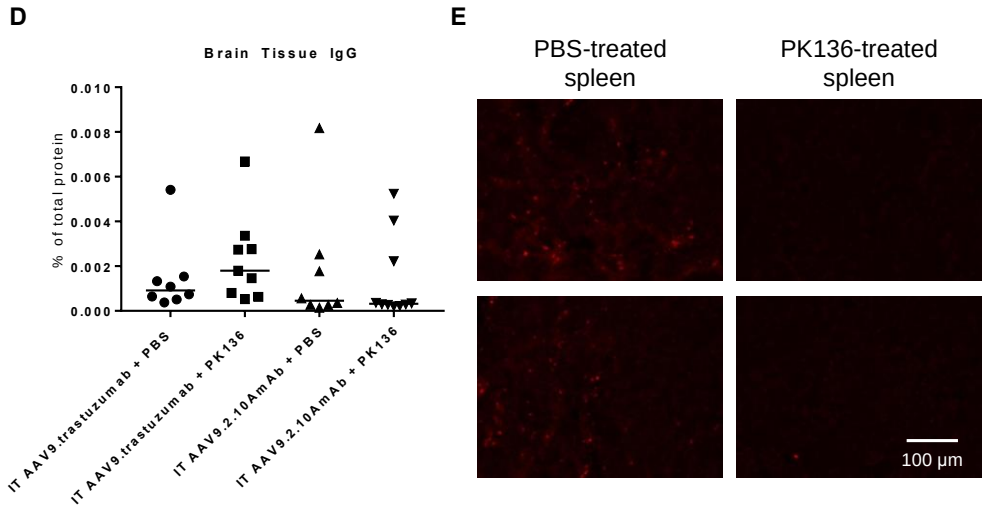

Fig. 5. IT AAV9.trastuzumab tumor prophylaxis in the setting of continuous NK cell depletion. (A) Kaplan-Meyer survival curves for mice that received IT AAV9.trastuzumab tumor prophylaxis or IT AAV9.2.10AmAb control treatment with or without continuous NK cell depletion using PK136 (anti-NK1.1 antibody). (B) Tabulated survival and statistical data for Fig. 5A. (C) *In situ* hybridization for *Ncr1* (*NKp46*) RNA (red) in formalin-fixed paraffin-embedded tumors harvested at necropsy from the experiment in Fig. 5A. DAPI (blue). (D) IgG transgene expression in brain tissue measured by protein A ELISA of brain homogenate and graphed as a percent of total protein in brain homogenate. (E) *In situ* hybridization of *Ncr1* RNA in formalin-fixed paraffin-embedded spleens harvested at necropsy.

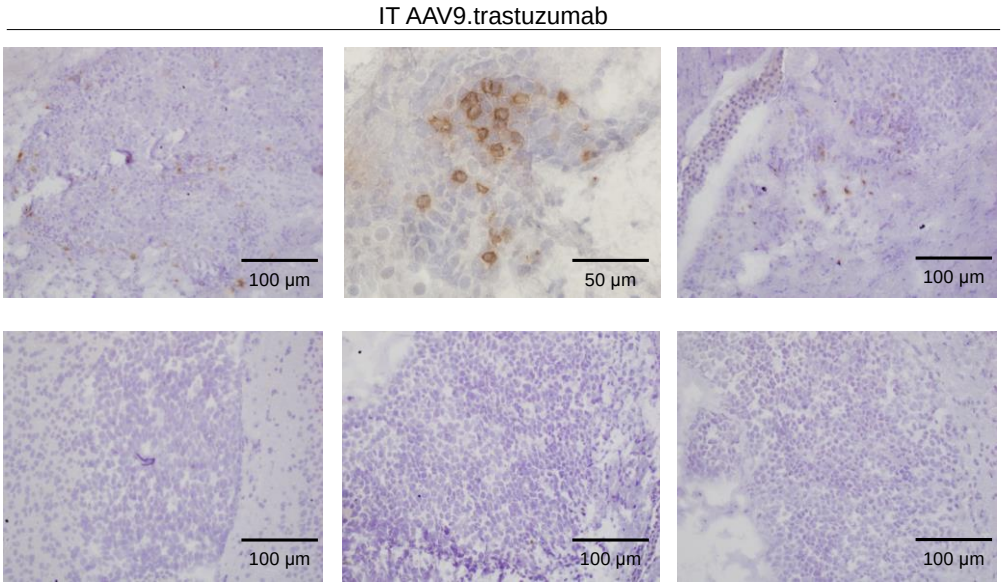

Fig. 6. NK cell immunohistochemical staining of day 20 tumors. Immunohistochemical staining for NK cells (Ly-49G2) performed on day 20 tumor cryosections.

A

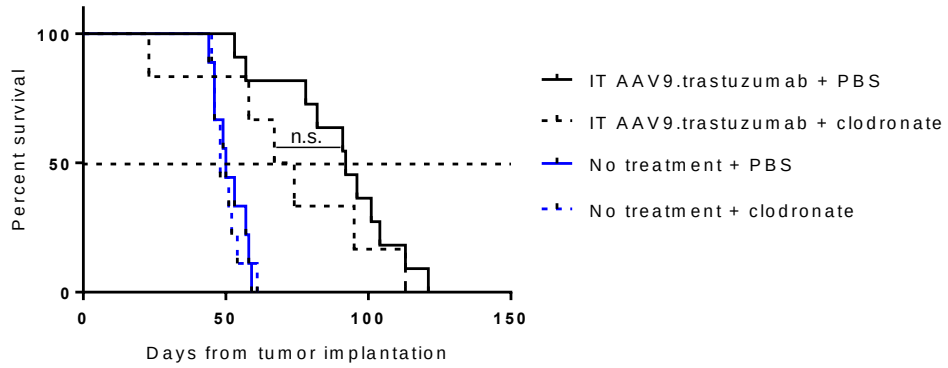

B

Treatment	*n*	Median survival (days)	p-value
IT AAV9.trastuzumab + PBS	11	92	<0.0001
IT AAV9.trastuzumab + clodronate	6	70.5	0.0117
No treatment + PBS	9	50	-
No treatment + clodronate	11	48	0.8462

C

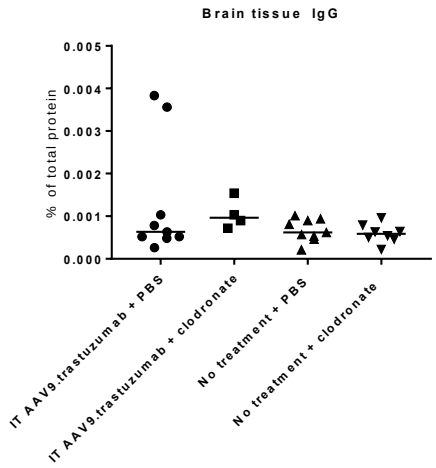

D

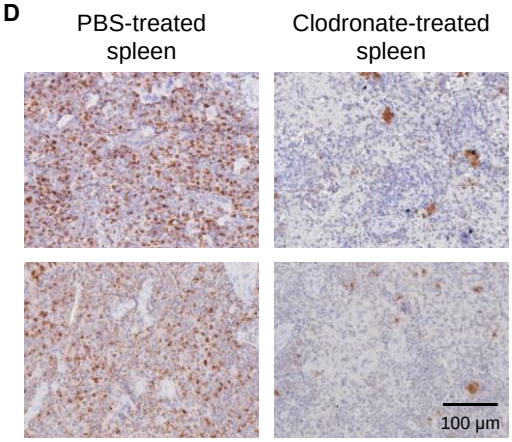

Fig. 7. IT AAV9.trastuzumab tumor prophylaxis in the setting of continuous systemic macrophage depletion. (A) Kaplan-Meyer survival curves for mice that received IT AAV9.trastuzumab tumor prophylaxis or IT AAV9.2.10AmAb control treatment with or without systemic macrophage depletion. (B) Tabulated survival and statistical data for Fig. 6A. (C) IgG transgene expression in brain tissue measured by protein A ELISA of brain homogenate and graphed as a percent of total protein in brain homogenate. (D) CD68 IHC staining of formalin-fixed paraffin-embedded spleens harvested at necropsy from animals treated with liposomal PBS or liposomal clodronate.

Supplementary Materials:

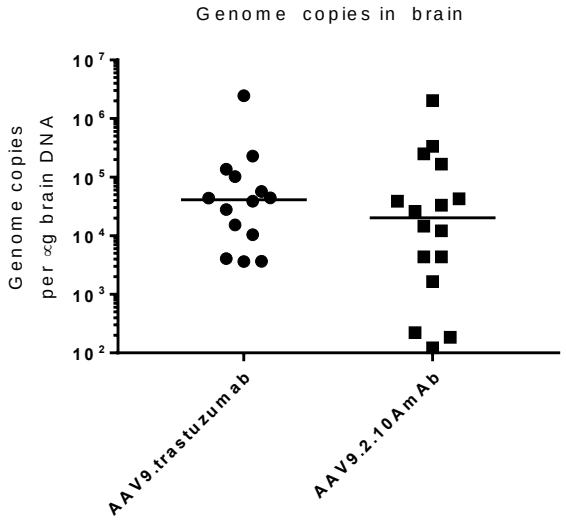

Fig S1. Biodistribution of vector genome copies in brain. AAV9 genome copies in brain tissue from experiment in Fig. 1 determined by qPCR.

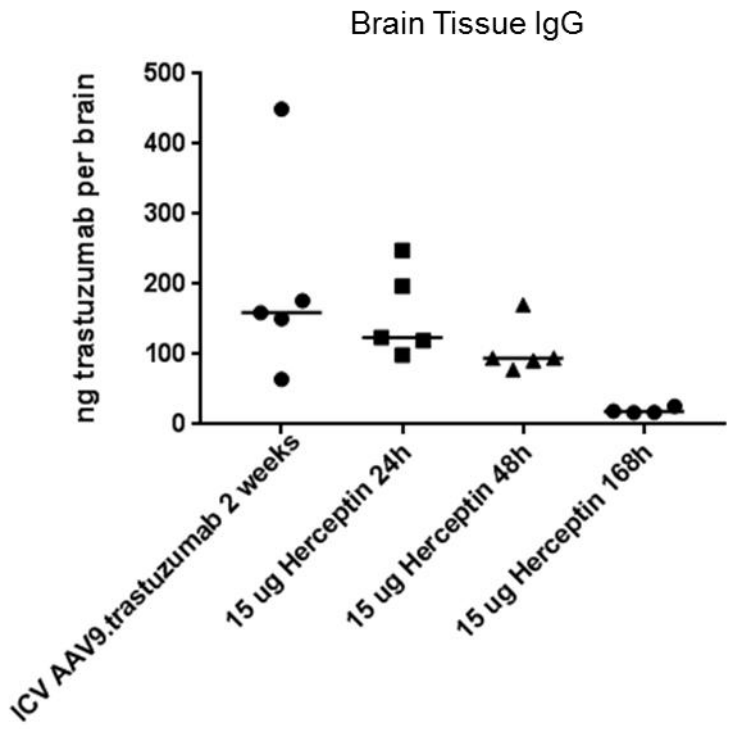

Fig S2. Trastuzumab quantified in brain tissue. 1e11 GC AAV9.trastuzumab or 15 µg Herceptin® in PBS was administered ICV to mice. Brains were harvested after the duration of time indicated for trastuzumab quantification in tissue.

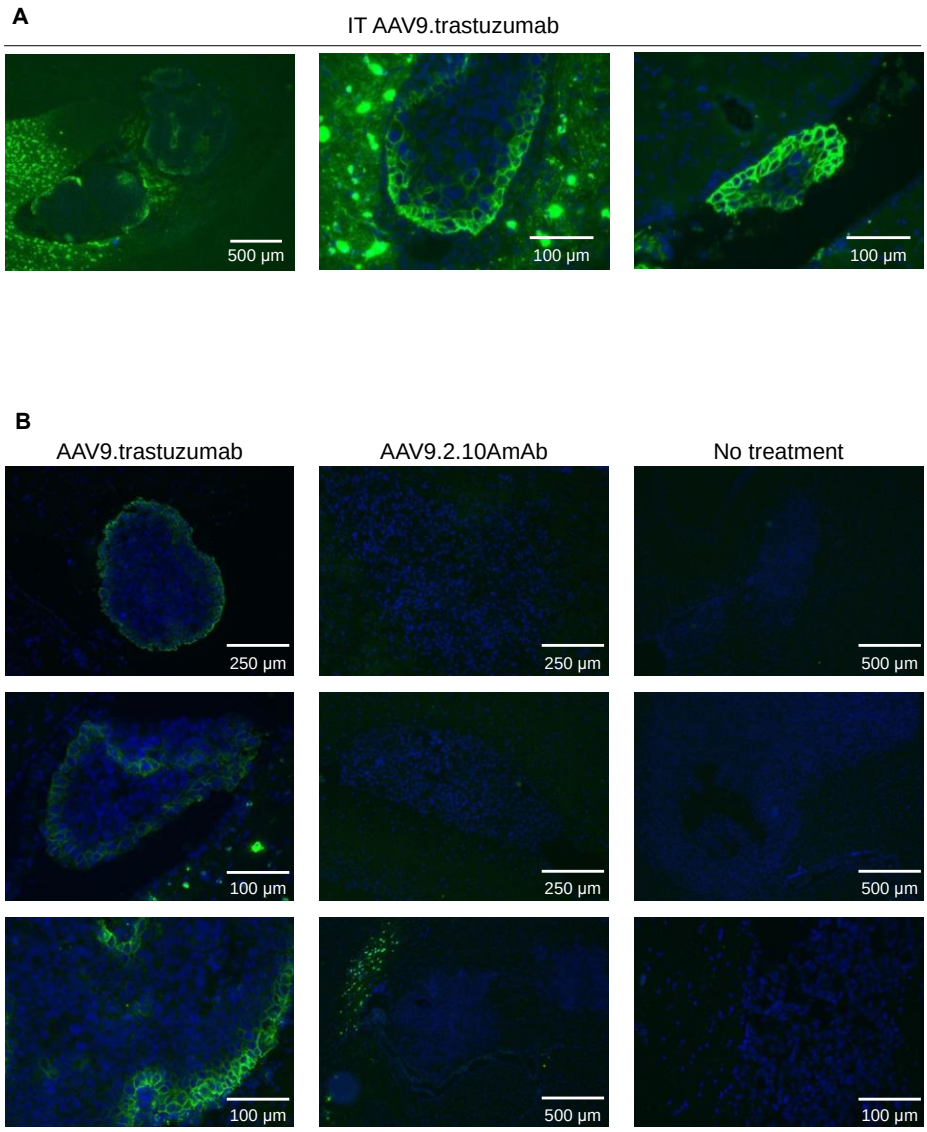

Fig S3. Anti-IgG immunofluorescence of day 20 and day 47 tumor cryosections. (A) Green channel (human/rhesus IgG) overexposures of day 47 tumors (Fig. 3D) from mice that received IT AAV9.trastuzumab prophylaxis. (B) anti-IgG immunofluorescence staining of day 20 tumor cryosections.

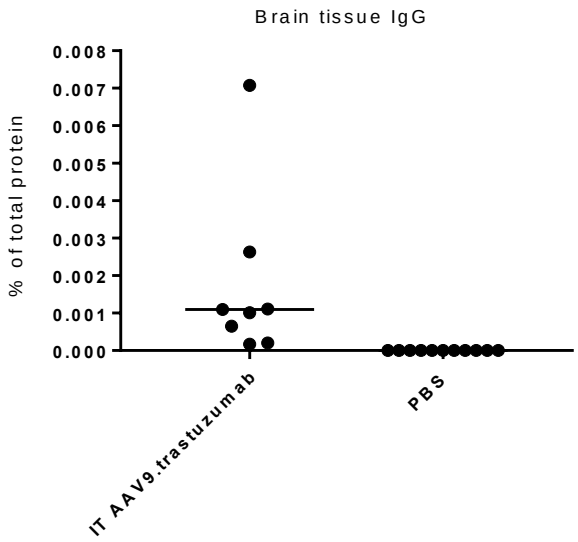

Fig S4. IgG expression in brain tissue. IgG transgene expression in brain tissue from experiment in Fig. 4 measured by protein A ELISA of brain homogenate and graphed as a percent of total protein in brain homogenate.

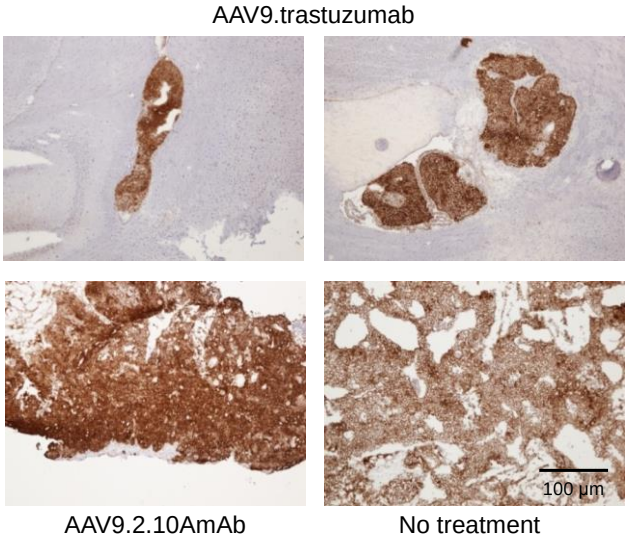

Fig S5. Human HER2 IHC staining of day 47 tumors. Positive HER2 immunohistochemistry staining of day 47 BT474.M1.ffluc tumors from the necropsies of mice in the experiment in Fig. 3D.

BIBLIOGRAPHY

1. Melnick, J.L., et al., *Association of 20-Millimicron Particles with Adenoviruses.* J Bacteriol, 1965. **90**(1): p. 4.
2. Calcedo, R. and J.M. Wilson, *Humoral Immune Response to AAV.* Front Immunol, 2013. **4**: p. 341.
3. Bell, P., et al., *Analysis of tumors arising in male B6C3F1 mice with and without AAV vector delivery to liver.* Mol Ther, 2006. **14**(1): p. 34-44.
4. Schlehofer, J.R., *The tumor suppressive properties of adeno-associated viruses.* Mutat Res, 1994. **305**(2): p. 303-13.
5. Dayton, R.D., D.B. Wang, and R.L. Klein, *The advent of AAV9 expands applications for brain and spinal cord gene delivery.* Expert Opin Biol Ther, 2012. **12**(6): p. 757-66.
6. Berns, K.I. and R.M. Linden, *The cryptic life style of adeno-associated virus.* Bioessays, 1995. **17**(3): p. 237-45.
7. Bartel, M., D. Schaffer, and H. Buning, *Enhancing the Clinical Potential of AAV Vectors by Capsid Engineering to Evade Pre-Existing Immunity.* Front Microbiol, 2011. **2**: p. 204.
8. Gao, G., et al., *Clades of Adeno-associated viruses are widely disseminated in human tissues.* J Virol, 2004. **78**(12): p. 6381-8.
9. Gao, G., et al., *Adeno-associated viruses undergo substantial evolution in primates during natural infections.* Proc Natl Acad Sci U S A, 2003. **100**(10): p. 6081-6.
10. Gao, G.P., et al., *Novel adeno-associated viruses from rhesus monkeys as vectors for human gene therapy.* Proc Natl Acad Sci U S A, 2002. **99**(18): p. 11854-9.
11. Maersch, S., et al., *Optimization of stealth adeno-associated virus vectors by randomization of immunogenic epitopes.* Virology, 2010. **397**(1): p. 167-75.
12. Maheshri, N., et al., *Directed evolution of adeno-associated virus yields enhanced gene delivery vectors.* Nat Biotechnol, 2006. **24**(2): p. 198-204.
13. Pillay, S., et al., *An essential receptor for adeno-associated virus infection.* Nature, 2016. **530**(7588): p. 108-12.
14. Bell, C.L., et al., *The AAV9 receptor and its modification to improve in vivo lung gene transfer in mice.* J. Clin. Invest., 2011. **121**(6): p. 2427-35.
15. Castle, M.J., et al., *Long-distance axonal transport of AAV9 is driven by dynein and kinesin-2 and is trafficked in a highly motile Rab7-positive compartment.* Mol Ther, 2014. **22**(3): p. 554-66.
16. Nonnenmacher, M. and T. Weber, *Adeno-associated virus 2 infection requires endocytosis through the CLIC/GEEC pathway.* Cell Host Microbe, 2011. **10**(6): p. 563-76.
17. Bartlett, J.S., R. Wilcher, and R.J. Samulski, *Infectious entry pathway of adeno-associated virus and adeno-associated virus vectors.* J Virol, 2000. **74**(6): p. 2777-85.
18. Ding, W., et al., *rAAV2 traffics through both the late and the recycling endosomes in a dose-dependent fashion.* Mol Ther, 2006. **13**(4): p. 671-82.
19. Bantel-Schaal, U., B. Hub, and J. Kartenbeck, *Endocytosis of adeno-associated virus type 5 leads to accumulation of virus particles in the Golgi compartment.* J Virol, 2002. **76**(5): p. 2340-9.
20. Sonntag, F., et al., *Adeno-associated virus type 2 capsids with externalized VP1/VP2 trafficking domains are generated prior to passage through the cytoplasm and are maintained until uncoating occurs in the nucleus.* J Virol, 2006. **80**(22): p. 11040-54.

21. Klein, R.L., D.B. Wang, and M.A. King, *Versatile somatic gene transfer for modeling neurodegenerative diseases.* Neurotox Res, 2009. **16**(3): p. 329-42.
22. McCown, T.J., *Adeno-Associated Virus (AAV) Vectors in the CNS.* Curr Gene Ther, 2011. **11**(3): p. 181-8.
23. Lentz, T.B., S.J. Gray, and R.J. Samulski, *Viral vectors for gene delivery to the central nervous system.* Neurobiol Dis, 2012. **48**(2): p. 179-88.
24. Lock, M., et al., *Rapid, simple, and versatile manufacturing of recombinant adeno-associated viral vectors at scale.* Hum Gene Ther, 2010. **21**(10): p. 1259-71.
25. Flotte, T.R., et al., *Phase 2 clinical trial of a recombinant adeno-associated viral vector expressing alpha1-antitrypsin: interim results.* Hum Gene Ther, 2011. **22**(10): p. 1239-47.
26. Wang, L., et al., *Sustained correction of disease in naive and AAV2-pretreated hemophilia B dogs: AAV2/8-mediated, liver-directed gene therapy.* Blood, 2005. **105**(8): p. 3079-86.
27. Calcedo, R., et al., *Worldwide epidemiology of neutralizing antibodies to adeno-associated viruses.* J Infect Dis, 2009. **199**(3): p. 381-90.
28. Boutin, S., et al., *Prevalence of serum IgG and neutralizing factors against adeno-associated virus (AAV) types 1, 2, 5, 6, 8, and 9 in the healthy population: implications for gene therapy using AAV vectors.* Hum Gene Ther, 2010. **21**(6): p. 704-12.
29. Mingozzi, F., et al., *Prevalence and pharmacological modulation of humoral immunity to AAV vectors in gene transfer to synovial tissue.* Gene Ther, 2013. **20**(4): p. 417-24.
30. Halbert, C.L., et al., *Prevalence of neutralizing antibodies against adeno-associated virus (AAV) types 2, 5, and 6 in cystic fibrosis and normal populations: Implications for gene therapy using AAV vectors.* Hum Gene Ther, 2006. **17**(4): p. 440-7.
31. Wang, L., et al., *Impact of pre-existing immunity on gene transfer to nonhuman primate liver with adeno-associated virus 8 vectors.* Hum Gene Ther, 2011. **22**(11): p. 1389-401.
32. Hurlbut, G.D., et al., *Preexisting immunity and low expression in primates highlight translational challenges for liver-directed AAV8-mediated gene therapy.* Mol Ther, 2010. **18**(11): p. 1983-94.
33. Monteilhet, V., et al., *A 10 patient case report on the impact of plasmapheresis upon neutralizing factors against adeno-associated virus (AAV) types 1, 2, 6, and 8.* Mol Ther, 2011. **19**(11): p. 2084-91.
34. Bryant, L.M., et al., *Lessons learned from the clinical development and market authorization of Glybera.* Hum Gene Ther Clin Dev, 2013. **24**(2): p. 55-64.
35. Silva, M.d., *FDA Advisory Committee Unanimously Recommends Approval of Investigational LUXTURNA™ (voretigene neparvovec) for Patients with Biallelic RPE65-mediated Inherited Retinal Disease*, in *Investigational LUXTURNA has the potential to be both the first pharmacologic treatment for an inherited retinal disease (IRD) and the first gene therapy for a genetic disease in the United States*. 2017, GLOBE NEWSWIRE: Philadelphia.
36. Eric Althoff, F.P., *Novartis receives first ever FDA approval for a CAR-T cell therapy, Kymriah(TM) (CTL019), for children and young adults with B-cell ALL that is refractory or has relapsed at least twice*. 2017, Novartis Corporate Media Relations Basel.
37. *Kymriah (tisagenlecleucel) Prescribing information*, N.P. Corporation, Editor.: East Hanover, New Jersey, USA.
38. Brinker, T., et al., *A new look at cerebrospinal fluid circulation.* Fluids Barriers CNS, 2014. **11**: p. 10.

39. J. Gordon McComb, *Recent research into the nature of cerebrospinal fluid formation and absorption.* Journal of Neurosurgery, 1983. **59**(3): p. 369-383.
40. Agamanolis, D., *Neuropathology*, in *An illustrated interactive course for medical students and residents*. 2012.
41. Gray, S.J., et al., *Global CNS gene delivery and evasion of anti-AAV-neutralizing antibodies by intrathecal AAV administration in non-human primates.* Gene Ther, 2013. **20**(4): p. 450-9.
42. Gray, S.J., et al., *Preclinical differences of intravascular AAV9 delivery to neurons and glia: a comparative study of adult mice and nonhuman primates.* Mol Ther, 2011. **19**(6): p. 1058-69.
43. Bevan, A.K., et al., *Systemic gene delivery in large species for targeting spinal cord, brain, and peripheral tissues for pediatric disorders.* Mol Ther, 2011. **19**(11): p. 1971-80.
44. Samaranch, L., et al., *Adeno-associated virus serotype 9 transduction in the central nervous system of nonhuman primates.* Hum Gene Ther, 2012. **23**(4): p. 382-9.
45. Foust, K.D., et al., *Intravascular AAV9 preferentially targets neonatal neurons and adult astrocytes.* Nat Biotechnol, 2009. **27**(1): p. 59-65.
46. Wang, D.B., et al., *Expansive gene transfer in the rat CNS rapidly produces amyotrophic lateral sclerosis relevant sequelae when TDP-43 is overexpressed.* Mol Ther, 2010. **18**(12): p. 2064-74.
47. Miyake, N., et al., *Global gene transfer into the CNS across the BBB after neonatal systemic delivery of single-stranded AAV vectors.* Brain Res, 2011. **1389**: p. 19-26.
48. Foust, K.D., et al., *Rescue of the spinal muscular atrophy phenotype in a mouse model by early postnatal delivery of SMN.* Nat Biotechnol, 2010. **28**(3): p. 271-4.
49. Hinderer, C., et al., *Widespread gene transfer in the central nervous system of cynomolgus macaques following delivery of AAV9 into the cisterna magna.* Mol Ther Methods Clin Dev, 2014. **1**: p. 14051.
50. Vite, C.H., et al., *Effective gene therapy for an inherited CNS disease in a large animal model.* Ann Neurol, 2005. **57**(3): p. 355-64.
51. McCurdy, V.J., et al., *Sustained normalization of neurological disease after intracranial gene therapy in a feline model.* Sci Transl Med, 2014. **6**(231): p. 231ra48.
52. Hinderer, C., et al., *Intrathecal gene therapy corrects CNS pathology in a feline model of mucopolysaccharidosis I.* Mol Ther, 2014. **22**(12): p. 2018-27.
53. Ommaya, A.K., *Subcutaneous reservoir and pump for sterile access to ventricular cerebrospinal fluid.* Lancet, 1963. **2**(7315): p. 983-4.
54. Sandberg, D.I., et al., *Ommaya reservoirs for the treatment of leptomeningeal metastases.* Neurosurgery, 2000. **47**(1): p. 49-54; discussion 54-5.
55. Vermeulen, M. and J. van Gijn, *The diagnosis of subarachnoid haemorrhage.* J Neurol Neurosurg Psychiatry, 1990. **53**(5): p. 365-72.
56. Cearley, C.N. and J.H. Wolfe, *Transduction characteristics of adeno-associated virus vectors expressing cap serotypes 7, 8, 9, and Rh10 in the mouse brain.* Mol Ther, 2006. **13**(3): p. 528-37.
57. Schuster, D.J., et al., *Biodistribution of adeno-associated virus serotype 9 (AAV9) vector after intrathecal and intravenous delivery in mouse.* Front Neuroanat, 2014. **8**: p. 42.
58. Samaranch, L., et al., *Strong cortical and spinal cord transduction after AAV7 and AAV9 delivery into the cerebrospinal fluid of nonhuman primates.* Hum Gene Ther, 2013. **24**(5): p. 526-32.

59. Federici, T., et al., *Robust spinal motor neuron transduction following intrathecal delivery of AAV9 in pigs.* Gene Ther, 2012. **19**(8): p. 852-9.
60. Lishner, M., et al., *Complications associated with Ommaya reservoirs in patients with cancer. The Princess Margaret Hospital experience and a review of the literature.* Arch Intern Med, 1990. **150**(1): p. 173-6.
61. Mead, P.A., et al., *Ommaya reservoir infections: a 16-year retrospective analysis.* J Infect, 2014. **68**(3): p. 225-30.
62. Szvalb, A.D., et al., *Ommaya reservoir-related infections: clinical manifestations and treatment outcomes.* J Infect, 2014. **68**(3): p. 216-24.
63. Obbens, E.A., et al., *Ommaya reservoirs in 387 cancer patients: a 15-year experience.* Neurology, 1985. **35**(9): p. 1274-8.
64. Dinndorf, P.A. and W.A. Bleyer, *Management of infectious complications of intraventricular reservoirs in cancer patients: low incidence and successful treatment without reservoir removal.* Cancer Drug Deliv, 1987. **4**(2): p. 105-17.
65. Gower, D.J. and V.C. Gower, *Infected Ommaya reservoirs.* Neurosurgery, 1988. **22**(6 Pt 1): p. 1116.
66. Mechleb, B., et al., *Late onset Ommaya reservoir infection due to Staphylococcus aureus: case report and review of Ommaya Infections.* J Infect, 2003. **46**(3): p. 196-8.
67. Perrin, R.G., et al., *Experience with Ommaya reservoir in 120 consecutive patients with meningeal malignancy.* Can J Neurol Sci, 1990. **17**(2): p. 190-2.
68. Jacobs, A., P. Clifford, and H.E. Kay, *The Ommaya reservoir in chemotherapy for malignant disease in the CNS.* Clin Oncol, 1981. **7**(2): p. 123-9.
69. Shapiro, W.R., et al., *Treatment of meningeal neoplasms.* Cancer Treat Rep, 1977. **61**(4): p. 733-43.
70. Bleyer, W.A., et al., *The Ommaya reservoir: newly recognized complications and recommendations for insertion and use.* Cancer, 1978. **41**(6): p. 2431-7.
71. DeAngelis, L.M., *Current diagnosis and treatment of leptomeningeal metastasis.* J Neurooncol, 1998. **38**(2-3): p. 245-52.
72. Quincke, H., *Lumbar Puncture*, in *Diseases of the Nervous System*, A. Church, Editor. 1909, Appleton: New York.
73. Johnson K., S.D. *Lumbar Puncture: Technique, indications, contraindications, and complications in adults.* . UpToDate, 2014. 1-14.
74. Eskey, C.J. and C.S. Ogilvy, *Fluoroscopy-guided lumbar puncture: decreased frequency of traumatic tap and implications for the assessment of CT-negative acute subarachnoid hemorrhage.* AJNR Am J Neuroradiol, 2001. **22**(3): p. 571-6.
75. Conroy, P.H., et al., *Real-time ultrasound-guided spinal anaesthesia: a prospective observational study of a new approach.* Anesthesiol Res Pract, 2013. **2013**: p. 525818.
76. Shaikh, F., et al., *Ultrasound imaging for lumbar punctures and epidural catheterisations: systematic review and meta-analysis.* BMJ, 2013. **346**: p. f1720.
77. Cronin, K., *Lumbar Puncture*, in *Textbook of Pediatric Emergency Medicine Procedures*, K.C. Henretig F., Editor. 1997, Lippincott Williams & Wilkins: Philadelphia. p. 541.
78. Tabaddor, K. and J.R. Lamorgese, *Lumbar epidermoid cyst following single spinal puncture. Case report.* J Bone Joint Surg Am, 1975. **57**(8): p. 1168-9.
79. Alstadhaug, K.B., et al., *Post-lumbar puncture headache.* Tidsskr Nor Laegeforen, 2012. **132**(7): p. 818-21.

80. Dripps, R.D. and L.D. Vandam, *Hazards of lumbar puncture.* J Am Med Assoc, 1951. **147**(12): p. 1118-21.
81. Paech, M.J., et al., *The volume of blood for epidural blood patch in obstetrics: a randomized, blinded clinical trial.* Anesth Analg, 2011. **113**(1): p. 126-33.
82. Evans, R.W., et al., *Assessment: prevention of post-lumbar puncture headaches: report of the therapeutics and technology assessment subcommittee of the american academy of neurology.* Neurology, 2000. **55**(7): p. 909-14.
83. Bezov, D., R.B. Lipton, and S. Ashina, *Post-dural puncture headache: part I diagnosis, epidemiology, etiology, and pathophysiology.* Headache, 2010. **50**(7): p. 1144-52.
84. Arendt, K., et al., *Atraumatic lumbar puncture needles: after all these years, are we still missing the point?* Neurologist, 2009. **15**(1): p. 17-20.
85. Lavi, R., et al., *Standard vs atraumatic Whitacre needle for diagnostic lumbar puncture: a randomized trial.* Neurology, 2006. **67**(8): p. 1492-4.
86. Crock, C., et al., *Headache after lumbar puncture: randomised crossover trial of 22-gauge versus 25-gauge needles.* Arch Dis Child, 2014. **99**(3): p. 203-7.
87. Chapman, P.H., E.R. Cosman, and M.A. Arnold, *The relationship between ventricular fluid pressure and body position in normal subjects and subjects with shunts: a telemetric study.* Neurosurgery, 1990. **26**(2): p. 181-9.
88. Hatfalvi, B.I., *Postulated mechanisms for postdural puncture headache and review of laboratory models. Clinical experience.* Reg Anesth, 1995. **20**(4): p. 329-36.
89. Vandam, L.D. and R.D. Dripps, *Long-term follow-up of patients who received 10,098 spinal anesthetics. IV. Neurological disease incident to traumatic lumbar puncture during spinal anesthesia.* J Am Med Assoc, 1960. **172**: p. 1483-7.
90. Jones, R.J., *The role of recumbency in the prevention and treatment of postspinal headache.* Anesth Analg, 1974. **53**(5): p. 788-96.
91. Camann, W.R., et al., *Effects of oral caffeine on postdural puncture headache. A double-blind, placebo-controlled trial.* Anesth Analg, 1990. **70**(2): p. 181-4.
92. Basurto Ona, X., D. Osorio, and X. Bonfill Cosp, *Drug therapy for treating post-dural puncture headache.* Cochrane Database of Systematic Reviews, 2015(7).
93. Gladstone, J.P., et al., *Spontaneous CSF leak treated with percutaneous CT-guided fibrin glue.* Neurology, 2005. **64**(10): p. 1818-9.
94. Schievink, W.I., et al., *Surgical treatment of spontaneous spinal cerebrospinal fluid leaks.* J Neurosurg, 1998. **88**(2): p. 243-6.
95. Adler, M.D., A.E. Comi, and A.R. Walker, *Acute hemorrhagic complication of diagnostic lumbar puncture.* Pediatr Emerg Care, 2001. **17**(3): p. 184-8.
96. Peltola, J., et al., *Spinal epidural haematoma complicating diagnostic lumbar puncture.* Lancet, 1996. **347**(8994): p. 131.
97. Baer, E.T., *Post-dural puncture bacterial meningitis.* Anesthesiology, 2006. **105**(2): p. 381-93.
98. Dodge , P.R. and M.N. Swartz *Bacterial Meningitis — a Review of Selected Aspects.* New England Journal of Medicine, 1965. **272**(19): p. 1003-1010.
99. McDonald, J.V. and T.E. Klump, *Intraspinal epidermoid tumors caused by lumbar puncture.* Arch Neurol, 1986. **43**(9): p. 936-9.
100. Halcrow, S.J., P.J. Crawford, and A.W. Craft, *Epidermoid spinal cord tumour after lumbar puncture.* Arch Dis Child, 1985. **60**(10): p. 978-9.

101. Kohler, G. and C. Milstein, *Continuous cultures of fused cells secreting antibody of predefined specificity.* Nature, 1975. **256**(5517): p. 495-7.
102. Nadler, L.M., et al., *Serotherapy of a patient with a monoclonal antibody directed against a human lymphoma-associated antigen.* Cancer Res, 1980. **40**(9): p. 3147-54.
103. Miller, R.A. and R. Levy, *Response of cutaneous T cell lymphoma to therapy with hybridoma monoclonal antibody.* Lancet, 1981. **2**(8240): p. 226-30.
104. Sears, H.F., et al., *Phase-I clinical trial of monoclonal antibody in treatment of gastrointestinal tumours.* Lancet, 1982. **1**(8275): p. 762-5.
105. 2014, N.M.A., *Physiology or Medicine 1984 - Press Release*. 1984, Nobelprize.org.
106. Reyes, F., et al., *ACVBP versus CHOP plus radiotherapy for localized aggressive lymphoma.* N Engl J Med, 2005. **352**(12): p. 1197-205.
107. Coiffier, B., *Rituximab in combination with CHOP improves survival in elderly patients with aggressive non-Hodgkin's lymphoma.* Semin Oncol, 2002. **29**(2 Suppl 6): p. 18-22.
108. Coiffier, B., et al., *CHOP chemotherapy plus rituximab compared with CHOP alone in elderly patients with diffuse large-B-cell lymphoma.* N Engl J Med, 2002. **346**(4): p. 235-42.
109. Roopenian, D.C. and S. Akilesh, *FcRn: the neonatal Fc receptor comes of age.* Nat Rev Immunol, 2007. **7**(9): p. 715-25.
110. Male, D.K., *Immunology*. 2013, Elsevier/Saunders,: United States. p. 1 online resource (x, 472 p.
111. Murphy, K.P., et al., *Janeway's immunobiology*. 8th ed. 2012, New York: Garland Science. xix, 868 p.
112. Levinson, W., *Review of Medical Microbiology and Immunology*. 11th ed. 2010, New York: McGraw Hill Medical. 632.
113. Chng, J., et al., *Cleavage efficient 2A peptides for high level monoclonal antibody expression in CHO cells.* mAbs, 2015. **7**(2): p. 403-412.
114. Balazs, A.B., et al., *Antibody-based protection against HIV infection by vectored immunoprophylaxis.* Nature, 2011. **481**(7379): p. 81-4.
115. Johnson, P.R., et al., *Vector-mediated gene transfer engenders long-lived neutralizing activity and protection against SIV infection in monkeys.* Nat Med, 2009. **15**(8): p. 901-6.
116. Cote, G.M., D.B. Sawyer, and B.A. Chabner, *ERBB2 inhibition and heart failure.* N Engl J Med, 2012. **367**(22): p. 2150-3.
117. Shenoy, C., et al., *Cardiovascular Complications of Breast Cancer Therapy in Older Adults.* The Oncologist, 2011. **16**(8): p. 1138-1143.
118. Baselga, J., *Phase I and II clinical trials of trastuzumab.* Ann Oncol, 2001. **12 Suppl 1**: p. S49-55.
119. Vu, T. and F.X. Claret, *Trastuzumab: updated mechanisms of action and resistance in breast cancer.* Front Oncol, 2012. **2**: p. 62.
120. Spector, N.L. and K.L. Blackwell, *Understanding the mechanisms behind trastuzumab therapy for human epidermal growth factor receptor 2-positive breast cancer.* J Clin Oncol, 2009. **27**(34): p. 5838-47.
121. Yarden, Y. and M.X. Sliwkowski, *Untangling the ErbB signalling network.* Nat Rev Mol Cell Biol, 2001. **2**(2): p. 127-37.
122. Park, J.W., et al., *Unraveling the biologic and clinical complexities of HER2.* Clin Breast Cancer, 2008. **8**(5): p. 392-401.

123. Pinkas-Kramarski, R., et al., *Diversification of Neu differentiation factor and epidermal growth factor signaling by combinatorial receptor interactions.* EMBO J, 1996. **15**(10): p. 2452-67.
124. Graus-Porta, D., et al., *ErbB-2, the preferred heterodimerization partner of all ErbB receptors, is a mediator of lateral signaling.* EMBO J, 1997. **16**(7): p. 1647-55.
125. Slamon, D.J., et al., *Human breast cancer: correlation of relapse and survival with amplification of the HER-2/neu oncogene.* Science, 1987. **235**(4785): p. 177-82.
126. Browne, B.C., et al., *HER-2 signaling and inhibition in breast cancer.* Curr Cancer Drug Targets, 2009. **9**(3): p. 419-38.
127. Loibl, S. and L. Gianni, *HER2-positive breast cancer.* Lancet, 2017. **389**(10087): p. 2415-2429.
128. Wolff, A.C., et al., *Recommendations for Human Epidermal Growth Factor Receptor 2 Testing in Breast Cancer: American Society of Clinical Oncology/College of American Pathologists Clinical Practice Guideline Update.* Journal of Clinical Oncology, 2013. **31**(31): p. 3997-4013.
129. Mustacchi, G., et al., *HER2-positive metastatic breast cancer: a changing scenario.* Crit Rev Oncol Hematol, 2015. **95**(1): p. 78-87.
130. Pauletti, G., et al., *Detection and quantitation of HER-2/neu gene amplification in human breast cancer archival material using fluorescence in situ hybridization.* Oncogene, 1996. **13**(1): p. 63-72.
131. Makino, K., et al., *Upregulation of IKKalpha/IKKbeta by integrin-linked kinase is required for HER2/neu-induced NF-kappaB antiapoptotic pathway.* Oncogene, 2004. **23**(21): p. 3883-7.
132. Bacus, S.S., et al., *AKT2 is frequently upregulated in HER-2/neu-positive breast cancers and may contribute to tumor aggressiveness by enhancing cell survival.* Oncogene, 2002. **21**(22): p. 3532-40.
133. Xia, W., et al., *Regulation of survivin by ErbB2 signaling: therapeutic implications for ErbB2-overexpressing breast cancers.* Cancer Res, 2006. **66**(3): p. 1640-7.
134. Gupta, S., *Trials and tribulations.* Nature, 2017. **548**(7666): p. S28-S31.
135. Fendly, B.M., et al., *Characterization of murine monoclonal antibodies reactive to either the human epidermal growth factor receptor or HER2/neu gene product.* Cancer Res, 1990. **50**(5): p. 1550-8.
136. Lewis, G.D., et al., *Differential responses of human tumor cell lines to anti-p185HER2 monoclonal antibodies.* Cancer Immunol Immunother, 1993. **37**(4): p. 255-63.
137. Carter, P., et al., *Humanization of an anti-p185HER2 antibody for human cancer therapy.* Proc Natl Acad Sci U S A, 1992. **89**(10): p. 4285-9.
138. Baselga, J., *Clinical trials of Herceptin(trastuzumab).* Eur J Cancer, 2001. **37 Suppl 1**: p. S18-24.
139. Shak, S., *Overview of the trastuzumab (Herceptin) anti-HER2 monoclonal antibody clinical program in HER2-overexpressing metastatic breast cancer. Herceptin Multinational Investigator Study Group.* Semin Oncol, 1999. **26**(4 Suppl 12): p. 71-7.
140. Baselga, J., et al., *Phase II study of weekly intravenous recombinant humanized anti-p185HER2 monoclonal antibody in patients with HER2/neu-overexpressing metastatic breast cancer.* J Clin Oncol, 1996. **14**(3): p. 737-44.

141. Baselga, J., et al., *Phase II study of weekly intravenous trastuzumab (Herceptin) in patients with HER2/neu-overexpressing metastatic breast cancer.* Semin Oncol, 1999. **26**(4 Suppl 12): p. 78-83.
142. Baselga, J., *Clinical trials of Herceptin(R) (trastuzumab).* Eur J Cancer, 2001. **37 Suppl 1**: p. 18-24.
143. Eiermann, W. and G. International Herceptin Study, *Trastuzumab combined with chemotherapy for the treatment of HER2-positive metastatic breast cancer: pivotal trial data.* Ann Oncol, 2001. **12 Suppl 1**: p. S57-62.
144. Romond, E.H., et al., *Trastuzumab plus adjuvant chemotherapy for operable HER2-positive breast cancer.* N Engl J Med, 2005. **353**(16): p. 1673-84.
145. Genentech, *Biotechnology Breakthrough in Breast Cancer Wins FDA Approval*, in *New Therapy for a Quarter of Women with Metastatic Breast Cancer; Testing for Protein Overexpression Critical* 1998: South San Francisco, California.
146. Genentech, *FDA Approves Herceptin for the Adjuvant Treatment of HER2-Positive Node-Positive Breast Cancer* 2006: South San Francisco, California.
147. Dieras, V. and T. Bachelot, *The success story of trastuzumab emtansine, a targeted therapy in HER2-positive breast cancer.* Target Oncol, 2014. **9**(2): p. 111-22.
148. von Minckwitz, G., et al., *Adjuvant Pertuzumab and Trastuzumab in Early HER2-Positive Breast Cancer.* N Engl J Med, 2017. **377**(2): p. 122-131.
149. Weiner, G.J., *Rituximab: mechanism of action.* Seminars in hematology, 2010. **47**(2): p. 115-123.
150. Vogel, C.L., et al., *Efficacy and safety of trastuzumab as a single agent in first-line treatment of HER2-overexpressing metastatic breast cancer.* J Clin Oncol, 2002. **20**(3): p. 719-26.
151. Clynes, R.A., et al., *Inhibitory Fc receptors modulate in vivo cytotoxicity against tumor targets.* Nat Med, 2000. **6**(4): p. 443-6.
152. Gennari, R., et al., *Pilot study of the mechanism of action of preoperative trastuzumab in patients with primary operable breast tumors overexpressing HER2.* Clin Cancer Res, 2004. **10**(17): p. 5650-5.
153. Arnould, L., et al., *Trastuzumab-based treatment of HER2-positive breast cancer: an antibody-dependent cellular cytotoxicity mechanism?* Br J Cancer, 2006. **94**(2): p. 259-67.
154. Yakes, F.M., et al., *Herceptin-induced inhibition of phosphatidylinositol-3 kinase and Akt Is required for antibody-mediated effects on p27, cyclin D1, and antitumor action.* Cancer Res, 2002. **62**(14): p. 4132-41.
155. Asanuma, H., et al., *Survivin expression is regulated by coexpression of human epidermal growth factor receptor 2 and epidermal growth factor receptor via phosphatidylinositol 3-kinase/AKT signaling pathway in breast cancer cells.* Cancer Res, 2005. **65**(23): p. 11018-25.
156. Molina, M.A., et al., *Trastuzumab (herceptin), a humanized anti-Her2 receptor monoclonal antibody, inhibits basal and activated Her2 ectodomain cleavage in breast cancer cells.* Cancer Res, 2001. **61**(12): p. 4744-9.
157. Xia, W., et al., *Truncated ErbB2 receptor (p95ErbB2) is regulated by heregulin through heterodimer formation with ErbB3 yet remains sensitive to the dual EGFR/ErbB2 kinase inhibitor GW572016.* Oncogene, 2004. **23**(3): p. 646-53.

158. Izumi, Y., et al., *Tumour biology: Herceptin acts as an anti-angiogenic cocktail.* Nature, 2002. **416**(6878): p. 279-280.
159. Pietras, R.J., et al., *Remission of human breast cancer xenografts on therapy with humanized monoclonal antibody to HER-2 receptor and DNA-reactive drugs.* Oncogene, 1998. **17**(17): p. 2235-49.
160. Pietras, R.J., et al., *Monoclonal antibody to HER-2/neureceptor modulates repair of radiation-induced DNA damage and enhances radiosensitivity of human breast cancer cells overexpressing this oncogene.* Cancer Res, 1999. **59**(6): p. 1347-55.
161. Slamon, D.J., et al., *Use of chemotherapy plus a monoclonal antibody against HER2 for metastatic breast cancer that overexpresses HER2.* N Engl J Med, 2001. **344**.
162. Park, Y., et al., *Current status of therapy for breast cancer worldwide and in Japan.* World J Clin Oncol, 2011. **2**(2): p. 125-34.
163. Onitilo, A.A., J.M. Engel, and R.V. Stankowski, *Cardiovascular toxicity associated with adjuvant trastuzumab therapy: prevalence, patient characteristics, and risk factors.* Therapeutic Advances in Drug Safety, 2014. **5**(4): p. 154-166.
164. Crone, S.A. and K.F. Lee, *Gene targeting reveals multiple essential functions of the neuregulin signaling system during development of the neuroendocrine and nervous systems.* Ann N Y Acad Sci, 2002. **971**: p. 547-53.
165. Garcia-Rivello, H., et al., *Dilated cardiomyopathy in Erb-b4-deficient ventricular muscle.* Am J Physiol Heart Circ Physiol, 2005. **289**(3): p. H1153-60.
166. Ozcelik, C., et al., *Conditional mutation of the ErbB2 (HER2) receptor in cardiomyocytes leads to dilated cardiomyopathy.* Proc Natl Acad Sci U S A, 2002. **99**(13): p. 8880-5.
167. De Keulenaer, G.W., K. Doggen, and K. Lemmens, *The Vulnerability of the Heart As a Pluricellular Paracrine Organ.* Lessons From Unexpected Triggers of Heart Failure in Targeted ErbB2 Anticancer Therapy, 2010. **106**(1): p. 35-46.
168. Pentassuglia, L. and D.B. Sawyer, *The role of Neuregulin-1beta/ErbB signaling in the heart.* Exp Cell Res, 2009. **315**(4): p. 627-37.
169. Moja, L., et al., *Trastuzumab containing regimens for early breast cancer.* Cochrane Database of Systematic Reviews, 2012(4).
170. Romond, E.H., et al., *Seven-Year Follow-Up Assessment of Cardiac Function in NSABP B-31, a Randomized Trial Comparing Doxorubicin and Cyclophosphamide Followed by Paclitaxel (ACP) With ACP Plus Trastuzumab As Adjuvant Therapy for Patients With Node-Positive, Human Epidermal Growth Factor Receptor 2–Positive Breast Cancer.* Journal of Clinical Oncology, 2012. **30**(31): p. 3792-3799.
171. Azambuja, E.d., et al., *Trastuzumab-Associated Cardiac Events at 8 Years of Median Follow-Up in the Herceptin Adjuvant Trial (BIG 1-01).* Journal of Clinical Oncology, 2014. **32**(20): p. 2159-2165.
172. Guarneri, V., et al., *Long-Term Cardiac Tolerability of Trastuzumab in Metastatic Breast Cancer: The M.D. Anderson Cancer Center Experience.* Journal of Clinical Oncology, 2006. **24**(25): p. 4107-4115.
173. Sendur, M.A.N., S. Aksoy, and K. Altundag, *Cardiotoxicity of novel HER2-targeted therapies.* Current Medical Research and Opinion, 2013. **29**(8): p. 1015-1024.
174. Bendell, J.C., et al., *Central nervous system metastases in women who receive trastuzumab-based therapy for metastatic breast carcinoma.* Cancer, 2003. **97**(12): p. 2972-7.

175. Lin, N.U., J.R. Bellon, and E.P. Winer, *CNS metastases in breast cancer.* J Clin Oncol, 2004. **22**(17): p. 3608-17.
176. Souglakos, J., et al., *Central nervous system relapse in patients with breast cancer is associated with advanced stages, with the presence of circulating occult tumor cells and with the HER2/neu status.* Breast Cancer Research, 2006. **8**(4): p. R36.
177. Clayton, A.J., et al., *Incidence of cerebral metastases in patients treated with trastuzumab for metastatic breast cancer.* Br J Cancer, 2004. **91**.
178. Stemmler, H.J., et al., *Characteristics of patients with brain metastases receiving trastuzumab for HER2 overexpressing metastatic breast cancer.* Breast, 2006. **15**(2): p. 219-25.
179. Yau, T., et al., *Incidence, pattern and timing of brain metastases among patients with advanced breast cancer treated with trastuzumab.* Acta Oncol, 2006. **45**(2): p. 196-201.
180. Barnholtz-Sloan, J.S., et al., *Incidence proportions of brain metastases in patients diagnosed (1973 to 2001) in the Metropolitan Detroit Cancer Surveillance System.* J Clin Oncol, 2004. **22**(14): p. 2865-72.
181. Tsukada, Y., et al., *Central nervous system metastasis from breast carcinoma. Autopsy study.* Cancer, 1983. **52**(12): p. 2349-54.
182. Patanaphan, V., O.M. Salazar, and R. Risco, *Breast cancer: metastatic patterns and their prognosis.* South Med J, 1988. **81**(9): p. 1109-12.
183. Wardley AM, D.S., Clayton AJ, et al., *High incidence of brain metastases in patients treated with trastuzumab for metastatic breast cancer at a large cancer center [abstract].* . Proc Am Soc Clin Oncol. , 2002. **241**.
184. Eitzen R, Z.L., Kaufman B, et al. , *High incidence of brain metastases (BM) in patients on trastuzumab (H) for advanced breast cancer [abstract].* . Proc Am Soc Clin Oncol, 2002. **31b**.
185. Bartolotti, M., E. Franceschi, and A.A. Brandes, *Treatment of brain metastases from HER-2-positive breast cancer: current status and new concepts.* Future Oncol, 2013. **9**(11): p. 1653-64.
186. Leyland-Jones, B., *Human epidermal growth factor receptor 2-positive breast cancer and central nervous system metastases.* J Clin Oncol, 2009. **27**(31): p. 5278-86.
187. Park, I.H., et al., *Concordant HER2 status between metastatic breast cancer cells in CSF and primary breast cancer tissue.* Breast Cancer Research and Treatment, 2010. **123**(1): p. 125-128.
188. Leone, J.P., et al., *Prognostic factors and survival according to tumour subtype in women presenting with breast cancer brain metastases at initial diagnosis.* Eur J Cancer, 2017. **74**: p. 17-25.
189. Martin, A.M., et al., *Brain Metastases in Newly Diagnosed Breast Cancer: A Population-Based Study.* JAMA Oncol, 2017.
190. Dawood, S., et al., *Prognosis of Women With Metastatic Breast Cancer by HER2 Status and Trastuzumab Treatment: An Institutional-Based Review.* Journal of Clinical Oncology, 2010. **28**(1): p. 92-98.
191. Kennecke, H., et al., *Metastatic behavior of breast cancer subtypes.* J Clin Oncol, 2010. **28**(20): p. 3271-7.
192. Gaedcke, J., et al., *Predominance of the basal type and HER-2/neu type in brain metastasis from breast cancer.* Mod Pathol, 2007. **20**(8): p. 864-70.

193. Gori, S., et al., *Central nervous system metastases in HER-2 positive metastatic breast cancer patients treated with trastuzumab: incidence, survival, and risk factors.* Oncologist, 2007. **12**(7): p. 766-73.
194. Lin, N.U. and E.P. Winer, *Brain metastases: the HER2 paradigm.* Clin Cancer Res, 2007. **13**(6): p. 1648-55.
195. Cho, S.Y. and H.Y. Choi, *Causes of death and metastatic patterns in patients with mammary cancer. Ten-year autopsy study.* Am J Clin Pathol, 1980. **73**(2): p. 232-4.
196. Lee, Y.T., *Breast carcinoma: pattern of metastasis at autopsy.* J Surg Oncol, 1983. **23**(3): p. 175-80.
197. Niikura, N., et al., *Changes in tumor expression of HER2 and hormone receptors status after neoadjuvant chemotherapy in 21,755 patients from the Japanese breast cancer registry.* Ann Oncol, 2016. **27**(3): p. 480-7.
198. Brufsky, A.M., et al., *Central nervous system metastases in patients with HER2-positive metastatic breast cancer: incidence, treatment, and survival in patients from registHER.* Clin Cancer Res, 2011. **17**(14): p. 4834-43.
199. Pieńkowski, T. and C.C. Zielinski, *Trastuzumab treatment in patients with breast cancer and metastatic CNS disease.* Annals of Oncology, 2010. **21**(5): p. 917-924.
200. Weil, R.J., et al., *Breast cancer metastasis to the central nervous system.* Am J Pathol, 2005. **167**(4): p. 913-20.
201. Kaal, E.C. and C.J. Vecht, *CNS complications of breast cancer: current and emerging treatment options.* CNS Drugs, 2007. **21**(7): p. 559-79.
202. Gabos, Z., et al., *Prognostic significance of human epidermal growth factor receptor positivity for the development of brain metastasis after newly diagnosed breast cancer.* J Clin Oncol, 2006. **24**(36): p. 5658-63.
203. Miller, K.D., et al., *Occult central nervous system involvement in patients with metastatic breast cancer: prevalence, predictive factors and impact on overall survival.* Ann Oncol, 2003. **14**(7): p. 1072-7.
204. Morikawa, A., et al., *Characteristics and Outcomes of Patients With Breast Cancer With Leptomeningeal Metastasis.* Clin Breast Cancer, 2017. **17**(1): p. 23-28.
205. Sahebjam, S., et al., *Experimental Treatments for Leptomeningeal Metastases From Solid Malignancies.* Cancer Control, 2017. **24**(1): p. 42-46.
206. Le Rhun, E., S. Taillibert, and M.C. Chamberlain, *Carcinomatous meningitis: Leptomeningeal metastases in solid tumors.* Surg Neurol Int, 2013. **4**(Suppl 4): p. S265-88.
207. Kim, H.J., et al., *Clinical outcome of central nervous system metastases from breast cancer: differences in survival depending on systemic treatment.* J Neurooncol, 2012. **106**(2): p. 303-13.
208. Yust-Katz, S., et al., *Breast cancer and leptomeningeal disease (LMD): hormone receptor status influences time to development of LMD and survival from LMD diagnosis.* J Neurooncol, 2013. **114**(2): p. 229-35.
209. Lin, N.U., *Breast cancer brain metastases: new directions in systemic therapy.* ecancermedicalscience, 2013. **7**: p. 307.
210. Cobleigh, M.A., et al., *Multinational study of the efficacy and safety of humanized anti-HER2 monoclonal antibody in women who have HER2-overexpressing metastatic breast cancer that has progressed after chemotherapy for metastatic disease.* J Clin Oncol, 1999. **17**(9): p. 2639-2648.

211. Kirsch, D.G., et al., *Survival after brain metastases from breast cancer in the trastuzumab era.* J Clin Oncol, 2005. **23**(9): p. 2114-6; author reply 2116-7.
212. Heinrich B, B.O., Siekiera W, et al. , *Development of brain metastases in metastatic breast cancer (MBC) responding to treatment with trastuzumab [abstract 147]. .* Proc Am Soc Clin Oncol 2003. **22**(37).
213. Bachelot, T., et al., *Lapatinib plus capecitabine in patients with previously untreated brain metastases from HER2-positive metastatic breast cancer (LANDSCAPE): a single-group phase 2 study.* The Lancet Oncology, 2013. **14**(1): p. 64-71.
214. Pivot, X., et al., *CEREBEL (EGF111438): A Phase III, Randomized, Open-Label Study of Lapatinib Plus Capecitabine Versus Trastuzumab Plus Capecitabine in Patients With Human Epidermal Growth Factor Receptor 2–Positive Metastatic Breast Cancer.* Journal of Clinical Oncology, 2015. **33**(14): p. 1564-1573.
215. Cascadian Therapeutics, I., *Cascadian Therapeutics' Lead Candidate, Tucatinib, Receives Orphan Drug Designation from FDA for Treatment of Breast Cancer Patients with Brain Metastases*. 2017, GlobeNewswire: Seattle.
216. Pestalozzi, B.C. and S. Brignoli, *Trastuzumab in CSF.* Journal of Clinical Oncology, 2000. **18**(11): p. 2349-2351.
217. Janin, G.B.a.A., *Passage of Humanized Monoclonal Antibodies Across the Blood-Brain Barrier: Relevance in the Treatment of Cancer Brain Metastases?* Journal of Applied Biopharmaceutics and Pharmacokinetics, 2014. **2**: p. 8.
218. Abuqayyas, L. and J.P. Balthasar, *Investigation of the role of FcgammaR and FcRn in mAb distribution to the brain.* Mol Pharm, 2013. **10**(5): p. 1505-13.
219. Zagouri, F., et al., *Intrathecal administration of trastuzumab for the treatment of meningeal carcinomatosis in HER2-positive metastatic breast cancer: a systematic review and pooled analysis.* Breast Cancer Res Treat, 2013. **139**(1): p. 13-22.
220. Bousquet, G., et al., *Intrathecal Trastuzumab Halts Progression of CNS Metastases in Breast Cancer.* J Clin Oncol, 2016. **34**(16): p. e151-5.
221. Colozza, M., et al., *Extended survival of a HER-2-positive metastatic breast cancer patient with brain metastases also treated with intrathecal trastuzumab.* Cancer Chemother Pharmacol, 2009. **63**(6): p. 1157-9.
222. Rubenstein, J.L., et al., *Phase I study of intraventricular administration of rituximab in patients with recurrent CNS and intraocular lymphoma.* J Clin Oncol, 2007. **25**(11): p. 1350-6.
223. Rubenstein, J.L., et al., *Multicenter phase 1 trial of intraventricular immunochemotherapy in recurrent CNS lymphoma.* Blood, 2013. **121**(5): p. 745-751.
224. Hollebecque, A., et al., *First case report of intrathecal panitumumab for treatment of meningeal carcinomatousis in an EGFR mutant lung adenocarcinoma patient.* Lung Cancer, 2013. **80**(1): p. 113-114.
225. Braen, A.P., et al., *A 4-week intrathecal toxicity and pharmacokinetic study with trastuzumab in cynomolgus monkeys.* Int J Toxicol, 2010. **29**(3): p. 259-67.
226. McKeage, K. and C.M. Perry, *Trastuzumab: a review of its use in the treatment of metastatic breast cancer overexpressing HER2.* Drugs, 2002. **62**(1): p. 209-43.
227. Leyland-Jones, B., et al., *Pharmacokinetics, safety, and efficacy of trastuzumab administered every three weeks in combination with paclitaxel.* J Clin Oncol, 2003. **21**(21): p. 3965-71.
228. *https://www.cancer.gov/types/common-cancers#1.* p. Accessed 21 July 2017.

229. Koo, T. and I.A. Kim, *Brain metastasis in human epidermal growth factor receptor 2-positive breast cancer: from biology to treatment.* Radiat Oncol J, 2016. **34**(1): p. 1-9.
230. Clayton, A.J., et al., *Incidence of cerebral metastases in patients treated with trastuzumab for metastatic breast cancer.* Br J Cancer, 2004. **91**(4): p. 639-43.
231. Mehta, A.I., A.M. Brufsky, and J.H. Sampson, *Therapeutic approaches for HER2-positive brain metastases: circumventing the blood-brain barrier.* Cancer Treat Rev, 2013. **39**(3): p. 261-9.
232. Forsyth, P.A., et al., *Prophylactic anticonvulsants in patients with brain tumour.* Can J Neurol Sci, 2003. **30**(2): p. 106-12.
233. Glantz, M.J., et al., *A randomized, blinded, placebo-controlled trial of divalproex sodium prophylaxis in adults with newly diagnosed brain tumors.* Neurology, 1996. **46**(4): p. 985-91.
234. Park, I.H., et al., *Trastuzumab treatment beyond brain progression in HER2-positive metastatic breast cancer.* Ann Oncol, 2009. **20**(1): p. 56-62.
235. Ramakrishna, N., et al., *Recommendations on disease management for patients with advanced human epidermal growth factor receptor 2-positive breast cancer and brain metastases: American Society of Clinical Oncology clinical practice guideline.* J Clin Oncol, 2014. **32**(19): p. 2100-8.
236. Stemmler, H.J., et al., *Ratio of trastuzumab levels in serum and cerebrospinal fluid is altered in HER2-positive breast cancer patients with brain metastases and impairment of blood-brain barrier.* Anticancer Drugs, 2007. **18**(1): p. 23-8.
237. Sperduto, P.W., et al., *Summary report on the graded prognostic assessment: an accurate and facile diagnosis-specific tool to estimate survival for patients with brain metastases.* J Clin Oncol, 2012. **30**(4): p. 419-25.
238. Slamon, D.J., et al., *Use of chemotherapy plus a monoclonal antibody against HER2 for metastatic breast cancer that overexpresses HER2.* N Engl J Med, 2001. **344**(11): p. 783-92.
239. Bergman, I., et al., *Pharmacokinetics of IgG and IgM anti-ganglioside antibodies in rats and monkeys after intrathecal administration.* J Pharmacol Exp Ther, 1998. **284**(1): p. 111-5.
240. Shi, Y., et al., *Trastuzumab triggers phagocytic killing of high HER2 cancer cells in vitro and in vivo by interaction with Fcgamma receptors on macrophages.* J Immunol, 2015. **194**(9): p. 4379-86.
241. Bruhns, P., *Properties of mouse and human IgG receptors and their contribution to disease models.* Blood, 2012. **119**(24): p. 5640-9.
242. Overdijk, M.B., et al., *Crosstalk between Human IgG Isotypes and Murine Effector Cells.* The Journal of Immunology, 2012.
243. Mayer, E.L. and N.U. Lin, *Long Term Follow-Up of National Surgical Adjuvant Breast and Bowel Project Trial B-31: How Well Can We Predict Cardiac Toxicity With Trastuzumab?* Journal of Clinical Oncology, 2012. **30**(31): p. 3.
244. de Azambuja, E., et al., *Trastuzumab-associated cardiac events at 8 years of median follow-up in the Herceptin Adjuvant trial (BIG 1-01).* J Clin Oncol, 2014. **32**(20): p. 2159-65.
245. Mantarro, S., et al., *Risk of severe cardiotoxicity following treatment with trastuzumab: a meta-analysis of randomized and cohort studies of 29,000 women with breast cancer.* Intern Emerg Med, 2016. **11**(1): p. 123-40.

246. Rivera, V.M., et al., *Long-term pharmacologically regulated expression of erythropoietin in primates following AAV-mediated gene transfer.* Blood, 2005. **105**(4): p. 1424-30.
247. Nathwani, A.C., et al., *Long-term safety and efficacy of factor IX gene therapy in hemophilia B.* N Engl J Med, 2014. **371**(21): p. 1994-2004.
248. Grossi, P.M., et al., *Efficacy of intracerebral microinfusion of trastuzumab in an athymic rat model of intracerebral metastatic breast cancer.* Clin Cancer Res, 2003. **9**(15): p. 5514-20.
249. Nakayama, A., et al., *Antitumor Activity of TAK-285, an Investigational, Non-Pgp Substrate HER2/EGFR Kinase Inhibitor, in Cultured Tumor Cells, Mouse and Rat Xenograft Tumors, and in an HER2-Positive Brain Metastasis Model.* J Cancer, 2013. **4**(7): p. 557-65.
250. Nanni, P., et al., *Multiorgan metastasis of human HER-2+ breast cancer in Rag2-/-;Il2rg-/- mice and treatment with PI3K inhibitor.* PLoS One, 2012. **7**(6): p. e39626.
251. Park, E.J., et al., *Ultrasound-mediated blood-brain/blood-tumor barrier disruption improves outcomes with trastuzumab in a breast cancer brain metastasis model.* J Control Release, 2012. **163**(3): p. 277-84.
252. Kodack, D.P., et al., *Combined targeting of HER2 and VEGFR2 for effective treatment of HER2-amplified breast cancer brain metastases.* Proc Natl Acad Sci U S A, 2012. **109**(45): p. E3119-27.
253. Gakhar, G., et al., *Hydronephrosis and urine retention in estrogen-implanted athymic nude mice.* Vet Pathol, 2009. **46**(3): p. 505-8.
254. Levin-Allerhand, J.A., K. Sokol, and J.D. Smith, *Safe and effective method for chronic 17beta-estradiol administration to mice.* Contemp Top Lab Anim Sci, 2003. **42**(6): p. 33-5.
255. Pearse, G., et al., *Urinary retention and cystitis associated with subcutaneous estradiol pellets in female nude mice.* Toxicol Pathol, 2009. **37**(2): p. 227-34.
256. Pestalozzi, B.C., et al., *Identifying breast cancer patients at risk for Central Nervous System (CNS) metastases in trials of the International Breast Cancer Study Group (IBCSG).* Annals of Oncology, 2006. **17**(6): p. 935-944.
257. Calias, P., et al., *Intrathecal delivery of protein therapeutics to the brain: a critical reassessment.* Pharmacol Ther, 2014. **144**(2): p. 114-22.
258. Mir, O., et al., *High-dose intrathecal trastuzumab for leptomeningeal metastases secondary to HER-2 overexpressing breast cancer.* Ann Oncol, 2008. **19**(11): p. 1978-80.
259. Kordbacheh, T., W.Y. Law, and I.E. Smith, *Sanctuary site leptomeningeal metastases in HER-2 positive breast cancer: A review in the era of trastuzumab.* Breast, 2016. **26**: p. 54-58.
260. Preusser M, B.A., Furtner J, Dieckmann D, Bartsch R, *Meningeosis carcinomatosa eines HER2-positiven Mammakarzinoms.* Tumorboard, 2013. **2**(1): p. 2.
261. Hofer, S., et al., *Intrathecal trastuzumab: dose matters.* Acta Oncol, 2012. **51**(7): p. 955-6.
262. Mego, M., et al., *Intrathecal administration of trastuzumab with cytarabine and methotrexate in breast cancer patients with leptomeningeal carcinomatosis.* Breast, 2011. **20**(5): p. 478-80.
263. Oliveira, M., et al., *Complete response in HER2+ leptomeningeal carcinomatosis from breast cancer with intrathecal trastuzumab.* Breast Cancer Res Treat, 2011. **127**(3): p. 841-4.

264. Ferrario, C., et al., *Intrathecal trastuzumab and thiotepa for leptomeningeal spread of breast cancer.* Ann Oncol, 2009. **20**(4): p. 792-5.
265. Allison, D.L., et al., *Intra-CSF trastuzumab in patients with neoplastic meningitis from breast cancer or primary brain tumors.* Journal of Clinical Oncology, 2009. **27**(15S): p. 2066-2066.
266. Stemmler, H.J., et al., *Application of intrathecal trastuzumab (Herceptintrade mark) for treatment of meningeal carcinomatosis in HER2-overexpressing metastatic breast cancer.* Oncol Rep, 2006. **15**(5): p. 1373-7.
267. Stemmler, H.J., et al., *Intrathecal trastuzumab (Herceptin) and methotrexate for meningeal carcinomatosis in HER2-overexpressing metastatic breast cancer: a case report.* Anticancer Drugs, 2008. **19**(8): p. 832-6.
268. Platini, C., J. Long, and S. Walter, *Meningeal carcinomatosis from breast cancer treated with intrathecal trastuzumab.* Lancet Oncol, 2006. **7**(9): p. 778-80.
269. Shojima, K., et al., *Application of intrathecal trastuzumab for treatment of meningeal carcinomatosis in HER2-overexpressing metastatic breast cancer.* Journal of Clinical Oncology, 2008. **26**(15_suppl): p. 1138-1138.
270. Laufman, L.R. and K.F. Forsthoefel, *Use of intrathecal trastuzumab in a patient with carcinomatous meningitis.* Clin Breast Cancer, 2001. **2**(3): p. 235.
271. Brandt, D.S., *Intrathecal trastuzumab: 46 months and no progression.* Community Oncology, 2012. **9**: p. 3.
272. Dumitrescu, C. and D. Lossignol, *Intrathecal Trastuzumab Treatment of the Neoplastic Meningitis due to Breast Cancer: A Case Report and Review of the Literature.* Case Rep Oncol Med, 2013. **2013**: p. 154674.
273. Park, W.Y., et al., *Intrathecal Trastuzumab Treatment in Patients with Breast Cancer and Leptomeningeal Carcinomatosis.* Cancer Res Treat, 2016. **48**(2): p. 843-7.
274. Pluchart, H., et al., *Long-Term Survivor with Intrathecal and Intravenous Trastuzumab Treatment in Metastatic Breast Cancer.* Target Oncol, 2016. **11**(5): p. 687-691.
275. Gulia, S., S. Gupta, and A. Singh, *Intrathecal trastuzumab for leptomeningeal carcinomatosis in patients with human epidermal growth factor receptor 2 positive breast cancer.* Indian Journal of Medical and Paediatric Oncology, 2016. **37**(3): p. 196-198.
276. Lu, N.T., et al., *Intrathecal trastuzumab: immunotherapy improves the prognosis of leptomeningeal metastases in HER-2+ breast cancer patient.* J Immunother Cancer, 2015. **3**: p. 41.